THE UNIVERSITY OF CALGARY

Rehabilitation of HC-Type Bridge Girders Using CFRP-Sheets/ Strips or External Post-Tensioning

by

Amr H. Riad

A THESIS

SUBMITTED TO THE FACULTY OF GRADUATE STUDIES

IN PARTIAL FULFILMENT OF THE REQUIREMENTS FOR THE

DEGREE OF MASTER OF SCIENCE

DEPARTMENT OF CIVIL ENGINEERING

CALGARY, ALBERTA

OCTOBER, 1998

ABSTRACT

An effective and economic method of rehabilitation needs to be developed for many reinforced concrete bridges, due to factors such as corrosion of the steel, greater permissible truck loads and changes to the design code. Testing of two HC-Type beams dismantled from a bridge near Calgary indicated that the flexural capacity of the beams was only 60% of the shear capacity. Thus enhancing the flexural capacity is the primary target of rehabilitation. Two more beams were repaired with Carbon Fibre Reinforced Plastic (CFRP)-strips, and were tested in flexure. The strips increased the capacity by only 12%. This was less than the expected. Further tests were performed in order to understand more about the behaviour of beams strengthened with CFRP-strips. Two other HC-beams were externally post-tensioned and tested to give the desired strength for the girders. External post-tensioning is recommended for increasing the flexural and the shear capacity of the beams.

ACKNOWLEDGEMENTS

First and foremost, praise and thanks to Almighty Allah, the Most Gracious, the Most Merciful, and peace be upon His Prophet.

I would like to express my deepest gratitude and appreciation to my supervisor, Dr. Nigel G. Shrive for his invaluable guidance, support and encouragement and for his profound patience throughout all the stages of this study. I also greatly appreciate the help and encouragement provided by Dr. Robert E. Loov and Dr. Gamil Tadros. The help of Dr. Ezz Y. Sayed-Ahmed throughout all stages of research is deeply appreciated. The assistance of Mr. Ken McWhinnie and Mr. Frank Iquinta is also greatly acknowledged. The technical assistance provided by Mr. Don McCullough, Mr. Don Anson and Mr. Terry Quinn is sincerely appreciated. I would like to thank all the sponsors without whom the project would not have survived: IRAP, CH2M Gore and Storrie Ltd., Sika Canada, ISIS Canada, Mitsubishi Chemical Corp., Graham Construction, Bridgeworks Inc., DYWIDAG Systems International Ltd., and UCAN Fasteners. This work was done under the auspices of ISIS Canada.

Finally, I would like to express my heartfelt appreciation to my family for lots of support, encouragement and love.

To A'alaa

TABLE OF CONTENTS

LIST OF TABLES

LIST OF FIGURES

LIST OF SYMBOLS

a	Depth of the equivalent rectangular stress block
A_f	Area of the CFRP-strips
A_{fs}	Area of the CFRP-sheets
A_p	Area of prestressing bars
A_s	Area of reinforcing bars
b	Width of compression flange
b_w	Width of the beams' web
B	Slab width
c	Depth of the neutral axis
c_y	Neutral axis depth assuming $f_{pr} = f_{py}$
C	Compressive Force
C_F	Constant used by Neubauer (1996)
d_f	Distance between the centre of the CFRP-strips and the top fibre of the beam
d_p	Distance between the centre of the horizontal DYWIDAG-bar and the top fibre of the beam
d_s	Distance between the centre of the reinforcement bars and the top fibre of the beam
d_v	Distance measured perpendicular to the neutral axis between the resultants of tensile and compressive forces
E	Modulus of elasticity of concrete
E_l	Modulus of elasticity of plate as used by Neubauer (1996)
E_s	Modulus of elasticity of steel
E_f	Modulus of elasticity of plate
f'_c	Concrete compressive strength
f'_{ck}	Concrete bond strength as used by Saeki et al. (1996)
f_{ctm}	Concrete surface tensile strength
f_{cu}	Concrete ultimate strength
f_f	Stress in the CFRP
f_{pe}	Effective stress in prestressing
f_{pr}	Stress in prestressing tendons at factored resistance
f_{py}	Yield stress of prestressing steel
f_y	Yield stress of reinforcing steel
f_{ult}	Ultimate stress in CFRP
F_{max}	Maximum allowable force in the prestressing bar
F_{ult}	Ultimate force in the prestressing bar
G_{IC}	Fracture energy at mode failure I
G_{IIC}	Fracture energy at mode failure II
G_f	Fracture energy
k_b	Constant used by Neubauer (1996)
k_c	Constant used by Neubauer (1996)
l_e	Effective length of tendon

l_{tmax} Maximum required bond length
L Length of Beam
L_b Bond length
L_{jd} Development length
M Bending moment
M_D Bending moments due to dead loads
M_L Bending moment due to live loads
M_f Factored moment
M_r Factored moment of resistance of the beam
M_n Nominal moment of the beam
N_f Factored normal force on the beam
P Applied load on beam
R Vertical support reaction
$R_{expected}$ Predicted reaction at support
s Spacing of stirrups
s_l Local slip between plate and concrete
s_{l0} Slip between plate and concrete at zero bond strength
t_l Thickness of CFRP-plate
T Tensile force
T_f Tensile force in the CFRP-strip
T_{max} Maximum tensile force
T_s Tensile force in the reinforcing steel
T_u Ultimate tensile capacity
v_f Factored shear stress
V_{cg} Factored shear resistance in concrete based on general method
V_D Shear force due to dead loads
V_f Factored shear force
V_{fg} Factored shear resistance in CFRP-sheets based on general method
V_{rg} Total factored shear resistance based on general method
V_{sg} Factored shear resistance in steel based on general method
w Width of CFRP-plate
$w_{O.W.}$ Self weight of the structure
$w_{F.C.}$ Weight of wearing surface
α Angle between bent-up bars and the longitudinal axis of the beam
α_1 $0.85 - 0.0015\, f'_c \geq 0.67$
β Factor accounting for shear resistance of cracked concrete
β_1 $0.97 - 0.0025\, f'_c \geq 0.67$
ΔL Difference in distance
ε_c Strain in the concrete top fibre
ε_{cu} Ultimate compressive strain in concrete
ε_f Strain in the CFRP-strips
ε_{fult} Ultimate strain in the CFRP-strip
ε_{lu} Ultimate strain in CFRP-strip as used by Neubauer (1996)
ε_s Strain in the reinforcing bars

ε_{sy} Yield strain in reinforcing bars
ε_x Longitudinal strain of flexural tension chord of the member
σ Shear stress
θ Angle of inclination of diagonal compressive stresses to the longitudinal axis of the member
λ Factor to account for low density concrete
τ_{ca} Bond stress of concrete
ϕ Bar diameter
ϕ_c Resistance factor for concrete
ϕ_f Resistance factor for CFRP-plates
ϕ_p Resistance factor for prestressing tendons and bars
ϕ_s Resistance factor for reinforcement

CHAPTER 1

INTRODUCTION

1. 1 General Problem

Rehabilitation and maintenance of reinforced concrete bridges has become one of the most important issues of the second part of the twentieth century. Every year governments spend large sums of money in the repair and renewal of infrastructure. In the USA more than 40 % of the 500,000 existing bridges are either structurally deficient or functionally obsolete (Klaiber et al. 1987). Several reasons can be found for the previous statement such as the general age of the structure, the steady increase of truck loads and traffic density, changes in the use of the structure, mistakes in design, deterioration due to environmental attack, or poor original construction, and poor maintenance practices. Munley (1994) states that there is a lack of funding to contain the rapidly increasing deterioration of bridges in the USA adequately. Over 200,000 bridges worth $78 billion are in critical need of repair. Repairs would cost $5.2 billion per year to keep bridge renewal at the current status quo.

In Canada no exact numbers have been found. More than 40 % of the bridges in Canada were built in the fifties and sixties, and most of them are in need of urgent rehabilitation (Neale 1997). The situation here is expected to be worse than in the USA, because of the more severe weather conditions, especially in the winter.

1. 2 General Methods of Rehabilitation

The solution of the problem of bridge deterioration needs extensive research. There are several methods, which have proven efficient to rehabilitate bridge girders. Among these methods are the use of external post-tensioning, which increases the flexural capacity of the beams. External post-tensioning has been successfully used in several projects, and has the advantage of being easy and reliable. Another method of rehabilitation is the use of external steel-plates to improve the beams' strength: also an easy and proven efficient method. This method however, has several disadvantages, such as corrosion of the steel-plates, the heavy weight of the steel, and extensive false work and splicing. An option which may be better is to use Carbon Fibre Reinforced Polymer-strips (CFRP-strips) instead of steel-plates. For the same required level of strengthening, less area of material is required with much less weight. CFRP-strips do not have the problems of corrosion or heavy false work. This new material has proven to be very promising in the area of rehabilitation.

1. 3 Scope of Research

During the mid-part of this century, over 1500 reinforced concrete bridges were constructed in Alberta, Canada using Type HC, G and E precast reinforced concrete beams. The bridge beams were inverted U-sections, which are put beside each other to make the bridge. The beams were mostly with short spans (from ≈ 8-12 m) and simply supported

even if the bridge has several spans. Some types of bridges have shear connectors, which allow the loads to be redistributed along the beams, and the other types do not have shear connectors. Over the years, these bridges began to have several problems. Frequently in winter, salt is spread on the bridge deck to melt the snow. The chloride ions in the solution accelerate the formation of rust in the steel reinforcement, as the chloride ions tend to lower the ph-value of the concrete. In addition to this, the concrete cover was too small in comparison of the amount of steel reinforcement put into the beams and too small to resist effectively the weather conditions the bridges face. Cracks appeared around the reinforcement exposing most of the steel in the mid-span of the girders. Another problem is outdated design Codes. These beams were designed using the truck loads and shear strength equations from what is now an older Code of Practice. The specifications in the current Code of Practice are for greater loads (about 45 % increase in truckloads): simultaneously, the shear design equations have been made more conservative. As a result, the old beams do not necessarily meet the new Code provisions and need immediate rehabilitation.

The focus will mainly be on one type of these beams. The HC-Type bridge beams are 11.6 m long and contain shear connectors between the beams. The beams have all the problems mentioned earlier and create a huge problem for Alberta Transportation and the City of Calgary. In order to determine the weaknesses of the beams and find an economic way to rehabilitate them, research was required. Eleven HC-Type beams dismantled from a bridge near Calgary were transported to the reinforced concrete laboratory in the University of Calgary to be tested. Several opportunities were available to rehabilitate the bridges. The

final decision was either to use Fibre Reinforced Polymers (FRP), or external post-tensioning. A practical and efficient method of rehabilitation had to be determined through an experimental programme. That programme is described in the thesis.

Existing knowledge about the two methods of rehabilitation, their techniques, advantages and problems, was assessed. The current state of the beams was examined in order to determine the direction of research. The examination of the beams involved visual inspection and testing to determine flexural and shear capacities. Rehabilitation with CFRP-strips and sheets was then attempted. Test results are described and compared to predictions based on theoretical analysis. Tests were also performed under cyclic loading. The beams rehabilitated with CFRP-strips were not as strong as expected and a truss model was used to explain the mode of failure of the beams. Tests on further beams (cast in the laboratory) provide experimental verification to the truss model. Some conclusions are drawn, and future design recommendations are made on the basis of the analysis and test results. Other beams were then post-tensioned. The layout of the cables and the anchorages were designed to be usable in the field. An analysis was performed to estimate the increase in performance of the beam: the results of the analysis and the tests are described: the different techniques of rehabilitation are reviewed, leading to overall conclusions, and final recommendations to rehabilitate the bridge girders.

CHAPTER 2

CARBON FIBRE SHEETS/STRIPS: STATE OF THE ART

EXTERNAL POST-TENSIONING: AN ALTERNATIVE

Experiments performed in North America, Europe and Japan concerning Carbon Fibres can be divided into three "generations". The first generation of tests was concerned with the determination of material properties. The second generation of tests was concerned with testing the material in civil engineering applications, while the third generation was concerned with design equations for using CFRP-sheets/strips in the rehabilitation of structures for improving flexural and shear capacity. All three types of experiments continue to be performed, as these materials are still new. More experimental work has to be done for CFRP to be understood as well as steel-reinforcing bars.

2. 1 Introductory Work

The following papers have helped to understand the first stage of the project in the thesis. The knowledge of concrete cracks, the effect of rust on reinforcement, lack of cover, concrete properties and methods of testing such large beams was useful.

2.1. 1 Corrosion and Bond Loss

Okada et al. (1988) deal with the analysis of beams that developed longitudinal cracks due to reinforcing bar corrosion. Corrosion was induced in the beams by spraying a chloride solution once a day on the beams over a period of about 22 weeks until longitudinal cracking was evident. It was found that the flexural-shear cracks that formed during the flexural test were fewer in the damaged beam than in the intact beam. This led to

the conclusion that there was considerable bond deterioration between the concrete and the main reinforcement. Although this deterioration was evident, the ratios of measured to calculated yield capacities for the intact and damaged beams were close to 1.0. The ratios of the ultimate measured and calculated flexural resistance were also compared and indicated that the ultimate capacity of the damaged beams was reduced by only about ten percent.

Raoof and Lin (1997) performed tests on a number of beams from which they had removed varying amounts of concrete cover (0% to 30%) to varying depths. Their general findings indicated that there is a limit to the amount of concrete cover that can be removed, beyond which there are significant strength loss. Removal of the concrete cover up to one millimeter above the main reinforcing steel level in different zones between the supports resulted in minimal ultimate strength losses. This removal of concrete around the reinforcing bar effectively simulates bond failure.

2.1. 2 Testing of Full Scale Bridge Girders

A number of bridge girders (Type G) were tested in 1985-1986 in order to determine their strengths in flexure and shear (Ghali 1986). The province of Alberta was interested in the possibility of increasing the truckloads on the bridges in Alberta. Eight G-Type beams with a span of about 9 m were tested, concentrating on the effect of eccentric loading on the shear and flexural capacities of each web. The torsional rigidity of the beams was found to be high so the effect of eccentric loading was minor.

Several conclusions were drawn from the survey: as expected the capacity of the beams was similar regardless of the deterioration of the cover or the cracks that they had. It

was found that there was little merit in testing the beams under eccentric loading because of their large torsional rigidity.

Mao, Alexander and Rogowsky (1997) performed 41 tests on 11 HC-Type girders. The tests aimed to assist the inspection and rating of existing bridges that use HC type stringers. The span of the girders was 10 metres and the condition of the girders varied from poor to good. It was necessary to look at different kinds of tests, such as flexural tests, shear tests on the full beam, shear tests on single webs, tests with eccentric loading and bond tests for single webs.

Calculations to predict maximum shear, flexure and torsional loads, as well as calculations for vertical deflections were based on the CSA Standard A23.3-94.

The following conclusions were drawn: the preliminary tests showed higher than expected concrete compression and steel yield strengths. The visual ratings of the beams did not necessarily indicate the actual strength of the beams (Several poorly graded beams have performed well in the tests). The flexural capacity of the beams is higher than truck loads. The beams failed in a ductile manner due to crushing of concrete top slab at the locations of the shear connectors. The locations of the shear connectors were considered locations of stress concentration. Torsion failure was unlikely unless uplift at the supports was restrained. Uncut and uncracked diaphragms allow load sharing between loaded and unloaded webs. The shear capacity is more than adequate, being higher than the flexural capacity. The report concluded with recommendations to maintain the beams and pay particular attention to corrosion in the stirrups.

2. 2 Testing Material Properties

As more tests were done in this preliminary stage, the most critical points with respect to CFRP-sheets were the effect of environmental exposure and the bond with the concrete. The other mechanical properties (tensile strength, modulus of elasticity, elongation etc.) were already known from manufacturers' tests. Much had been done for the use of CFRP sheets/strips in the field of aerospace research.

There is a lack of knowledge in the area of appropriate selection of materials, manufacturing process and overall durability of these materials. However, many researchers have attempted to write about the properties of composite materials. The selection of the right composite should ideally be based on the composites' properties: the relaxation and creep, the moisture resistance, the alkali resistance, the thermal stability (which is critical for resins), the resistance to salt water and the fatigue behaviour. But the economic aspect should not be ignored, as well as the unique needs of each project in itself. The high cost of composite materials may be reduced by taking into consideration that the high accuracy needed in the aerospace field (where the composites originally came from) was not needed in civil engineering.

A good manufacturing process is important to get a reliable material too. Norris, Saadatmanesh and Ehsani (1997) state that CFRP-sheets are composed almost entirely of carbon atoms, the fibres are generally available as bundles of 500-150,000 filaments of approximately five microns in diameter called "yarn". Continuous fibre sheets are made of parallel yarns attached to a flexible backing tape for handling. Since there is no adhesion between fibres, a polymer or resin matrix is used to transmit the forces between the fibres. In general, the best quality of composite is fabricated using a prepeg and autoclave cure

based process, and the highest variability would be found in composites fabricated by the wet lay-up or spray-up type of process. A reduction factor of 0.45-0.6 for strength in the long-term uses was suggested by Kabhari (1997) when using the wet lay-up process.

2.2. 1 Effect of Environmental Exposure

Karbhari and Seible (1996), and Karbhari (1997) suggest that the carbon fibre composites are the best available choice in terms of resistance to environmental effects, as the glass fibres are weak in moisture resistance and thermal stability. Some reduction factors were proposed in terms of reliable strength in short-term and long-term applications. The suggested reduction factors for carbon fibre composites were as high as 0.9-0.95, while for the E-glass composites they were as low as 0.25-0.7.

Meier (1992) and Neale and Labossière (1991) also stated that glass fibres are the most popular of the reinforcing fibres, since they are economical to produce. However, their susceptibility to alkaline and acid solutions, as well as their potentially inferior fatigue behaviour, restricts the use of GFRP-sheets for strengthening structures. Carbon and aramid have strength and stiffness properties that are superior to glass fibres, but since carbon fibres are approximately twice as stiff as aramid fibres and less susceptible to deterioration than glass, their use is favoured for strengthening structures.

Karbhari, and Engineer (1996a), (1996b), Karbhari, Engineer and Eckel (1997), focused their investigation on the effect of short-term environmental exposure on the interfacial fracture energies between the concrete and the composite material. Durability of CFRP-sheets or strips under different climates is a very important issue. Peel tests were performed on a series of layers of CFRP-strips glued to different concrete blocks. Figure

2.1 shows the apparatus used in the peel tests. Each set (CFRP-strip + concrete) was subjected to one of the five following environments for a period of sixty days:

1) Ambient conditions at 20° C (as control tests).

2) Immersion at fresh water in 20° C.

3) Immersion in synthetic seawater at 20° C.

4) Exposure to -15.5° C.

5) Freeze-thaw exposure as represented by 24h alternate cycles of -15.5°C to +20°C.

The high humidity and moisture content would affect the reaction between the concrete and the epoxy and weaken the bond between them. Short-term exposure to water or seawater has very little effect on the levels of the flexural mode of failure although significant levels are seen in the shear of the epoxy resin. Exposure to subzero temperature has a positive effect by increasing the stiffness of the composites.

The selection of the right resin though, could neutralize some of the environmental effects. Chajes et al. (1996) stated that the important factors taken into consideration in the matter of the better adhesive were:

1) average shear stress at failure (a good adhesive should not be the cause of failure in terms of its shear stress),

2) pot-life of the adhesive,

3) sensitivity to the mixing ratio

4) working viscosity

5) cost.

The epoxies bond very well with concrete, have a low coefficient of thermal expansion, and a low shrinkage upon cure. The good bond between epoxie resins and concrete in a rough climate was proven by Calder (1982) and Lloyd and Calder (1982) in a two year-long monitoring programme on a bridge in England. Also J. K. McKenna and M. A. Erki (1993) noticed the dependence of the force transfer between concrete and steel plates as well as the CFRP-plates on the shear strength of the adhesive (polymer, epoxy, etc.), and recommended epoxies. There are other types of adhesives, which are cheaper but have poorer performance under different environmental conditions.

2.2. 2 The Bond between CFRP and Concrete

Bond or peeling out is the mode of failure of the composite plates from concrete. The high tensile strength of the composite materials makes the tensile failure in the material rare. To develop rehabilitation procedures for concrete structures involving externally applied composite plates, a good understanding of the behaviour and strength of bond is needed.

There are several factors which affect the bond: a) internal influences: like chemical activity, electrochemical activity, ph-level of concrete, internal cracks and internal moisture of concrete, b) interfacial influences: like thermal effects and moisture difference at the epoxy, c) external influences: like humidity, temperature, temperature cycling and ultra violet rays. Internal cracks in concrete, for instance, could cause initial debonding in the area near the supports where the sheets end, where high shear stresses and a rapid change of moment occur, which would lead finally to lower than expected flexural or shear capacity for the structure.

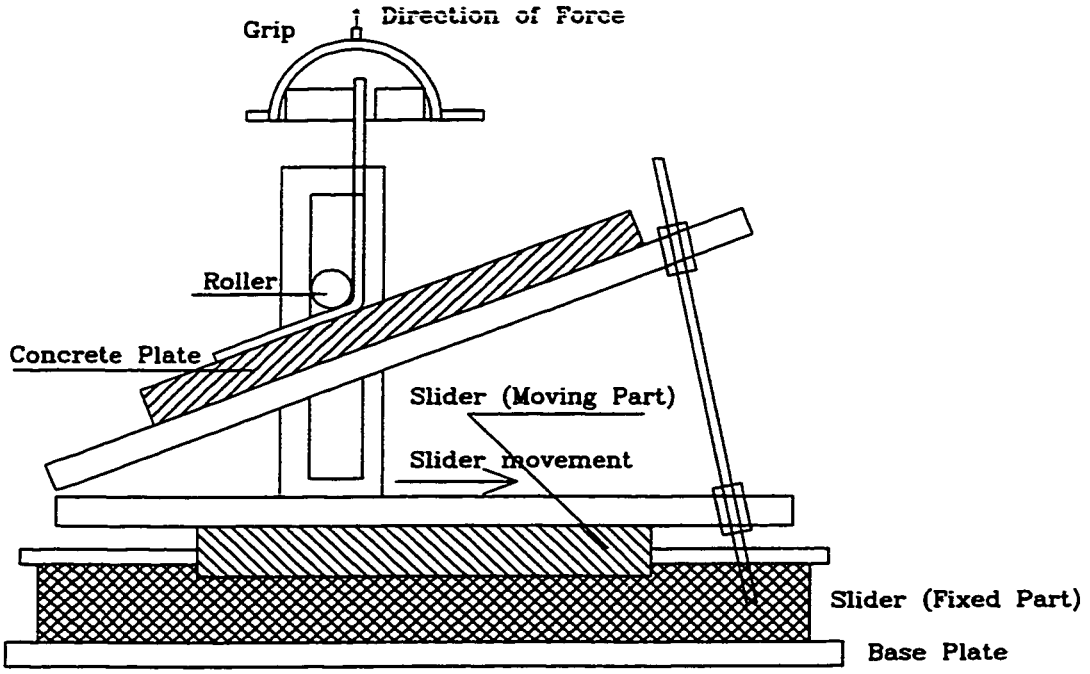

Figure 2.1 Details of the Peel Test Apparatus

In the field there are several aspects which may cause debonding or peel between the concrete and the composite material. Imperfect bonding, debonding cracking due to flexural cracking in concrete or failure of concrete in pure shear, non-uniformity in concrete surface, fatigue due to cyclic loading, incomplete or poor wetout of fibre as well as the presence of large resin-rich zones, could reduce the capacity of the section.

Karbhari (1995), Karbhari, Engineer and Eckel (1997) stated that there are four mechanisms of adhesion between concrete and composite: mechanical interlock, diffusion theory, electronic theory and absorption theory. The most important mechanism is the mechanical interlock depending very much on the irregularities of the concrete surface, that is why it is very important to have a relatively rough surface and a good resin to be sure that a strong bond appears between the concrete and the composite. The five different types of failure or potential crack paths (Figure 2.2) are either through the concrete (peel failure), or interfacial failure between concrete and adhesive, cohesive failure in the adhesive, interfacial crack between the adhesive and the composite, or an alternating crack between the two interfaces.

One advantage of the peel test is that the test is a direct method to measure the work of detachment because bond failure proceeds at a controlled rate. Another advantage is that failure can be achieved under a mixed mode of loading. Thereby the critical interfacial fracture energy under both loading modes I and II (G_{IC} and G_{IIC} respectively) can be evaluated. Figure 2.3 shows a schematic failure in mixed modes I and II. A key result from the tests is the effect of the resin used, where two types of resin were used, one with resin to hardener ratios of 2:1 (resin A) and the other 4:1 (resin B). Also the peel angle (20° to

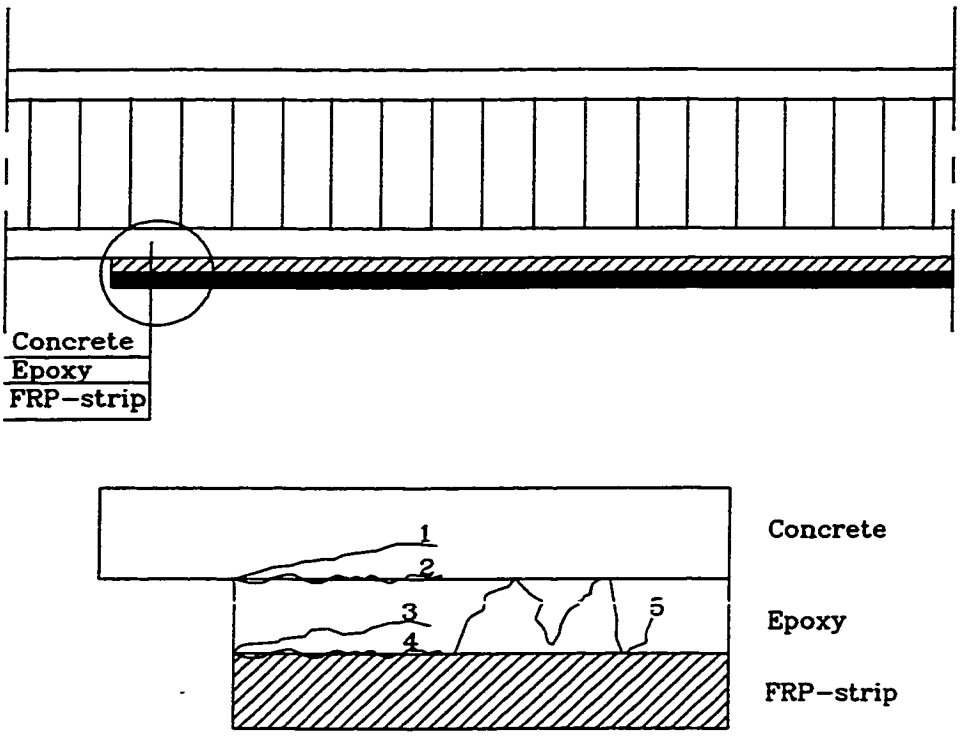

1: Peel failure into concrete

2: Interfacial failure between concrete and adhesive

3: cohesive failure in the adhesive

4: Interfacial crack between the adhesive and the composite

5: Alternating crack path between the two interfaces

Figure 2.2 Potential Crack Paths

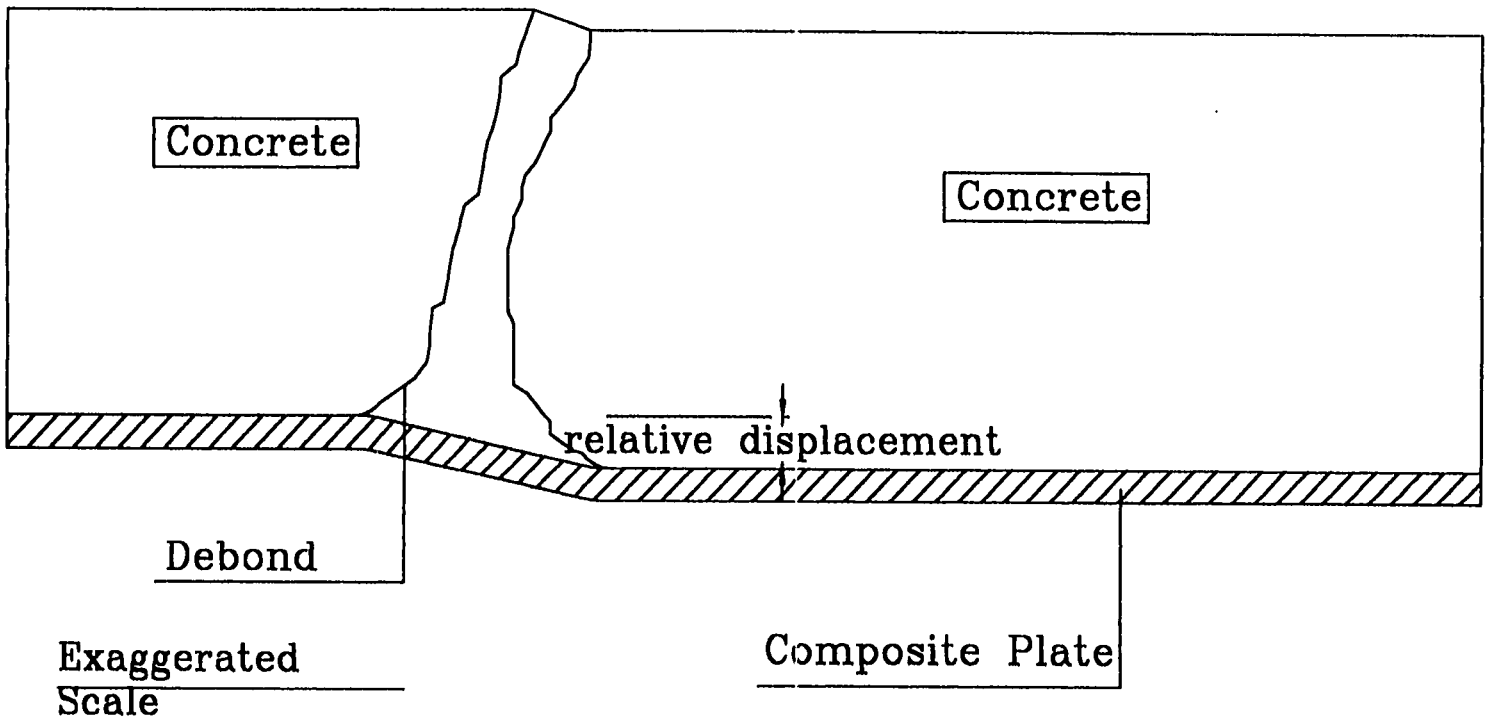

Figure 2.3 Schematic of failure mode in debonding due to relative movement and interfacial debonding at the concrete-composite

140°) was an important factor to determine which mode governs failure. From the results it should be noted that G_{IC} values are dependent on the properties of the interface, whereas G_{IIC} values are dependent on the properties of the epoxy. Values achieved by resin A were higher than those achieved with resin B.

The choice of the resin system is a very important factor in raising the fracture energy of the system. The overall shape of the profile of the peel force as a function of the peel angle was the same under all conditions using glassfibre or carbonfibre (the force declined as the peel angle increased). The peel force needed under conditions F (freeze), and FT (freeze thaw) was much higher than needed for SW (salt water) or the other conditions.

Chajes et al. (1996) did a series of tests on bond and force transfer between composite material plates and concrete. An experimental programme of two different stages was performed by testing graphite/epoxy composite material plates adhered to concrete in a single lap test. In stage I, a constant bond length was used in all tests.

The following parameters were changed: Surface preparation method, type of adhesive, and concrete strength to see the effect of each factor on the average bond strength. One inch wide graphite/epoxy composite plate bonded to a concrete block (6″ × 6″× 9″) with a 3inche bond length was tested.

At first three types of surface preparation were used on concrete of the same strength and with the same type of epoxy.

1) No surface preparation (plate bonded to the "as cast" concrete)

2) Grinding with a stone to give a smooth finish

3) Mechanically abrading with a wire wheel to give a finish near sandblasting.

The average bond shear stress at failure was, as expected, highest with the mechanical abrading. The results showed the need for a mechanical bond between the concrete, the epoxy, and the composite plate.

A series of tests was performed to eliminate the effect of concrete compressive strength. Figure 2.4 shows the machine used in the testing programme. It was found that the average shear stress at failure varied almost linearly with the concrete strength throughout the tests.

Varying only the bond length in order to examine the force transfer from the composite to the concrete was the second part of the project. The same single lap test was used with the same size of concrete specimen with bond lengths of 2 inches, 4 inches, 6 inches and 8 inches. Strain gauges were glued on the plate to measure the force transferred. For all bond lengths, at loads below failure load, the strain in the plate decreased at a fairly uniform rate until the strain became small (all the force was transferred to the concrete). For the 6 inch and 8 inch bond lengths the strain distribution indicated progressive failure. The stress-strain curve becomes flat at the beginning of the bond because concrete begins to fail in this area. A very short bond length (here 2 inches) caused a lower failure load due to " bond shortage". This term means that there is insufficient area to transfer the force to the concrete. The authors also observed that the average bond stress at failure decreased as bonded length increases. This is because a certain minimum length is required to develop the force at maximum bond strength. At lengths beyond the minimum, maximum bond strength is not developed as the force is spread over a greater area. Some equations were predicted to help design the bond length for the composite material. The shear stress and the average bond resistance were given by two simple and understandable equations:

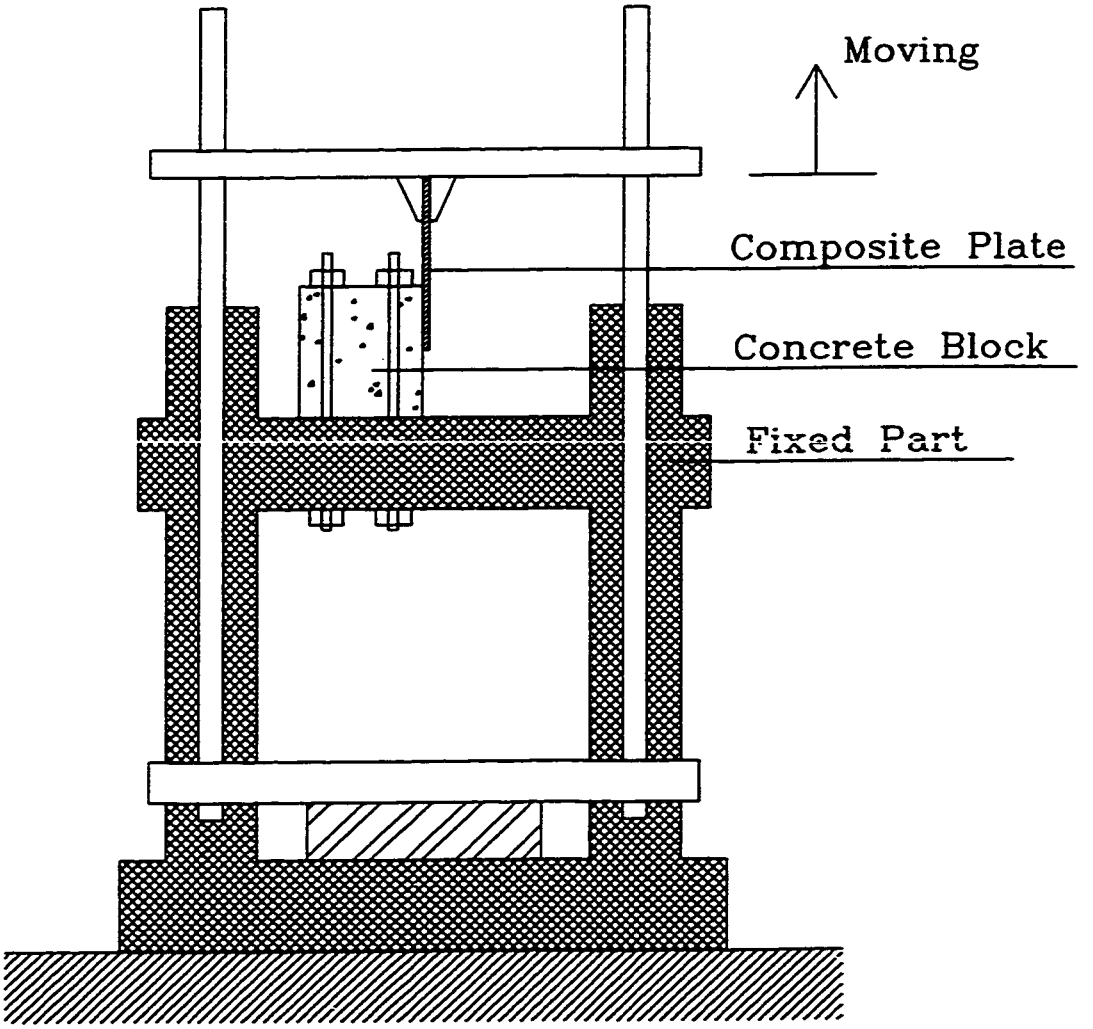

30,000 lb. (135 kN) Tinius Olsen Machine

Figure 2.4 Single Lap Shear Bond Test-Setup

$$\tau = \frac{F_1 - F_2}{w \Delta L}$$

$$R = \tau w = \frac{F_1 - F_2}{\Delta L}$$

Where: τ Is the shear stress, F_1 and F_2 are the forces in the composite plates at gauges 1 and 2, w is the width of the composite plate, and ΔL is the distance between the gauges 1 and 2. Based on the idealized representation of the force transfer, the ultimate capacity T_u of a joint having a bond length L_b, and a bond development length L_{jd} is:

$$T_u = R L_b \qquad L_b < L_{jd}$$

$$T_u = R L_{jd} \qquad L_b > L_{jd}$$

These equations need further research.

2.2. 3 Other Properties

Finally, J. K. McKenna and M. A. Erki (1993), Neale K. and Labossière P. (1991) summarized some other factors, which affect the performance of FRP-sheets:

1) The load duration. Some laboratory tests have shown that under a sustained load, the stress-strain curve will not remain linear and there will be a certain "yield" at the end.
2) Fatigue resistance: for up to 10,000,000 cycles carbon fibres maintain 80% of their monotonic strength.
3) Environmental effects and temperature. Differences in temperature cause the material to weaken since the fibres have different coefficients of thermal expansion.

4) Fire: The polymer matrix is very susceptible to fire, however one can use additives to improve the fire resistance.

The conclusions can be summarized that the research work showed it was obvious that a stiff epoxy is the key for better results. A stiff epoxy can guarantee the transfer of forces (through shear flow) from the beam to the sheets. The CFRP-sheets are the best way to rehabilitate weak beams in flexure, showing better performance than both glass and aramid fibres. CFRP-sheets are about 10 times higher in the initial cost, but about 10 times lighter in weight. By considering the fact that the material cost will only be 20% of the total cost of the project (labour, working period, false forms, maintenance, etc.), it can also be said that the CFRP-sheets could be more economic as well. The fire resistance is an issue to discuss, but is of less importance for bridge systems, while fatigue behaviour is shown to be a good point for using the composite materials.

2. 3 Applying CFRP-Sheets/Strips on Concrete Structures

The other method of testing is testing these materials after applying them on concrete structures. This is the main purpose of using the CFRP-sheets/strips. Their use concentrates on the rehabilitation of beams or columns in shear (mainly FRP-sheets) or flexure (mainly FRP-strips). Most tests were directed towards the rehabilitation of bridges and bridge girders either in flexure or in shear.

2.3. 1 The effect of End-Anchorage

With respect to the application of external reinforcement to reinforced concrete beams a thesis (Jansze 1997) about strengthening beams with "steel-plates" was considered. The thesis is not directly related to CFRP-strips, but it contains some very important principles, which apply as well for the CFRP-strips. Important features from the

thesis include the end anchor failure, the strut and tie theory and the truss analogy in the finite element model.

The thesis is a report on the strengthening of concrete beams with external reinforcement. Steel plates were adhered with epoxy resin to the tension sides of concrete beams. Several parameters were inspected in a practical parametric study. The results of this parametric study were verified using a numerical finite element model.

There are several problems with the use of steel plates to strengthen concrete structures, particularly at the ends of the plates. Shear failure appears in these areas due to weak anchorage between the plates and the concrete. The lack of shear reinforcement between the level of the concrete and the level of the plates causes shear cracks (concrete struts between cracked ties) where the force is transferred to the plates. Therefore many reports have included a shear failure based on a strut and tie model.

Most of the recent reports included applying internal or external shear reinforcement to flexural strengthening with plates. Figure 2.5 shows a truss model used by Pichler (1993) to analyze the end portion of the beam with vertical bolts acting as anchors.

Part I: The Experimental Work:

Two beams were failed in the first tests with a span of 2400 mm and third point loading. One beam was plain (no external steel), while the other had a steel plate attached to its tension side in order to increase the flexural capacity. After testing these two beams in flexure two different modes of failure were noted.

Conventional flexural failure was observed in the first beam whereas there was failure at the end of the steel plate (the author calls it: plate end shear) for the other beam.

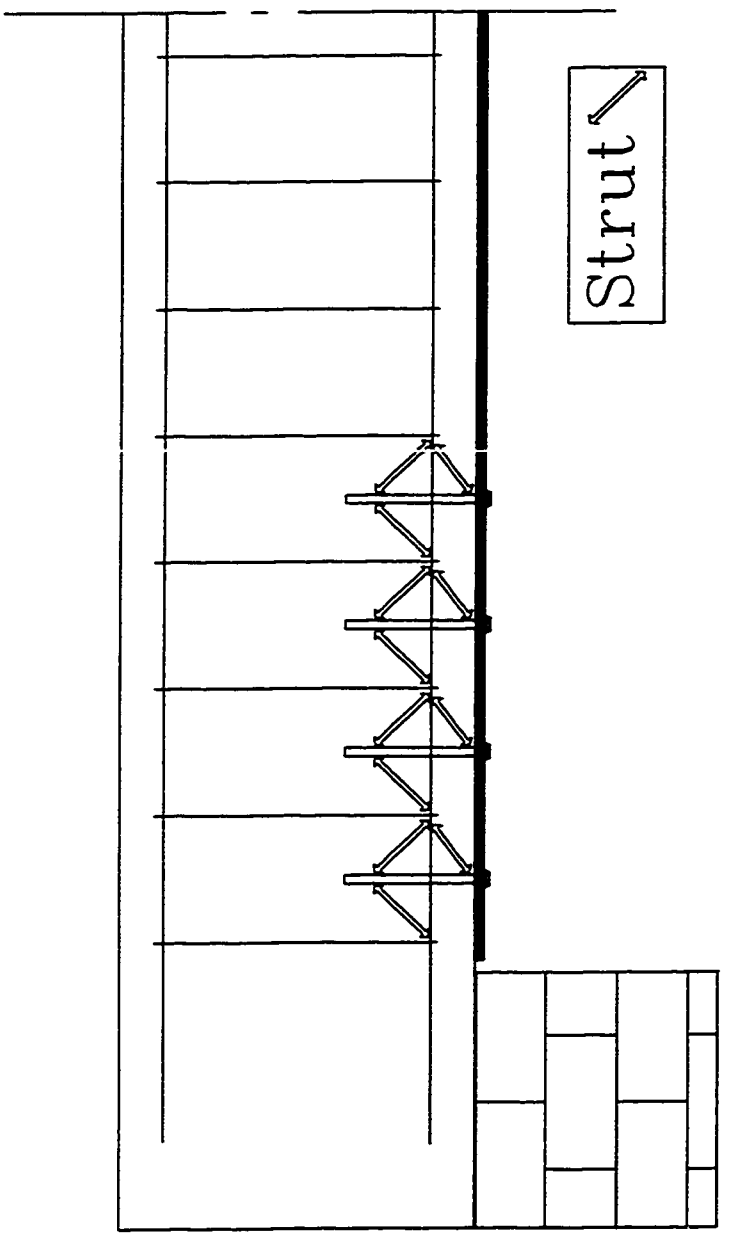

Figure 2.5 The Strut and Tie Model Suggested by Pichler (1993)

The expected strengthening ratio of 3.4 was not achieved as the beam failed at only 2.2 times the original moment. After the plate had separated, the beam responded similarly to a conventionally reinforced beam. The author concluded that the problem of end anchorage should be the focus of the investigations.

Experimental modeling was the next step, as due to symmetry only half of the beam had to be tested if the correct end conditions were achieved. A concrete of strength 45.5 MPa after 28 days, and steel reinforcing bars of yield strength 592 MPa and steel plates of 550 MPa were used for the tests. After casting, the surface of the tension sides of the beam was prepared through grit blasting before the epoxy resin and plates were applied. Several parameters were investigated to determine the most efficient way to strengthen the beams. The unplated length is the distance between the support and the beginning of the plate. The unplated length was varied in one series of tests; the influence of bolts in the end anchorage was investigated in another series. Cyclic loading, the cross section of the plates, the width and the depth of the section were examined as well. One of the major variables was the unplated length of the beam. In the tests the unplated length was varied from 100 mm to 300 mm in a series of 6 beams. The maximum load capacity was achieved when the unplated length was minimum. As the unplated length rose to 300 mm the mode of failure seemed to be changing from shear at the end plate to conventional flexure failure. It is important to notice that the ratio of the unplated length to the plated is the important parameter. The shear span is 800 mm with 300 mm left from the shear length exposed. This is almost half of the shear span, which is of course damaging to the strengthening idea. The bond length would of course decrease dramatically and the shear and normal stresses would increase at the end of the plate by increasing the unplated length.

The influence of the addition of bolts at the end of the plate was found to be a very important aspect. The addition of bolts prevented endplate shear or at least delayed such shear. As a result, with bolts there was a more ductile failure rather than the brittle failure mode of endplate shear. Before strengthening, at 25 mm from the plate end, a 12.5 mm diameter hole was drilled through the steel plate. After the concrete member was strengthened with the external steel plate, an approximately 90 mm deep hole was drilled through the steel plate into the bottom of the concrete member. An 80 to 85 mm bolt was glued in the hole with epoxy thus providing additional anchorage for the plate. Additional prestressing forces were added to some of the bolts (P=10 kN, 25 kN, 2 × 10 kN or 3 × 10 kN) and the others were left without nuts (no prestressing force). The failure mechanism which occurred with bolted ends was different than before (Figure 2.6) and the load needed to crush the beam is increased. The peeling crack, usually causing plate end shear, could not occur in the presence of the bolts. As a result of increasing the load, increased shear stresses at the concrete-epoxy interface occurred, which led to interface plasticity. In the case of two or three bolts, the failure load was increased more. By virtue of the larger prestressed zone with increased normal compressive stresses, the interface failed at a higher load. The deflection curves of the reference beam and the beam with plates with bolted ends were the same until the reference beam reached failure. The bolt therefore played a passive role up to this point.

It seemed that due to lack of "suspension reinforcement" (extra external vertical reinforcement to transfer the forces from the level of the steel plate to the compression zone) several cracks were formed in the level of the plain concrete between the level of the reinforcing bars and the level of the steel plate, forming concrete struts, not finding steel

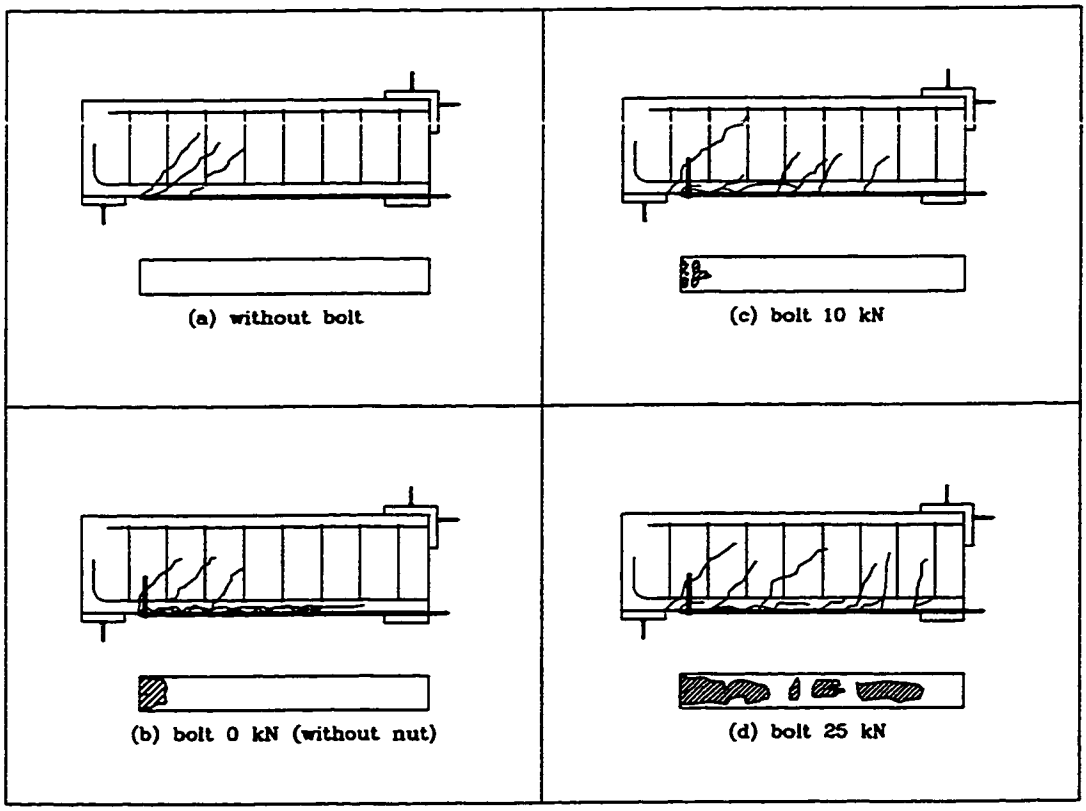

Figure 2.6 The effect of the Prestressed Bolts on the Mode of Failure of the Beams

ties to balance their forces. The recommendation of the author was to add at the end zone several bolts at a certain spacing instead of one bolt with a bigger force.

The next parameter tested was the influence of repeated loading. The beams were subjected to cyclic loading of 35%-80% of the maximum static load at a frequency of 6 Hz. These values were chosen after a pilot test to investigate the critical upper and lower load levels for crack initiation in the anchorage zone. 7 beams were then tested, subjected to an average number of 2,000,000 cycles to reach failure. No failure occurred in the beams despite this high number of cycles.

The influence of the plate cross section, the width of the plates and the height of the section were investigated as well to see their effect on the maximum force to fail the beams.

A numerical truss model (Figure 2.7) was developed by the author, taking into consideration that the materials have non-linear properties in the plastic state. The focus of the numerical model was to concentrate on the ends of the plate to analyze the principal stresses in this area to verify the experimental work and produce general equations.

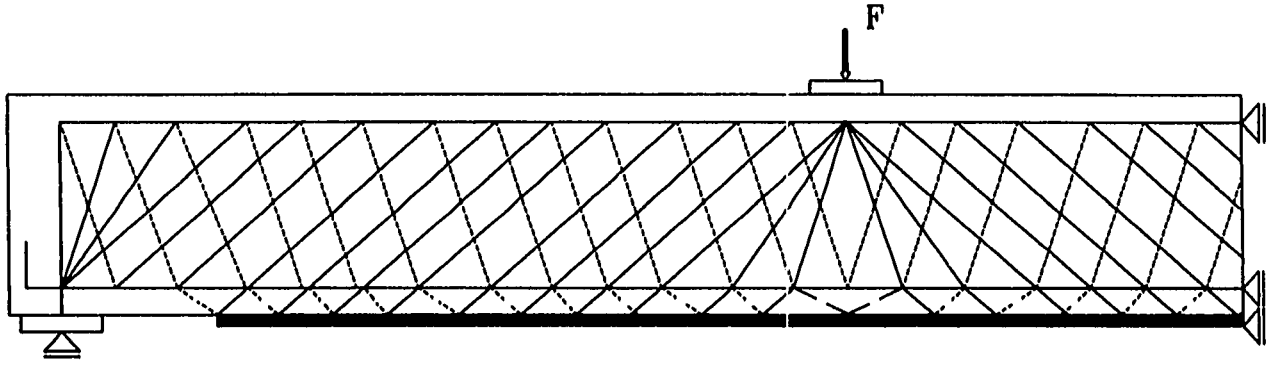

Figure 2.7 The Truss model used by Jansze (1997) for the Finite Element Analysis

2.3. 2 Rehabilitation of a Real Bridge

Walser and Steiner (1996) describe the rehabilitation of the Oberriet-Meiningen Bridge in Germany. The bridge deck was made of a reinforced concrete slab, which was designed according to an outdated code of practice. The traffic loads have subsequently doubled and the slab was deemed to be unsafe. Several methods of rehabilitation were proposed. The method chosen was to strengthen the tension side of the slab with Carbon Fibre Reinforced Plastic- (CFRP)-strips, and at the same time to increase the slab thickness by having an additional layer of reinforced concrete in the compression zone. The CFRP-strips used were 80 mm wide and 1.2 mm thick. A total of 160 strips 4 m long were bonded to the slab at 750 mm intervals.

The calculations made for the rehabilitation were based on full compatibility between the strips, the epoxy and the concrete and then proceeding with a conventional method of strain relations and equilibrium of forces. The design was such that failure would occur in the CFRP-strip prior to yielding of the steel. A total strengthening factor of 2.4 was achieved to meet the safety requirements of the bridge.

The application of the CFRP-strips included several steps. The underside of the bridge was prepared by blast cleaning, which produced the roughness layer of 0.5-1.0 mm required for bonding, in addition to cleaning the surface. The good achievement of bond also relies on the relative humidity in the air. Epoxy mortar was used to fill the bigger cavities after having the surface even. Immediately after the final cleaning the epoxy was applied, so that the surface had no chance to get dirty again. The epoxy was applied as coned shape on the CFRP-strips. This shape has the advantage that when pressing the strip

against the beam, the maximum amount of air-bubbles was pushed out and that excellent adhesion is achieved.

The author had no experimental tests to verify his calculations. He assumed full compatibility at the ultimate stage of loading, which is shown later in the thesis to be incorrect. The author did not take any bond effect into consideration, which would probably mean that he has an error in his calculations.

Neubauer and Rostàzy (1996) suggested a design procedure for strengthening reinforced concrete beams and frames with Carbon Fibre Reinforced Plastic-plates (CFRP-strips or plates).

A truss analogy was used to determine a design for the beam (Figure 2.8). The first condition was to have enough concrete in the compression zone to equilibrate the tension in the plates. For equilibrium, extra external vertical reinforcement was the only possible solution to transfer the force from the compression zone to the plates on the bottom. The zone of the end anchor was of particular concern because the plates had to end before the supports.

This means the plates ended in a zone where $T \neq 0$. The bond length is usually a problem along this zone. The design procedure went through three phases:

1) Design for Bending.

2) Design for shear.

3) Design of the end anchor.

The design procedure used for bending is the same procedure used in conventional design for reinforced concrete. Some limitations, resulting from experimental results, for the strain were established by the authors in order to prevent separation of the plate from the concrete

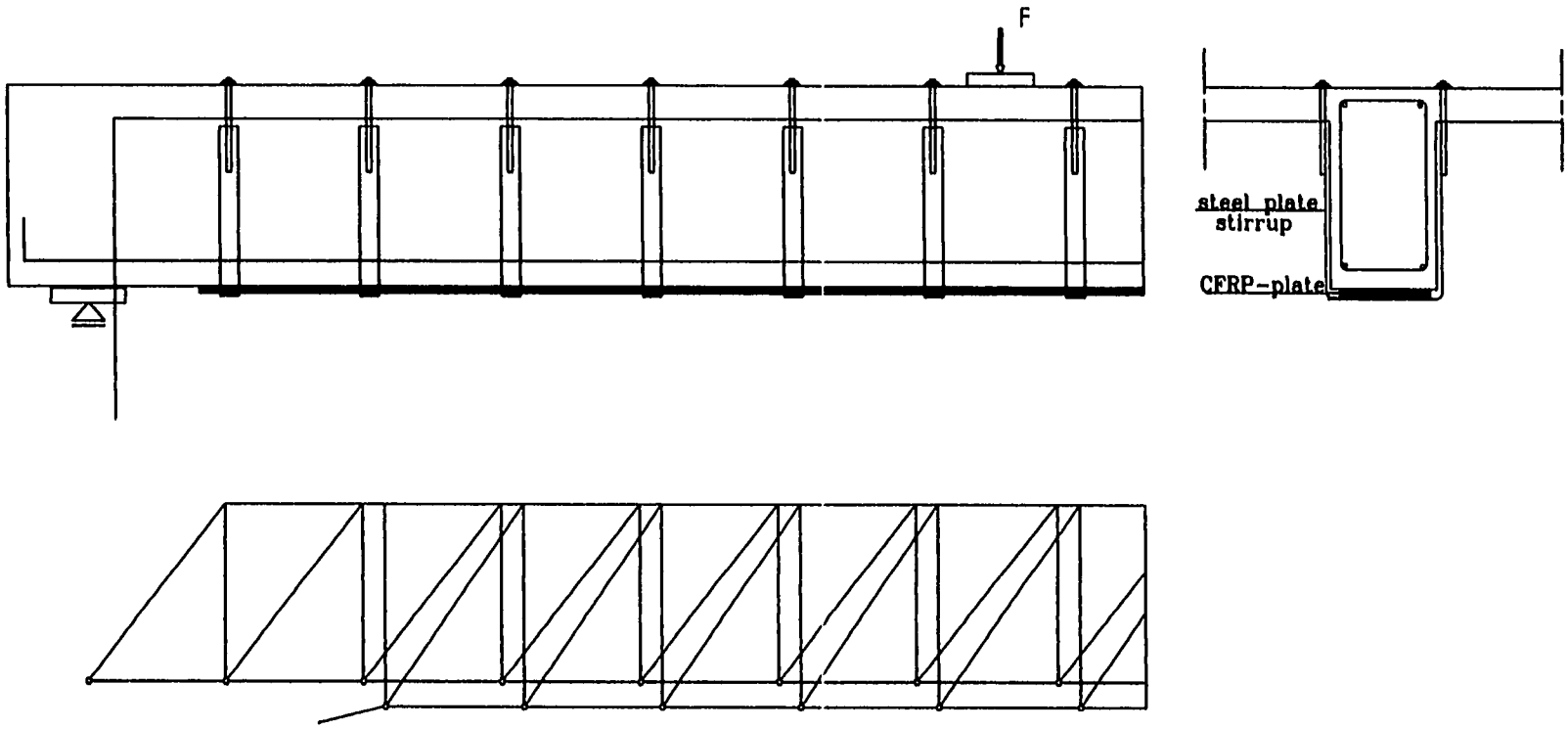

Figure 2. 8 Truss Model and Proposed Method of Rehabilitation

Neubauer and Rostàzy (1996)

at bending cracks and to avoid yielding of internal reinforcement at service loads. The ultimate strain in the CFRP-strip has to be limited by:

$$\varepsilon_{lu} \leq 5\varepsilon_{sy}$$

$$\varepsilon_{lu} \leq 0.5\varepsilon_{cu}$$

where the lower value applies. Other than that, the assumption of full strain compatibility, and the normal design method were used.

The design for shear followed conventional design methods in several ways as well, but even if the internal stirrups were enough to resist the whole shear of the beam, it was essential to have a set of external stirrups to have equilibrium for the outer CFRP-plates. The number and size of external stirrups have to be sufficient to resist tension transfer from the CFRP-plates.

The design of the plate end anchorage was of great concern as the plate end anchorage is the area where failure happened. Fifty one bond tests were done varying several parameters like bond length l_t, plate width b_l, plate thickness t_l and concrete cube strength f_{cc}. In all tests a sudden brittle failure occurred, but there was a big difference between the failure in concrete with lower f_{cc}, and the concrete with higher f_{cc}. With the lower strength concrete separation happened consistently. With the higher strength of concrete, a strange type of failure occurred, as the CFRP-plate tore off. However, the test results matched sufficiently "the engineering model of the bond strength of glued reinforcement for concrete members" made by Holzenkämpfer (1994). The equation used by Holzenkämpfer for the fracture energy needed to debond the glued reinforcement from the concrete is:

$$G_f = \int_0^{slo} \tau s_l \, ds_l \approx C_F \, f_{ctm}$$

Where C_F is a constant and f_{ctm} the concrete's surface tensile strength. This led to the equation of the maximum tensile force as well as the maximum effective bond length, after which the bond length does not have any effect on the fracture energy.

$$T_{max} = 0.4 k_b \, k_c \, b_l \sqrt{E_l \, t_l \, f_{ctm}}$$

$$l_{t\,max} = \sqrt{\frac{E_l \, t_l}{4 f_{ctm}}}$$

These were the equations concerning steel plates. With the same concept, only the constants of the equations change for CFRP-plates.

There are several applications for strengthening concrete structures with CFRP, but the author indicates that always in narrow deep elements (beams, frames etc.), the vertical steel reinforcement is essential to keep the beam in equilibrium.

Garden et al. (1997) worked on an experimental parametric study to decide the possibility of repairing RC-beams with CFRP-plates. A theoretical comparison between the CFRP-plates and the steel plate can be summarized in the following points: Steel plates have disadvantages (with respect to CFRP-plates) like transporting, handling and installing heavy plates, forming of joints due to limited delivery lengths, corrosion of plates, labor- and material intensive work during and after installation (curing time), lower strength to weight ratio and high maintenance costs.

Smaller beams in cross sectional area and span were used (100×100×1000 mm) to allow a higher number of beams to be tested. In the meantime a higher number of parameters can be changed. The parameters changed were the shear span/ depth ratio, the

composite plate aspect ratio and the type of anchorage used in the tests. Three series of beams were tested, as well as two control beams without composite plates on the bottom. A low tensile reinforcement ratio and a high shear reinforcement ratio were used to force the beams to fail in bending instead of the expected failure in shear due to the very short span.

Some important results were observed and conclusions drawn from the tests. In all plated cases, failure was accompanied by separation of concrete cover from internal reinforcement as shown in Figure 2.9. This type of failure means that the concrete itself, being the weakest material in the composite section, fails before the plate and the adhesive. The results also indicated that the anchorage system is a very important issue and the stronger the anchorage system is, the higher the capacity of the beam will be. It turned out that the highest capacity is reached with full anchorage of the plate between the plate and the supports, which is not practical in the field: beams would have to be jacked off their supports in order to place the strips between them and the support, which is expensive. Another important issue is the aspect ratio of the plate itself. It turns out that the thin wide plate develops a higher capacity in the beams than the thick narrow one (provided they have the same cross-sectional area). The composite action of the plates and the concrete was examined in the tests. Strain profiles were drawn and the plates generally produced a strain equal, or very nearly equal, to the strain in the bottom of the beam. The neutral axis position was noticed to be lower in plated beams than in unplated beams, which indicated a higher compression zone in the concrete to balance against the tension in the plated beams. Observing some results of shear forces at ends of anchored plates and comparing them with the calculations based on the elastic theory; it seemed that the elastic theory underestimates the bond stresses between the plate and the concrete. The author states that the failure due

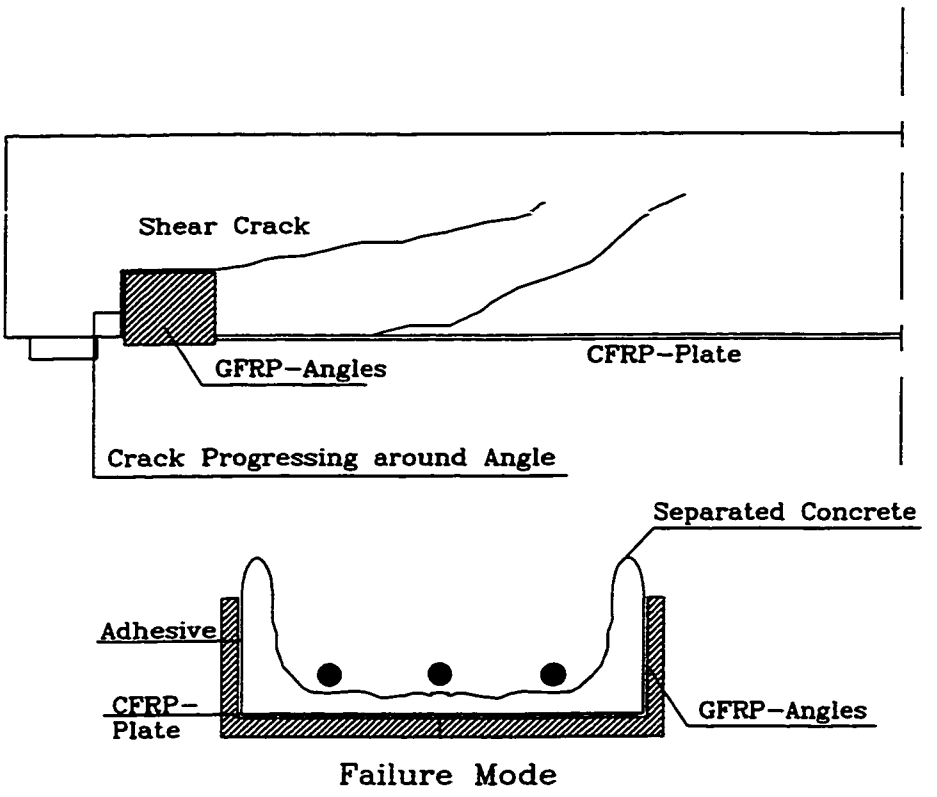

Figure 2.9 The End Anchorage and The Cracks at Failure, Garden et al. (1997)

to bond stresses would theoretically happen in the adherent itself because both interfaces (between the concrete and the adhesive and between the adhesive and the strip) have practically the same axial force on them.

The actual case was that the failure always happened in the concrete because the concrete was the weakest of the three materials. This programme of work indicated the important role of the end anchor to increase the failure load of the beams.

In general, the research programme recommended the use of CFRP-plates instead of steel plates in repair of R/C beams.

Norris, Saadatmanesh and Ehsani (1997) compared numerical computer analysis and laboratory testing to assess an approximate method for designing carbon fibre reinforced structures. Nineteen beams reinforced with steel and carbon fibre were tested under different flexure and shear loads. The main variables in the tests were the type of carbon fibre, the orientation of the fibres in relation to the axis of the beam, as well as the span of the beam and shear span. Some of the beams were cracked prior to applying the CF-sheets on them to simulate the case in the field.

The beams were analyzed based on the conventional theory of compatibility and the concrete compressive stress block. An approximate analysis of stresses and strains was conducted to compare with laboratory results.

The testing programme included 13 beams with a span of 2440 mm tested for flexure (Figure 2.10) and six beams with a span of 1220 mm tested for shear (Figure 2.11). There was a little difference between the various sorts of fibres used; the continuous fibre sheets behaved much like the stitched or the woven fabrics. There was no difference between the precracked beams and the uncracked ones at the ultimate level. The previous

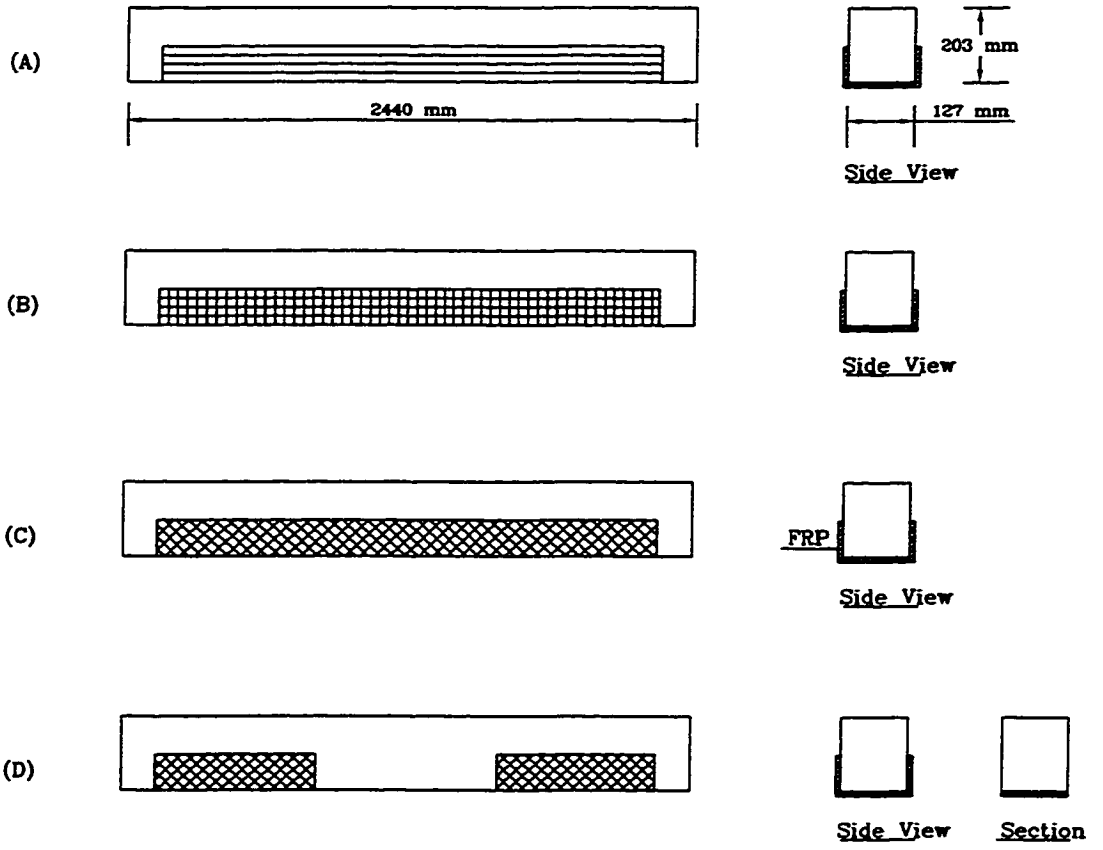

Figure 2.10 The Different Orientations of Fibres in Flexure Test

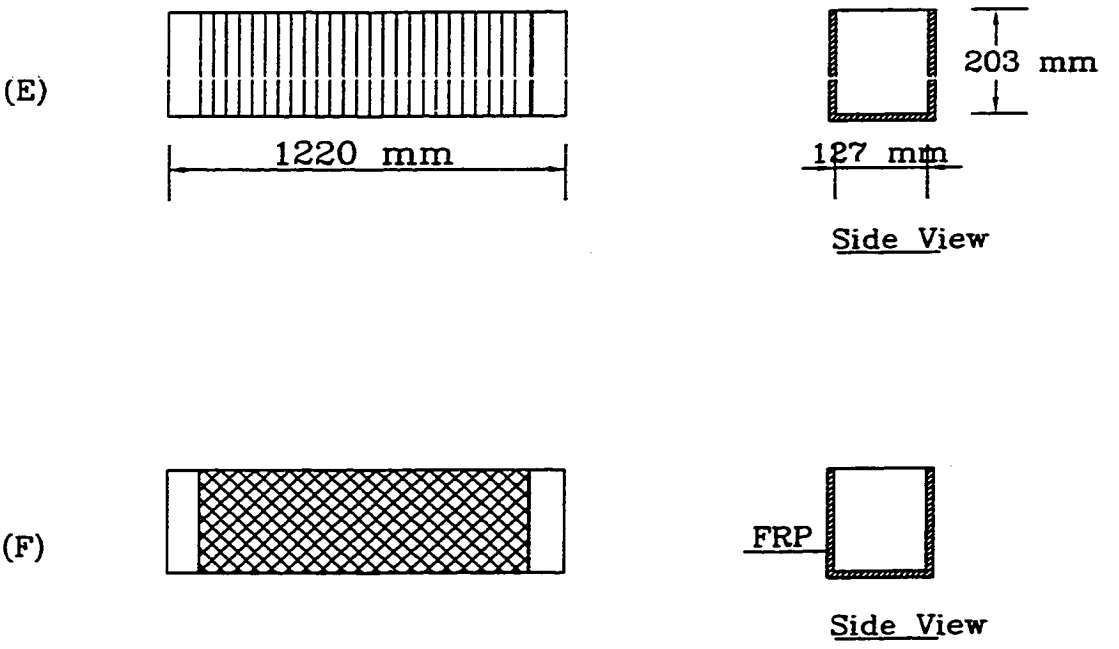

Figure 2.11 The Different Orientations of Fibre used in Shear Test

statement is logical because the beams were designed to have the same ultimate capacity. The most significant differences were due to various fibre orientations and web coverage systems. It was also proven, by comparing the stress in the steel reinforcing bars in the control beams and the retrofitted beams, that the steel was sharing forces with the carbon fibres in the retrofitted beams. The experimental work matched the analytical results well, which gave confidence in the method of design used. The most important conclusion was that an increase in strength and stiffness was seen in every specimen to which CFRP was applied, regardless of the fibre orientation. There was also a consistent, direct correlation seen between the magnitude of the increase in strength and the brittleness of failure. In both shear and flexural specimens, when the fibres were placed perpendicular to cracks in the beam, the result was higher stiffness with brittle failure caused by concrete rupture. Where double CFRP layers were used, the fibres placed transverse to the first layer tended to contain the fractured concrete, but the rupture was still abrupt because of the fibres perpendicular to the cracks. When fibres were placed obliquely to the cracks, the increase in stiffness was less and the mode of failure was more ductile. The ductile mode of failure was seen with the 45° fibres crossing flexural cracks and fibres placed vertically on the web across diagonal shear cracks. It was also noted that the magnitude of the increase was directly related to the development length of the fibres on both sides of the cracks.

Saeki, Shimura, Izumo and Horiguchi (1997) used more advanced technology in Japan. A series of beams was tested to determine the amount of strengthening the beams gained through using prestressed (uniaxial and biaxial) aramid-FRP sheets. The aim of the project was to decide whether to use these materials as prestressed materials to rehabilitate

damaged bridges in Japan. The results of the static experiments showed improvement in shear and flexure capacities as well as effectiveness in prestressing.

Three main modes of failure were expected and on that basis a series of 8 Tee-beams (span of 2500 mm and height of 300 mm) was chosen. The beams were expected to fail either in flexure (crushing in concrete), shear (yield in stirrups or in the wrapped sheets) or in peeling off by bond. The variables in these 8 concrete beams were the stirrups, the amount and alignment of the sheets, and the amount of artificial cracks made in the beams before testing. Some calculations were done prior to testing to predict the expected load at failure, and the mode of failure of each beam. At ultimate load in bending, the authors assumed full compatibility between the sheets and the concrete. A conventional method was used to calculate the strains in the elements. The effect of the sheets was considered in calculating the shear capacities of the beams. The truss model was used to calculate the forces in the stirrups and in the aramid sheets by assuming a crack angle of 45°. The aramid-FRP sheets were placed both vertically and horizontally to enhance the beams in bending and shear as well as to restrain crack propagation. By calculating the peeling capacity of the beams, the authors considered three different types of peeling cracks. Failure will either happen between the concrete and the epoxy, in the layer of epoxy itself, or inside the surface of the concrete, which was the case in these beams. This failure meant that the bond strength of the whole structure was equal to the shear strength of the concrete. To calculate the bond strength the author used an equation from the Japanese Society of Civil Engineers, (1986) as follows:

$$\tau_{ca} = 0.112 \times f_{ck}^{'\,2/3}$$

Where τ_{ca} is the bond stress.

The test results showed that the bending capacity of the beams was increased by about 24% with the use of a bonded prestressed aramid sheet of uniaxial texture and by about 17% by bending the sheet to a biaxial texture. The shear capacity was increased by 36% with the use of prestressed aramid sheets of biaxial texture. These results were very close to the expected values from calculations.

Hisabe et al. (1997) led another testing program in Japan, examining the enhancement of shear capacity of beams by applying CF-sheets. Reinforced concrete beams (150×250×2400 mm) with f_{cu}=35 MPa were used in the tests. 4 mm stirrups @150 mm and 3 D-22 reinforcing bars were used as steel reinforcement. Two layers of CF-sheets were applied each time, one with horizontal adherence and one with vertical adherence. Epoxy resin (non-solvent type) was used as an adhesive. A control specimen without CF-sheets reinforcement was tested first, followed by the rest of the series of beams. The main variables changed in the program were the height of CF-sheets and the anchorage of the sheets to the beams. Heights of 10, 15, 20 and 25 cm were tried as shown in Figure 2.12, as well as M-16 chemical anchorage or no anchorage at all. The last specimen (CF-sheets height = 25 cm) was totally wrapped with CF-sheets.

It was noted after the tests that the specimen, where no end anchors were used, had a CF-sheet peeling and maximum capacity occurred simultaneously. However, in the specimen where anchors were used to hold the CF-sheets the shear crack occurred along the plate and the concrete beam near the supports was cracked along the plate without the fracture and peeling. The last specimen (wrapped totally with CF-sheets) had failed in bending prior to shear failure.

Numerical results matched initial expectations that the higher the CF-sheets were glued the higher the load to cause shear cracking. The specimen, where anchors were used to fix the CF-sheets had larger values of maximum ultimate load than those with free ends for the same height of CF-sheets. Furthermore it was found that adhering the CF-sheet above the neutral axis caused the shear crack to be controlled and shear resistance to be increased.

Tests performed on prestressed concrete I-girders wrapped with CFRP-sheets by Drimoussis and Cheng (1994), Cheng, Hutchinson and Rizkalla (1997), were aimed at determining the increase in the shear strength of I-girders. Different types of sheets were applied at different locations and at different angles on the beams. In some tests the sheets were glued vertically on the webs of the beams, while in others the sheets were placed horizontally. Sheets were also applied at inclinations of 45 degrees, crossing each other. This latter configuration was found to give the maximum shear capacity for the P/C beams. The increases in capacity obtained were in the range from 9% to 56%. The main problem encountered was bond failure between the CFRP-sheets and the reinforced concrete.

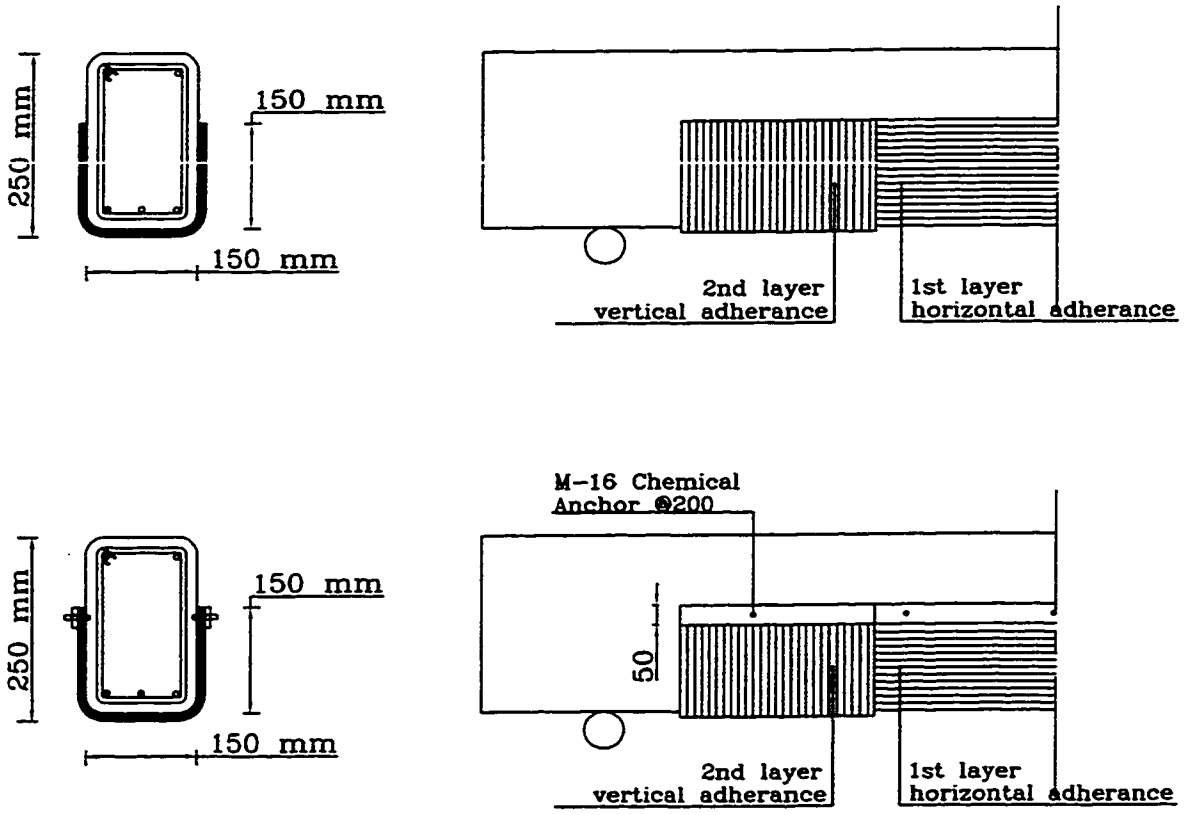

Figure 2.12 Alignment of CF-sheets in the Beams tested

Alexander and Cheng (1996), tested 3 full scale E-Type girders in shear after they were wrapped with CFRP-sheets. Sheets were wrapped vertically from the inner side of the beam's webs along the whole span. An eccentric loading system was used in the tests to obtain the maximum capacity of each web. The tests showed the shear capacity of the beams was increased by 21 to 55%. It was observed that the sheets had no effect on the failure mode, nor on the onset of inclined cracking. Four G-Type girders were therefore tested. These girders were described to be marginally weak in shear because of the increased truckloads over the years, and the changes in the shear design equations, which have now more strict measures than before. Under two-point loading the beams failed in flexure, so an eccentric loading system was used to fail the beams in shear. An increase of 21% in the shear capacity was gained by wrapping the webs with CFRP-sheets. This increase in strength was thought to occur through two main mechanisms. First, the sheets held the shear cracks together increasing the interface shear, and second the sheets also 'bridged' the shear cracks and transferred shear above these cracks, thus acting like external stirrups.

An existing bridge has also been rehabilitated with CFRP-sheets. The sheets were wrapped on the webs in two different manners; vertically throughout the whole length or vertically but with 50 mm spacing between the 250 mm wide sheets. This was done to assess the durability of the material under field conditions and to determine the actual cost of doing such work. Rehabilitation is being pursued further. Reinforced concrete bridge beams (G-Type) have been tested under eccentric loading to assess their flexural and shear capacities. Additional tests are scheduled with beams wrapped with CFRP- or GFRP-sheets, to see the effect of wrapping these beams with different materials.

2. 4 Different Applications of CFRP

The application of CFRP in civil engineering have not stopped at the rehabilitation and strengthening of existing beams in flexure or shear. CFRP has been used to reinforce newly built beams. CFRP-rods were manufactured to be tested and used in several areas in building or rehabilitation as well, because of the advantages they have (relatively light weight, no corrosion, easy to handle etc.). Other applications for CFRP are fabricated sections (L-shapes, C-shapes and I-shapes) to be used in the future in building trusses and portal frames.

A method of rehabilitation for reinforced concrete beams using CFRP-rods was suggested by Crasto et al. (1997). Composite rods, with adhesive, were embedded into grooves cut into the tensile face of the beam. 2.6 m long beams were cast. The cross-sectional area of the beams was 457 mm wide × 152 mm high. Four rectangular grooves 12.7 mm deep and 10.2 mm wide were machined into the tensile face of the beams. The rods (ϕ = 8 mm) were then embedded into the grooves with epoxy and were allowed to cure overnight. When tested in flexure, the beams showed results similar to those with equivalent cross-section area strengthened with CFRP-plates, but a less catastrophic failure happened at ultimate. With the rods, a concrete compression failure happened first, followed by a secondary failure in the composite (partial rod debonding and fracture).

Several disadvantages were described about the use of CFRP-plates versus the use of rods. The optimum bonding of plates requires careful and consistent surface preparation and the application of pressure during adhesive cure, to promote intimate contact between adhesive and adherents and to minimize voids. Free edge, residual and thermal stresses, with the environmental conditions can cause plate debonding and loss of reinforcing

capability over time. Also the plates cover the whole bottom face of the beam which prevents the drainage of water. The paper concludes that using CFRP-rods for rehabilitation is very promising and the use of FRP-rods would be a revolution in civil engineering in the near future.

In reviewing the work on fibre reinforced materials, it seems that the technology has progressed well and is now in a settled phase. Testing and field applications have been performed world-wide to determine the behaviour of the new material. The material, in most cases, has shown high performance, which makes it worth examining for use in the bridge rehabilitation in Alberta.

Up till now, only empirical design has been used. There have been some attempts to analyze the behaviour of composite materials, but solid and reliable design equations are still to be determined. Due to the fast developments in the field of composite materials and the numerous field applications, it is expected that the next bridge design code will include a chapter on the methods of design using CFRP-materials using the huge amount of data coming out of the tests.

2. 5 External Post-Tensioning

External post-tensioning is a safe, simple and economic method to enhance the flexural, as well as the shear-capacities of reinforced concrete structures. Many structures over the years have been rehabilitated using this method. Avoidance of severe cracks in flexure, elimination of large deflections, and replacement of corroded steel are among several other applications solved by adding post-tensioned bars/ strands to the structure. Experimental research, in most of the cases, has verified the various code methods to design beams prestressed with unbonded tendons. In a few cases researchers argue that the structure would lose a great amount of capacity due to lack of bond between concrete and bars.

Pisani and Nicoli (1996) interpret this confusion in the introduction of their work, quoting from Walter and Miehlbradt (1990), and Rozvany and Woods (1969) that the use of externally unbonded tendons does not increase the capacity of beams as calculated if no losses due to lack of bond are assumed. On the other hand Muller and Gauthier (1990), Naaman and Alkhairi (1991a, b) , and Mattock et al. (1971) among others state that there are no significant differences due to lack of bond in the external post-tensioning method.

To verify this last statement a numerical method is suggested by Pisani (1996): The numerical algorithm determines the displacements of each point along the beams for the concrete beams and for the tendon as well. At each step of loading of the beam the difference of the deflection between the tendons and the concrete can be determined. Several assumptions were made in this method: the shear deformations are neglected, provided there is adequate shear reinforcement in the beam, the tensile strength of concrete is neglected, and the creep effects are not included.

The results of this method were compared with 3 different experimental programmes, including 23 different tests. The different configurations of structures to be tested shown in Figure 2.13 included reinforced concrete rectangular beams, T-beams and slabs with unbonded prestressed tendons. In the experimental tests failure always occurred due to concrete crushing after yielding of the steel. Although the third group of tests (slabs) did not contain any unprestressed reinforcing steel, the slabs showed ductile behaviour, although this behaviour was not a consequence of yielding of reinforcement. (Some slabs behaved totally elastically and reverted to almost zero deflection after removal of the loads). The results of the three groups of tests showed the good level of precision attained by the mathematical model. The deflection as well as the maximum capacity were predicted by the model.

The third part of the paper was the numerical modeling of similar beams with external unbonded tendons. The results of the analysis showed that there is no difference when the beams were still behaving elastically. The reason for that is the high stiffness of the concrete substructure compared to the low levels of loading. When the unprestressed steel starts to yield, the externally prestressed beams are less stiff than the internally prestressed beams. At this stage the stiffness of the concrete substructure drops to low values, and the increase of the capacity of the beams is due to the increase in the tensile stress in the tendons. The internally prestressed tendons tend to behave as free cables subjected to distributed vertical loads, while the external tendons, because of their free movement in the vertical direction, keep their polygonal shape that follows the concrete deflections only where the deviators are located. The external tendons have therefore lower

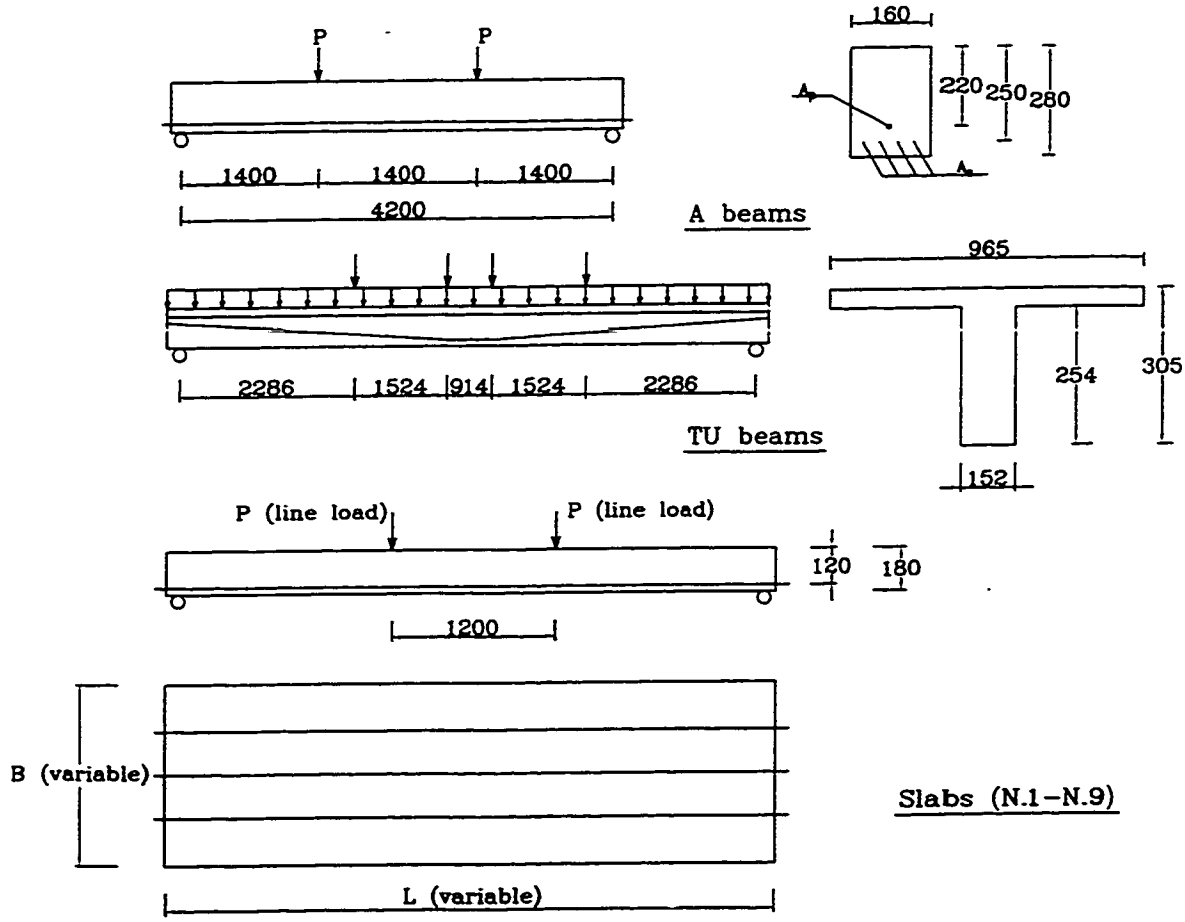

Figure 2.13 Experimental Verification of Mathematical Model

deflection for the same loading. The paper concludes that the capacity of the externally prestressed beams is less than the internally prestressed beams. However, the difference between the two methods is not significant.

In other analytic attempts, Iványi and Buschmeyer (1996a) worked on a design concept of strengthening bridge superstructures with external prestressing. The capacity of the beams prestressed with and without bond does not differ under service loads as was stated earlier by the same authors before (1996b). At the ultimate state there is a small difference in the capacity, which could be ignored when looking carefully at the costs of each method. The external post-tensioning to existing structures is a simple and economic way to enhance the strength of the structure.

Points to be considered in the design of external prestressing cables include corrosion protection, safe transfer of the prestressing forces to the bridge superstructure, and an easy to apply cable layout. Easy maintenance and inspection of the cables should be taken into consideration as well. Due to the experience the authors have in the field of external post-tensioning, there are two types of anchoring preferred in working as shown in Figure 2.14:

Method A: the cross beam anchorage, where the tendons are directly anchored to the end crossbeam. The end beam may need strengthening due to prestressing itself, to resist the tensile forces coming from the original prestressing.

Method B: the anchor block, where the prestressing tendons are anchored to a concrete block, cast in the vicinity of the beam end. The concrete block is then fixed to the beam with prestressing bars.

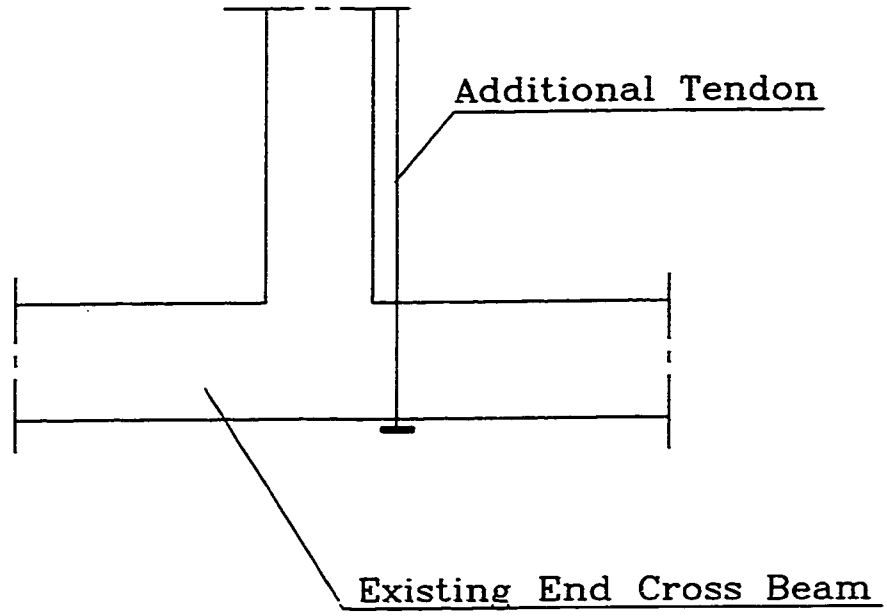

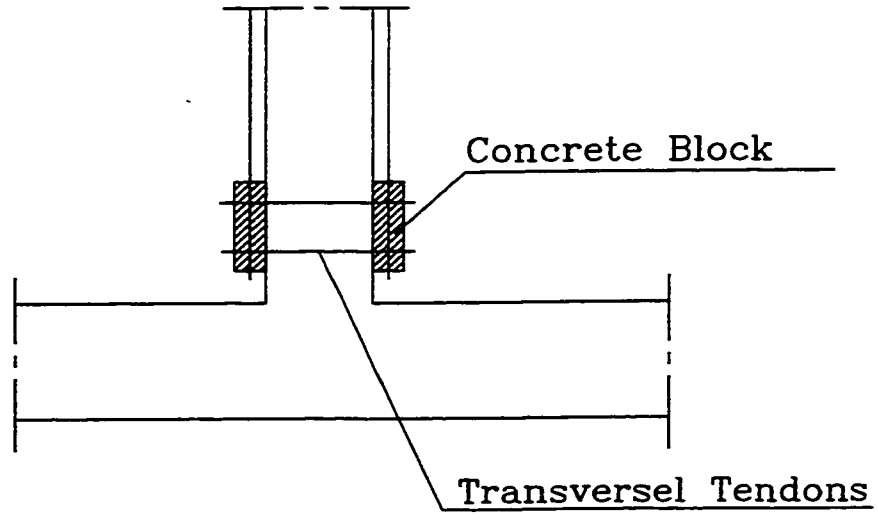

Figure 2.14 Different Types of Anchors as suggested by Iványi and Buschmeyer (1996)

The paper concludes by giving details of some bridges strengthened using this design concept, which have been monitored to verify the success of the method of external post-tensioning.

Some practical cases for using external post-tensioning in strengthening concrete structures were mentioned by Shawwaf (1996). An example of his work is the Won Hyo Bridge in Seoul, Korea. The bridge contained 10 main spans of 100 m, and 2 end spans of 60 m. The cross-section of the bridge was a twin cell post-tensioned concrete box girder. The deck width is 20 m and the depth varies between 6 m at the pier to 2.1 m at the midspans. The bridge was constructed using the cantilever method, containing a hinge at the midspan of each girder. Some years after the completion of construction, it was noticed that the girders were sagging at the midspan hinges. The sagging varied between 5 and 20 cm. The repair of the bridge involved adding 12 external DYWIDAG tendons of 19-0.6 strands each to the girders. The strands were anchored to a concrete block cast next to the webs of the box girders and prestressed with 36 mm DYWIDAG bars to the web. The concrete block was to guarantee the transfer of forces from the tendons to the bridge. Precautions were taken to ensure that the tendons would not corrode: the strands were placed in polyethelene pipes and were cement-grouted after stressing. By this method, the bridge was cambered to its normal level. The bridge is now successfully resisting full live loading without any further sagging.

Another practical example was done by Robson and Craig (1996). A bridge in the United Kingdom was constructed in the mid seventies. The bridge contained 50 m main spans , and 20 m end spans. The bridge was originally a post-tensioned structure and its cross-section was a single box section. The problems encountered in the bridge in 1994

were that two prestressing tendons had failed, and individual wire failure was encountered in other tendons. The tendons were mainly corroded at the anchors or deflectors, where no cementitious grout was used.

Several solutions were suggested, but the most reliable solution was to replace the old tendons with new ones, providing good protection from corrosion for the tendons. Two kinds of prestress were applied; temporary prestress, to ensure that the cracks did not develop between the precast members until the permanent prestress was applied, and permanent prestress, to guarantee the safety of the bridge under live and dead loads. The bridge is expected to act safely after this project is finished.

In conclusion there are two possible methods of rehabilitation to increase the strength and improve durability of the beams: using CFRP-sheets/ strips or external post-tensioning. Using CFRP-sheets/ strips was proven to be efficient in some projects, although there are some problems such as anchorage to prevent end-delamination: and the creep of the epoxies needs to be determined. More research work is needed to develop a rational design procedure. As for external post-tensioning, the procedures and design are well established.

This thesis will concentrate in examining these methods to rehabilitate a certain type of girder in Alberta. These girders have deeper webs than those previously rehabilitated with CFRP. A rational design procedure will be used to predict the increases in the strength from both methods of rehabilitation.

CHAPTER 3

DESCRIPTION OF TEST FRAME AND INITIAL TESTING PROGRAMME

3. 1 Introduction

Examination of the literature has shown that certain features of deteriorating reinforced concrete beams are important for strength. Hence the current state of the beams involved in this project was assessed with emphasis on those features: the geometry of the beams, the material properties, the cracks in the webs, the state of the diaphragms and the state of the deck. Initial calculations regarding the flexural and shear capacities of the beams were made.

Two different test arrangements were developed. The main arrangement was used to test all the large beams under flexural, shear and cyclic loads. Two different loading rams were used depending on the maximum expected load in the tests. A completely different test system (the small frame) was used to perform flexural tests on three other beams. These latter tests did not need to be performed in the main test frame, as the beams were smaller in span and needed less load capacity.

3. 2 Current State of Bridge Beams

The project involved testing 8 precast reinforced concrete HC-type beams. The length of the beams was 11.6 m: the cross section is shown in Figure 3.1. Each beam had two diaphragms, one on each end. Non-destructive tests were performed with a Schmidt

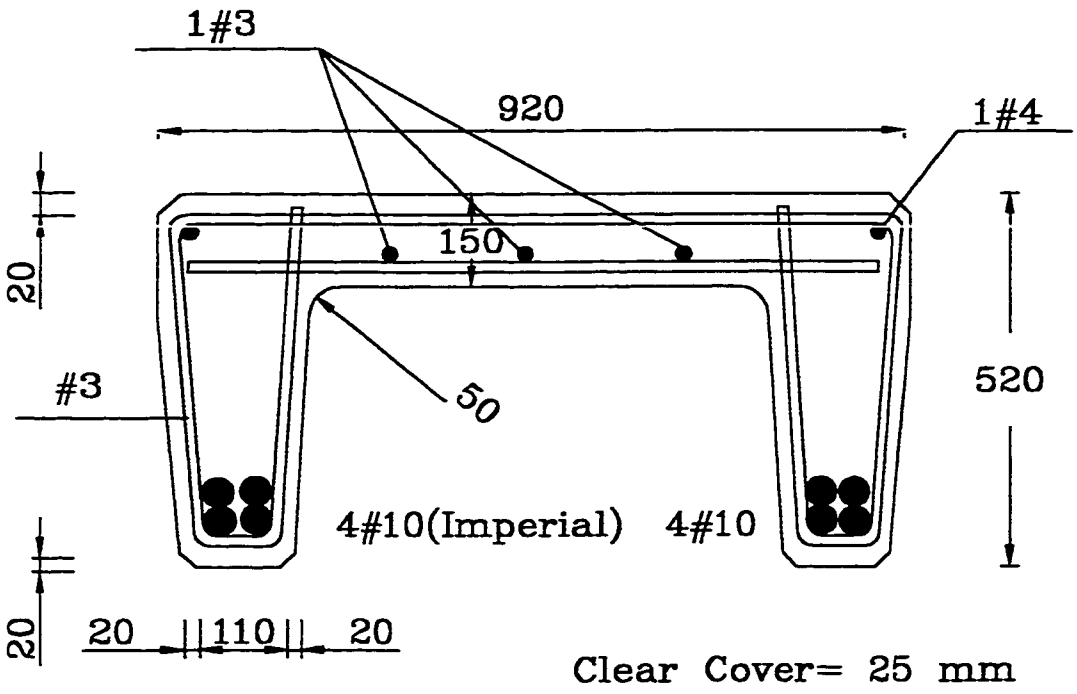

Figure 3.1 Girder HC-Type

For Strirrup Spacing see Figure 3.9

hammer to determine the strength of the concrete. Readings varied between 35 and 45 MPa. Cores extracted after the flexural and shear tests, indicated that the strength of the concrete was 45-55 MPa. Tensile testing of the reinforcing bars revealed the steel yield strength to be about 350 MPa.

The beams were inspected visually (amount of exposed steel, depth of exposure, number of shear cracks, number of bond cracks, width of cracks and condition of stirrups). It was expected that these inspections would suggest which bridge girders were weaker /stronger.

The visual inspection provided the following pieces of information. The diaphragms were badly damaged during bridge dismantling because their reinforcement was light. There was exposed steel in most of the webs. The depths of exposure varied between 20 mm to almost 150 mm, the greater exposure typically being in midspan. There was obvious rust on the steel and some stirrups were broken. Bond cracks were visible at the ends of the beams, most probably because of steel rusting as well. There were no obvious shear cracks or flexure cracks. Some webs were patched with relatively new patching, but it seemed very weakly bonded to the original concrete. Figures 3.2 and 3.3 give an example of one beam visually inspected, and show the cracks and the exposure of the steel reinforcement.

3. 3 Initial Calculations

Initial calculations of the flexural resistance and expected deflection at failure of an undamaged beam with the cross-section as already shown in Figure 3.1 were made to ensure the testing apparatus was adequate for the tests. Also, these calculations provided a

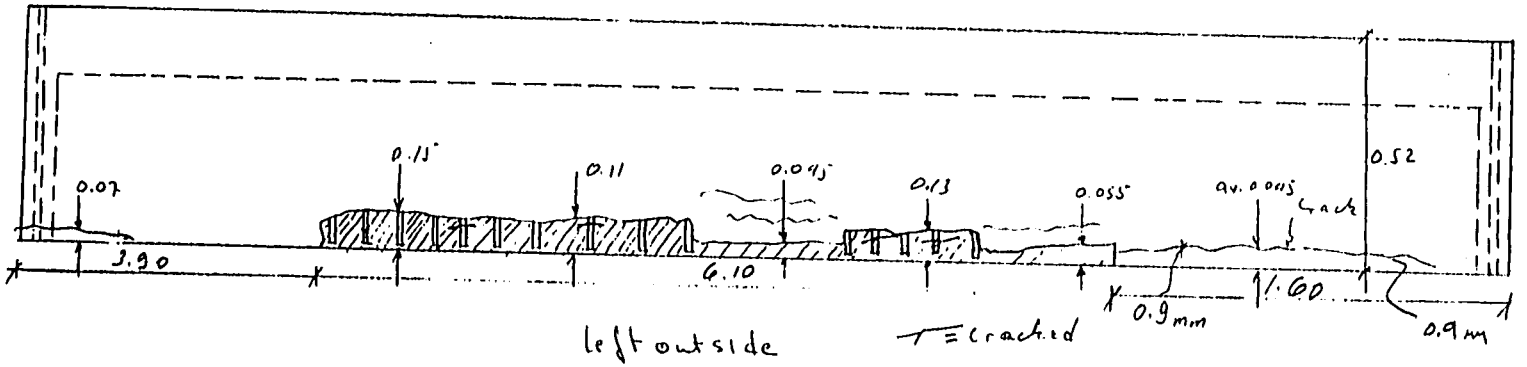

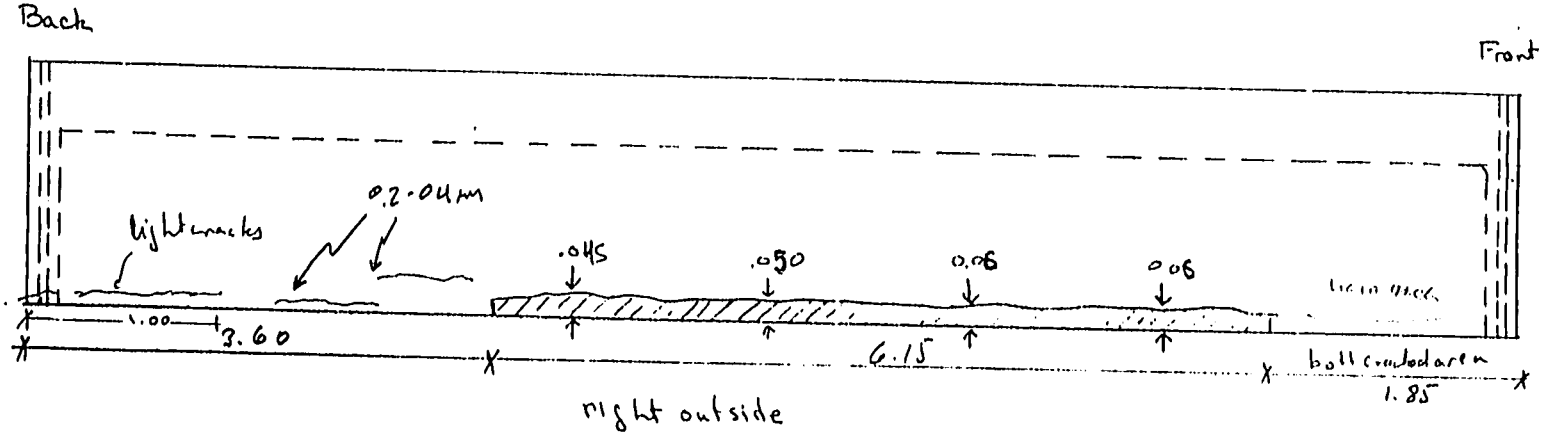

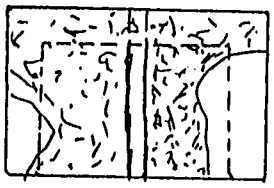

Back Diaphragm
(not bad)

NOTE① DEPTH OF BEAM IS 508m ON PLAN BUT AVERAGES ABOUT 520m IN ACTUALITY. 520m WAS USED IN DETERMINING DEPTH OF SPALLING.

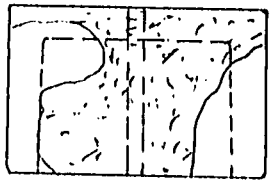

Front Diaphragm

Figure 3.2 Visual Inspection of Beam B4

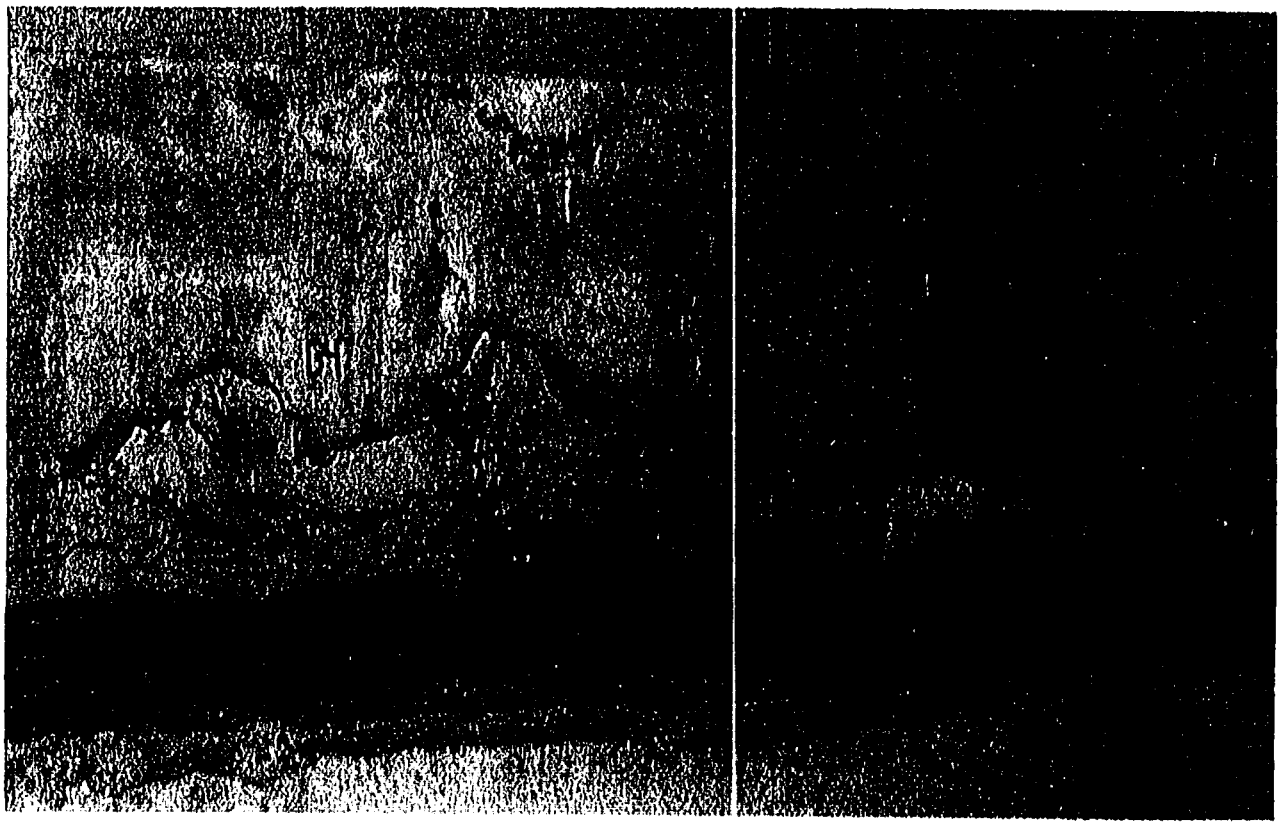

Figure 3.3 The Current Condition of the Beam

reference point for the results of the tests. Calculations of the actual resistance of the beams are included as well.

3.3. 1 Flexure

The non-destructive tests performed with the Schmidt hammer to determine the strength of the concrete provided results, which varied between 35 and 45 MPa so an average value of 40 MPa was used in the calculations. Resistance was calculated based on CSA-A23.3-94. The maximum flexural capacity was found to be 786 kN·m, which converts with the span and loading conditions to a maximum applied load of 338 kN.

3.3. 2 Deflection

The deflection corresponding to a maximum elastic moment in the beam of 338 kN·m was calculated using the method of virtual work. The modulus of elasticity of the concrete and the effective moment of inertia were estimated according to CSA Standard A23.3-94. The deflection at yield was calculated to be 42 mm.

3.3. 3 Shear

Using the general method of the CSA Standard A23.3-94 the angle of shear cracking was calculated to be 36°. The shear capacity was estimated to be 380 kN at the critical section of the girder, which converts, with the span and loading conditions of the shear test, to a maximum applied load of 500 kN. The simplified method was used to verify the results from the general method, and similar results were calculated.

3.3. 4Required Capacity

The design truckloads according to the CHBDC, as suggested by Dorton (1994), are shown in Figure 3.4. The maximum moment due to live load was calculated from several trials by the use of influence lines. As the width of the specified truck in the Code is 1.80 m

while the width of the beams was only 0.92 m, only one-half of the axle load was used to calculate the moment. As seen in Figure 3.4 there are two alternatives to calculate the moment: either to take the full axle load (1), or to take 64 % of the wheel load in addition to a certain uniform live load.

The calculations showed that the second alternative is the more critical one. The maximum moment calculated for live load only was:

$$M_{L.L.} = 376\,kN \cdot m$$

The moment of the dead load of the beam was calculated as well:

$$w_{O.W.} = 60\,kN = 5.2\,kN/m$$

$$w_{F.C.} = 0.8\,kN/m$$

$$M_{D.L.} = \frac{(5.2+0.8)\times 11.6^2}{8} = 101\,kN \cdot m$$

The total factored moment of the beam (including impact effect):

$$M_f = 1.25\times 101 + 1.5\times 1.3\times 376 = 860\,kN \cdot m$$

This is the required ultimate capacity of each bridge girder.

3. 4 Test Frame

3.4. 1 Main Test Frame

The main testing arrangement was primarily built for the testing of the beams in their condition before testing. The testing arrangement was made containing the following items: the loading frame, the loading system (ram, distribution beams, and connectors and spacers), the measuring equipment and the supporting system (Figure. 3.5). Due to the tight spacing in the laboratory a special supporting element had to be designed. The test span

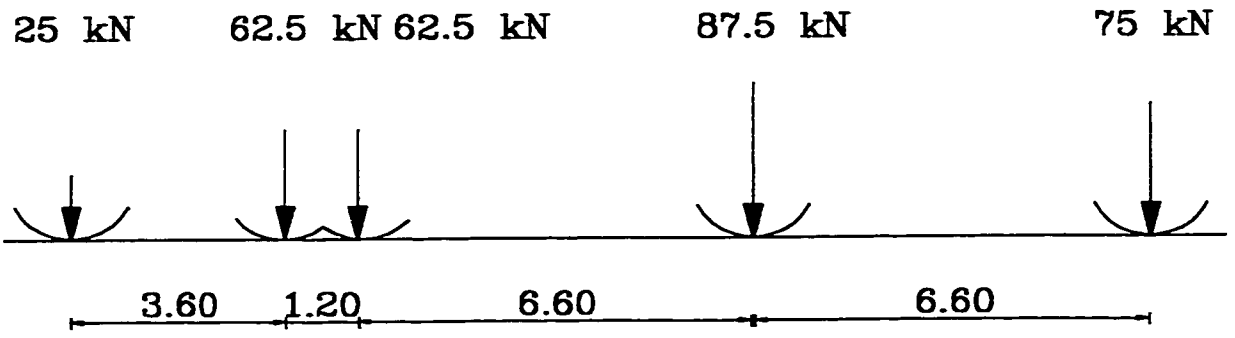

(1)

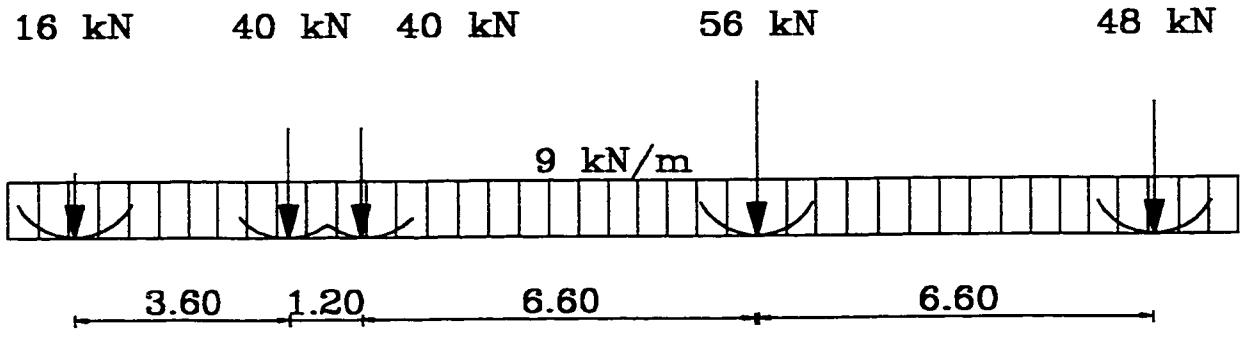

(2)

Figure 3. 4 Truck loads as specified in the CHBDC

was 10.5 m (beam length 11.6 m). The loading frame was centred at mid-span, with the load being applied to each web of the beam at two points 600 mm from the centerline in each direction. The simply supported beams were thus loaded at four points (two on each web) 1200 mm apart simulating the distance between truck wheels as specified in the Canadian Highway and Bridge Design Code. The loading results in a zone of constant moment over the mid-span. It was therefore possible to measure strains and deflections in more than one spot in the critical moment zone. The following components will be discussed in detail:

Loading frame.

Loading system.

Measuring equipment.

Supporting System.

3.4.1. 1 Loading Frame

The steel loading frame spans 2500 mm, with a clear height of 3300 mm. The steel frame was checked under the maximum loading capacity of the ram. All components of the steel frame were found safe under the maximum load of the ram.

3.4.1. 2 Loading System

The loading rams

A closed-loop electro-hydraulic loading ram with a maximum capacity of 500 kN, working with hydraulic oil pressure of maximum 20.7 MPa was calibrated to a maximum error of ± 2.5 kN and used in the initial flexure and cyclic tests. Tests were stroke controlled to avoid catastrophic failure of the beams. A load cell with 1500 kN capacity was calibrated to a maximum error of ± 2.5 kN and attached to the ram actuator to measure

the applied load on the beam, and a hemi-spherical seat with a maximum capacity of 600 kN was added to the load cell to ensure centrality of load relative to the ram. For the shear tests, as well as the tests after repair, a greater load capacity was needed. Therefore, an Enerpac hydraulic loading ram was used. The 2000 kN double acting ram operated by an electric power pump. These tests were controlled by observation of the operator, as there was no automatic control on the machine. The same load cell was used, but a spherical seat with a greater capacity (1000 kN) was put into the system.

The load distribution beams

An H-grid was manufactured out of three I-beams W 200×59 as shown in Figure 3.6. The distribution beams applied loads at four points on the beam two on each web. The beams were designed to resist the maximum load of the loading ram. For the tests with the Enerpac machine, the grid was redesigned and the top I-beam was welded to a similar section, while stiffeners were added to the bottom beams.

Load connectors and spacers (above I-beams)

Because the actuator had only 150 mm stroke, spacers were added just before the test to maximize the stroke which would be applied to the specimen. These were chosen as steel plates (150 mm× 150 mm) with about 20 mm thickness each. A teflon plate greased with vaseline was put on top of a thin stainless steel plate on the top I-beam to ensure that there was no eccentric loading on the loading ram.

Load connectors (underneath I-beams)

4 sets of neoprene pads were used, with one set at each loading point. Each set contained 4 pads 150×130×12.5 mm, which were stacked alternately with three 0.5 mm stainless steel plates. The steel plates ensure little lateral deformation of the stacks.

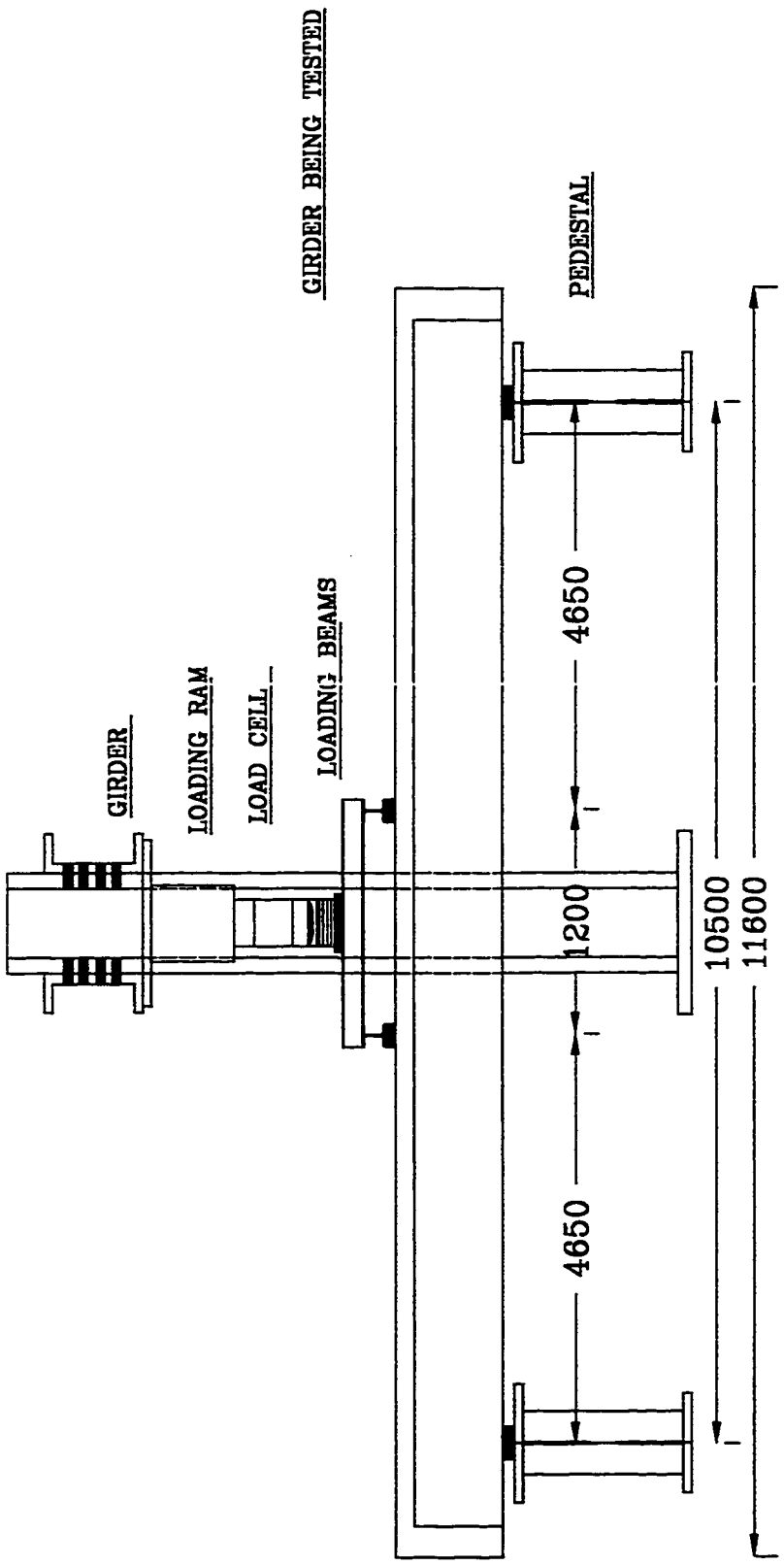

Figure 3.5 Arrangement of Test Frame

3.4.1. 3 The Measuring Equipment

Throughout the tests several types of measurement were made. One hundred mm Linear Strain Conversion Transducers (LSCs) were calibrated to a maximum error of ± 0.5 mm and used to measure the vertical deflection of the beams. For the horizontal deflection 25 mm LSCs were used, as the expected horizontal movement was small. The 25 mm LSCs were calibrated to a maximum error of ± 0.125 mm. Steel strain gauges were glued to the reinforcing steel and the CFRP-sheets/ strips for measuring strain. To measure compressive strain in the concrete, 50 mm long concrete strain gauges were used to be less sensitive to the irregularities in the concrete and to be more representative to the behaviour of concrete. The gauges were single axis electric gauges with 120 Ω resistance. LSCs were used to measure the strain on the tension side of the concrete, as strain gauges would become disfunctional once the concrete started cracking.

3.4.1. 4 Error Analysis

A simplified error analysis has been conducted to estimate the maximum possible error in the bending moments. Several factors were taken into consideration while calculating the error. One of the most important factors was the maximum possible error in estimating the self weight of the beams. The self weight of the beams was roughly estimated to be 60 kN, based on the cross-sectional area and the length given by Alberta Transportation and a unit weight of concrete of 24 kN/m^3. As there were several parts fallen off the webs, and the unit weight was not experimentally validated, a maximum estimated error of ± 4 % (2.4 kN) should be considered. The errors provided by the readings of the load cell were taken into consideration as well. The load cell was calibrated to a maximum error of ± 2.5 kN.

The "simulation method" was used to determine the maximum error in the calculated bending moment. The bending moment is a function of the total self weight W and concentrated applied load P, thus the error of the bending moment will be a function of the errors of W and P using the same equation.

$$M = 2.3P + 1.4W$$

The previous equation would give a maximum estimated error of ± 10 kN · m in the readings of the moments. As will be shown, this value would be around ± 1% of the values of the calculated moments.

3.4.1. 5 The Supporting System

Load cells of maximum capacity of 300 kN were placed under each corner of the bridge girder under test. These load cells measured the load transmitted down to the supporting pedestals (Figure 3.7). To accommodate geometric irregularities due to the deformed state and the non-uniformity of the bottom of the bridge girders, 150×150×12.5 mm neoprene pads were put on top of the load cells. The neoprene pads were reinforced with thin steel plates as in the loading system. Sometimes a steel-shim was needed under one or two corners to ensure stability of the girder during testing.

Pedestals

Two different types of pedestal were used. At one end of the beam the standard laboratory pedestals (Figure 3.7a) would not fit. Another pedestal therefore had to be designed and fabricated to support the two webs of the beam (Figure 3.7b). The pedestal was designed to hold more than the maximum expected reaction on each web with minimum deformation, so that it would not affect the test results. The pedestals, as well as

the loading frame, were bolted to the loading floor by 750 mm long 50 mm diameter anchor bolts to ensure safety.

3.4. 2 Smaller Test Frame

For the smaller beams the Amsler beam-testing machine was used. The Amsler machine is a frame with a built-in loading ram with a capacity of 2000 kN and built-in supporting elements, which can be adjusted anywhere from 100 mm to 2600 mm in span. The frame was set to a test span of 2000 mm with the load applied in the midspan. Load was distributed through an I-beam to two points on the beam, 250 mm apart. The tests performed were stroke controlled.

3. 5 Initial Testing Programme

Two beams were chosen from a total of 11 beams in the lab. The choice was mainly based on the results of the visual inspection, trying to choose the beams in the "best" condition (no rust in steel reinforcement, good web condition, no broken stirrups), and the beam in the "worst" condition. The choice was made in order to determine the range of capacities of the beams, if any.

3.5. 1 Flexural Testing

Test 1:

The first flexural test was performed on the beam considered to be in the best condition. The test span was 10.5 m (beam length 11.6 m). Strain gauges were put on the conrete slab, while the vertical deflection was measured at midspan. Initial load increments were 50 kN with readings taken every 10 kN but after 300 kN the beam was loaded to failure. The beam was inspected after each load increment. Failure occurred at 360 kN in a web which had been previously repaired. The mortar of the patch seemed to be weakly

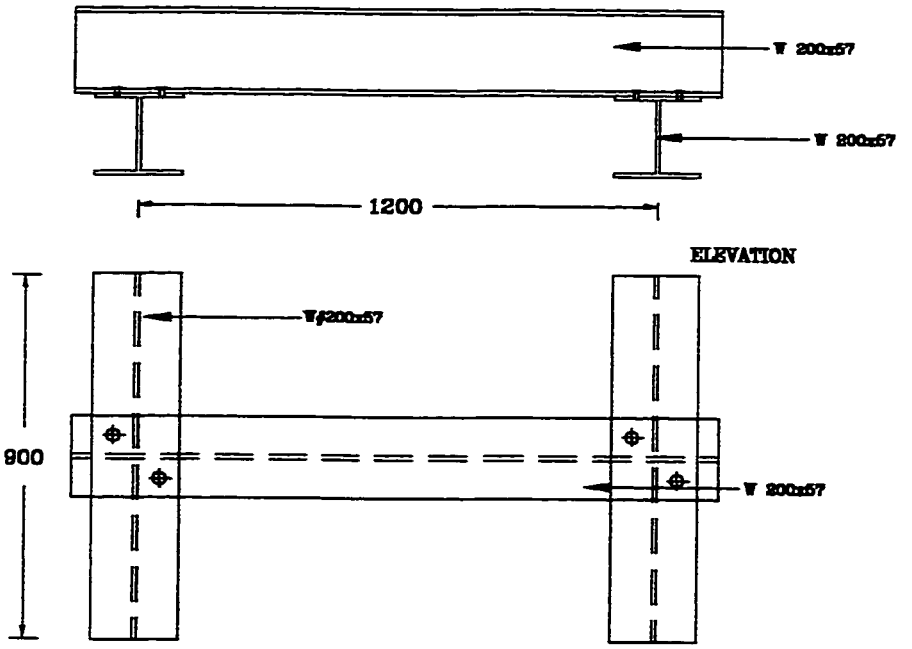

Figure 3.6 The H-Grid Loading System

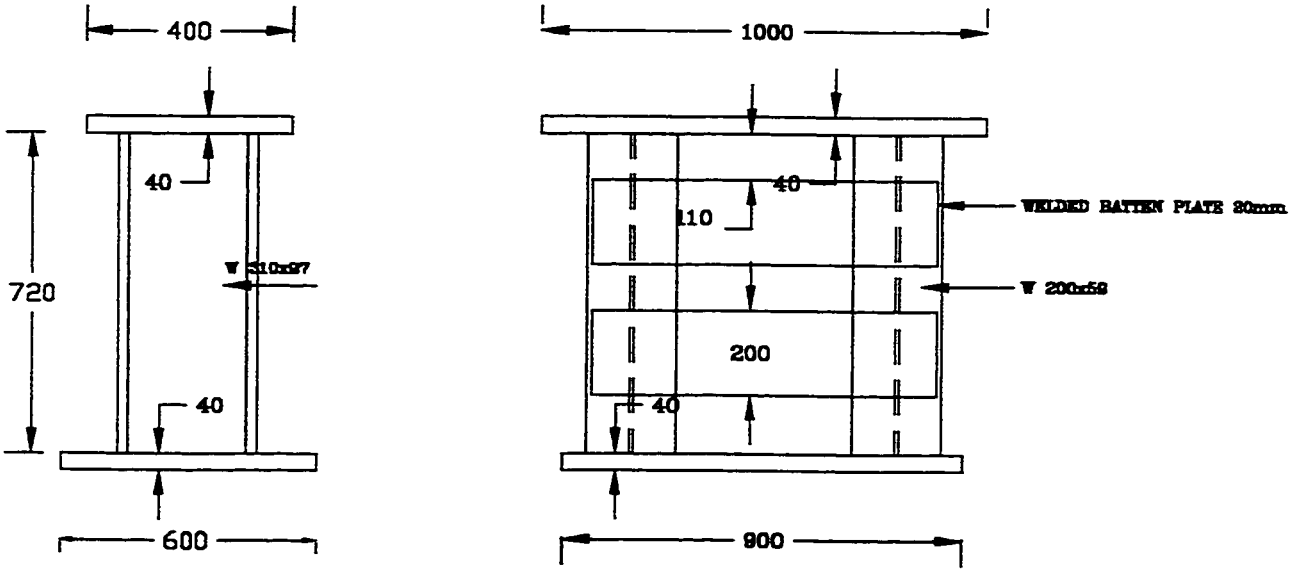

Figure 3.7 a. Existing Pedestal, b. Designed Pedestal

bonded to the original concrete. At the large deflections near maximum moment, pieces of the patch fell away, revealing corroded reinforcement. The test was stopped after the tension steel yielded and some of the concrete in the compression zone started to crush, but prior to total collapse. This allowed the same beam to be tested in shear. The permanent deflection of the beam after unloading was 75 mm. Only strain in the concrete was measured because there was no exposed steel on which to put gauges. The reactions at the four support points were measured as well.

Test 2:

The beam deemed to be in the worst condition was also tested in flexure. This beam had severe cracks all along its span, the steel was exposed and rusted, and some stirrups near the mid-span were rusted through. The configuration of the frame, the loading ram and test sequence that was used in the first test was repeated. Yield occurred at 352 kN, with wide flexural cracks at the mid-span in the bottom of the webs. Again the beam was not loaded to total collapse, so it also could be tested in shear. The permanent deflection of the beam after unloading was 80 mm. The strain in the concrete, the strain in the exposed steel, vertical and horizontal deflections and the reactions at the four supported points were measured.

3.5. 2 Shear Testing

Test 3:

Based on the compression field theory, the angle of the plane of failure in shear (θ) was calculated to be 36 degrees, providing a calculated shear span of about 760 mm. This span was increased to 1150 mm for the shear tests, while the total span under load was 8500 mm as shown in Figure 3.8. The same loading system was used as before with the

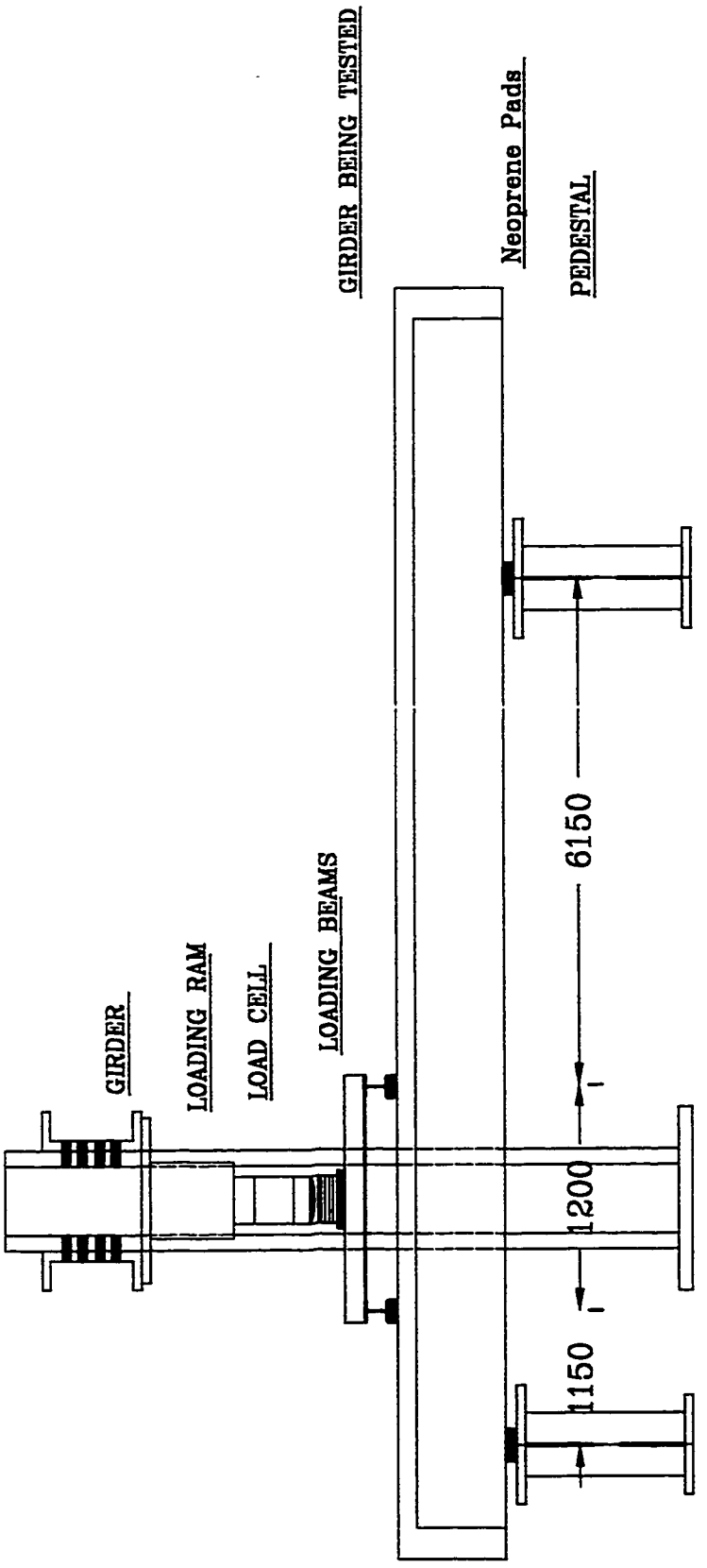

Figure 3.8 Arrangement of Shear Tests

loading ram was now 1750 mm away from the end diaphragm. With the spreader beam, the loading points closest to the end of the beam were thus only 1150 mm away from the diaphragm. There was no sign of distress even when the actuator had achieved its maximum capacity at 475 kN. This load implies a reaction at the end diaphragm of 371 kN, slightly less than the estimated shear capacity. The shear capacity of the girders therefore appeared to be higher than their flexural capacity for the loading condition applied. Deflection was measured at the point of maximum moment and the reactions were measured at the critical end only.

Test 4:

The second shear test was on the second beam. In order to increase the reaction at the end of interest, the overall span was decreased to 8000 mm and the whole load was applied 1150 mm from the end under test. The maximum reaction on the end of interest in this configuration was calculated to be 400 kN. Before the end of the test a crack parallel to the tension reinforcement developed in one web. The crack appeared to be either a bearing failure or the extension of a pre-existing bond crack (the concrete cover fell away at this crack). A few small diagonal tension cracks appeared but seemed to be incidental to the failure: more load was needed for a pure shear failure. This result confirms that the shear capacity of the girders is higher than the flexural capacity. As in the previous shear test, deflection was measured at the point of maximum moment and the reactions were measured at the critical end only.

Test 5:

The type of failure in test 4 raised a major concern. Was there bearing failure because the load cells had a smaller bearing area under the web compared to the actual

bearing area used in-situ? It would have been pointless to rehabilitate the girders to resist more shear and flexure if they would fail in bearing at the supports.

Using the same configuration as test 4, the second end of the first beam was tested to check its bearing capacity. This time the in-situ end conditions were simulated by placing a steel W 200x59 with 150 mm wide neopreane pad under the end-diaphragms instead of using two concentrated supports (the two load-cells). This had the positive effect of distributing the load along the whole length of the end diaphragm, reducing the effect of "point" loads on the two webs. The beam was loaded until the actuator reached its maximum capacity (475 kN) without any serious effects on the end-diaphragm of the beam. No failure occurred under this loading, with only a few minor cracks appearing.

Test 6:

After tests 4 and 5 it became clear that the maximum capacity of the actuator produces a shear force less than the total shear capacity of the girders. The Enerpac jack with a capacity of 2000 kN was used to determine the actual shear resistance of the bridge girders. The testing arrangement was changed to accommodate this actuator. The second end of the first beam (considered to be in the "best" condition: same end as in test 5) was tested under the same configuration as tests 4 and 5. The beam was loaded directly to failure. Yield developed at 600 kN, and failure occurred at 645 kN. The reaction at the tested end was therefore 544 kN. At first, the cover spalled off at a previously marked bond crack. Two major cracks then developed in each web. The first crack began to propagate from the end of the bond crack, which was approximately at the end of the last curtailed reinforcing bar (Figure 3.9, 3.10). The second crack propagated from the bottom of the

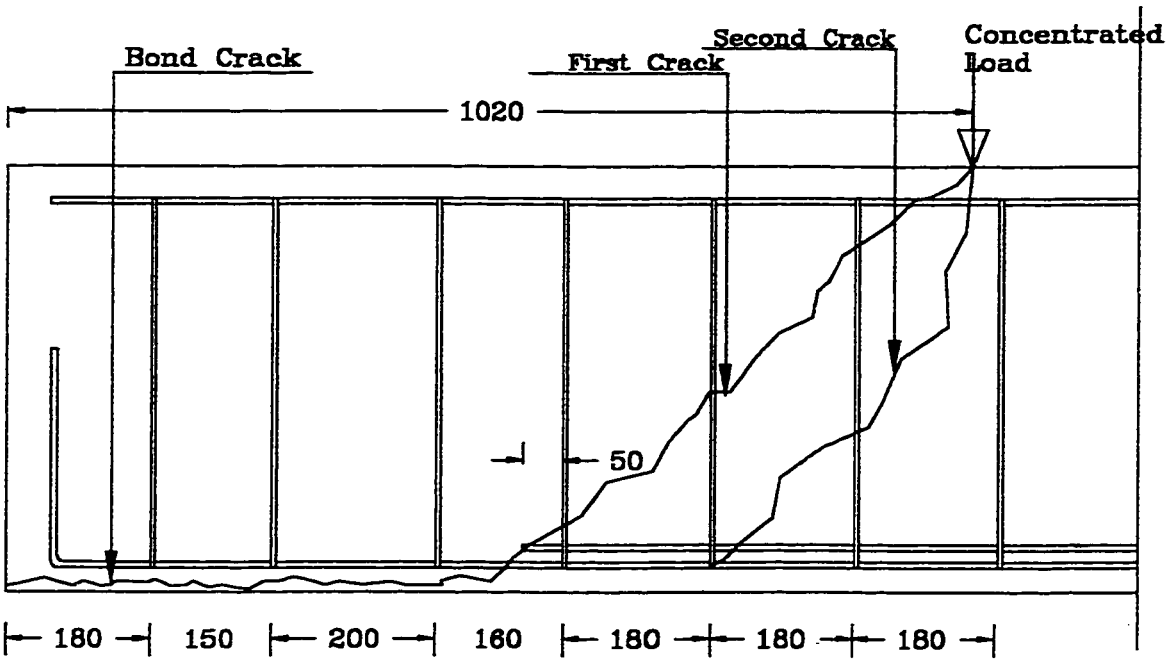

Figure 3.9 Crack Pattern at Failure after Shear

Showing Cracks in Relation to Tensile Reinforcement and Stirrups

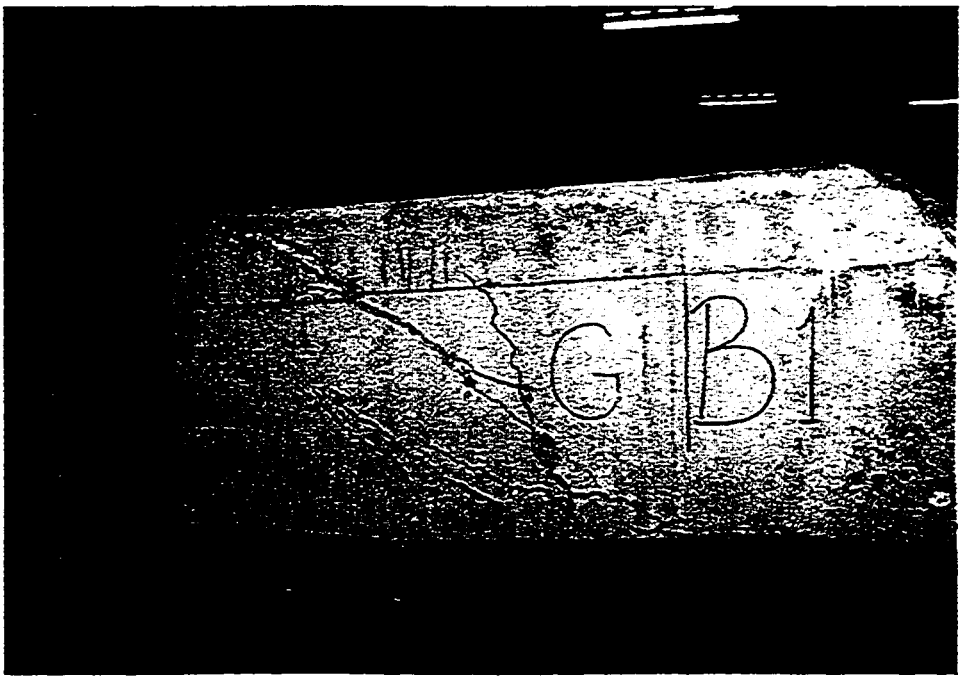

Figure 3.10 Cracks after Shear Test as in Figure 3.9

third stirrup and met the first crack at the point of application of the concentrated load. Compression failure began in the top flange of the beam and the test was stopped.

Test 7:

The same procedure was used for the second end of the second beam ("worst" condition). Surprisingly failure occurred at a higher load (665 kN) with a reaction of 561 kN at the tested end. The same propagation of cracks was noticed, together with a compression failure.

The major results of the tests are summarized in Table3.1.

BEAM	Best	Worst
Cover	Mostly Existing	Mostly Spalled off
Tested span in flexure	10500 mm	10500 mm
Max. flexural load	360 kN	352 kN
Max. vertical deflection	94.6 mm	94.3 mm
Max. permanent deflection	75 mm	80 mm
Tested span in shear	8000 mm	8000 mm
Max. shear load	645 kN	665 kN

Table 3.1 Summary of Major Results of the Tests

3. 6 Results and Discussion

In test 1 the vertical deflections were larger than expected by calculation (42 mm at yield) as shown in Figure 3.11, but there was no significant difference between the two webs due to the initial deformed shapes of the beam. The beam yielded at about 330 kN with rapidly increasing deflection until the test was stopped. The reactions indicated that there were differences between the four supporting points due to a torsional moment that happened because the webs had different levels at testing. The difference between the maximum and the minimum reaction was about 10% (see Figure 3.12). There was a slight increase in the reactions of the webs with less damage near the end of the test. No obvious compression failure occurred, but the readings in the strain gauges on the concrete increased very quickly after about 90% of the maximum load was reached (Figure 3.13).

The test 2 results were very similar to those of test 1, with a slight reduction in the deflection readings (Figure 3.14). Figure 3.15 shows the steel strain at mid-span, which could be measured on the second beam with its exposed steel at mid-span. These strains support the results obtained from the concrete gauges and indicate yielding in the steel at a load of 340 kN.

The results of the bending tests were within the expected range from the initial calculations, whereas the shear results were substantially higher than calculated with the shear equations. Shear friction theory (Loov R. E. 1997) was therefore used to analyze the beams. The calculations involved reasonable assumptions on the spacing of the stirrups, the yield strength of the steel, the bond length of the steel and the ultimate compressive strength of the concrete. The theory provided an estimated maximum load of 568 kN, which meant that the actual loads were 13% to 17% higher than predicted. The theory

correctly predicted that the critical zone would be at the end of the last curtailed reinforcing bar, which was the case in all four webs tested. The second crack that occurred from the bottom of the fourth stirrup matched the shear friction theory as well. In the theory, possible planes of failure are checked. A free body diagram is drawn of each plane of failure, and equilibrium demanded, involving the amount of tension steel, the amount of stirrups and the angle of the plane (θ).

At this stage some conclusions were drawn: the flexural strength of the girders is only about 60% of the shear strength. An increase in the flexural capacity would be more advisable than increasing the already good shear capacity. Bearing failure is not likely to occur because the site conditions for bearing are much better than the experimental arrangement. It was noticed that there was no big difference between the beam that was thought to be in a good shape and the one that was thought to be in a bad shape. It seemed that the rust apparent in the beams had not penetrated in the reinforcing bars deeply and the concrete, which fell from the bottom of the webs was not carrying loads because it was under tension and only acting as a cover. As a result, it was decided to deal with all beams in the same way except where there was severe damage and obvious cracking.

As the tests indicated the need to increase the flexural capacity of the beams, the testing programme continued with the focus on this point. The idea of gluing Carbon Fibre Reinforced Polymer (CFRP)-strips to the soffits of the beams after patching them seemed at this stage to be one potential solution. Another solution was to post-tension the beams using DYWIDAG-bars. Both solutions were studied in detail. The governing factors in preferring one over the other would be the total cost and effectiveness of each solution.

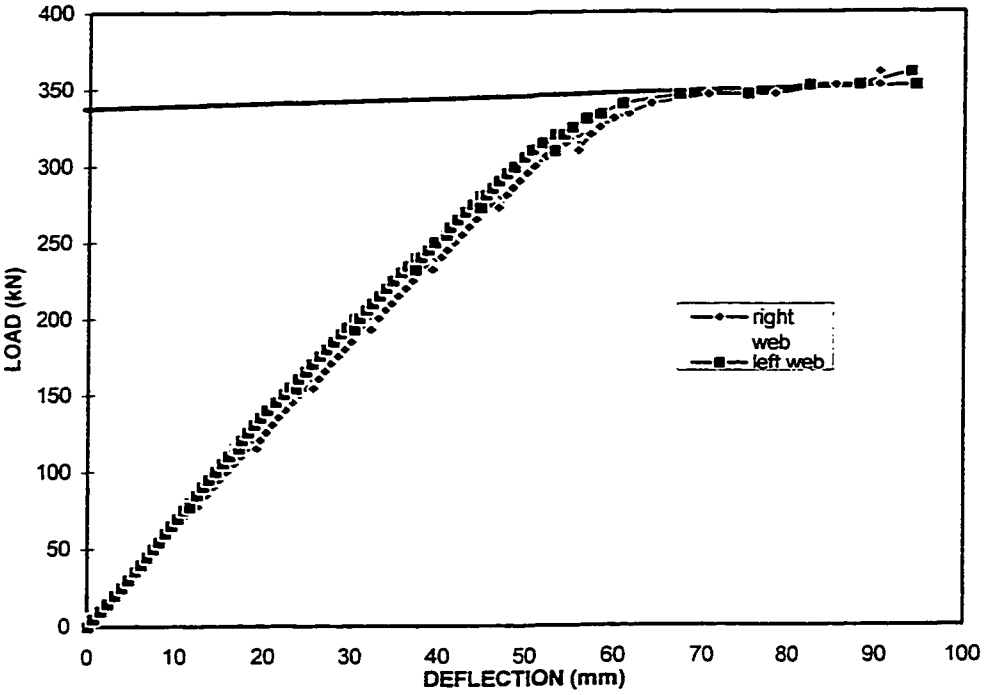

Figure 3.11 Deflection at Mid-span of the Good Beam; Flexural Test

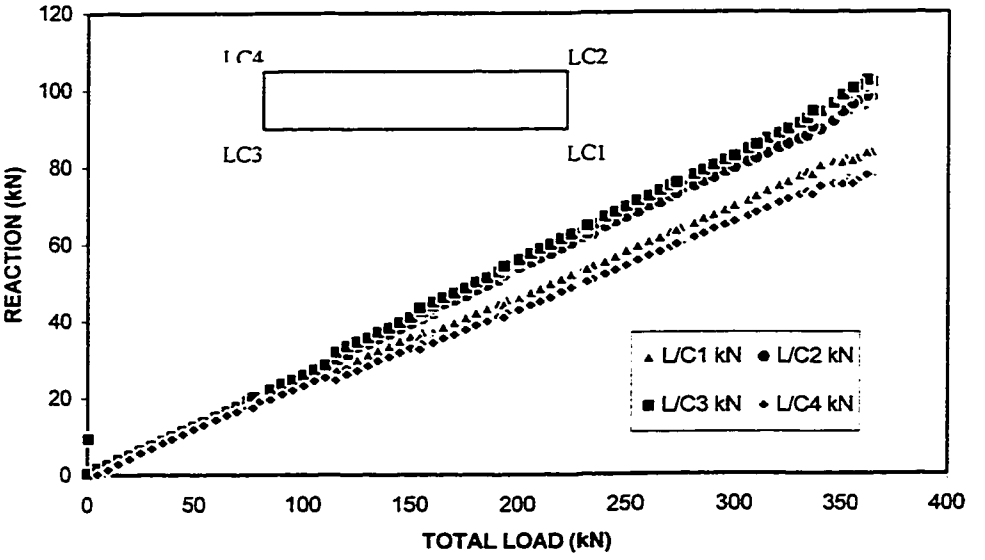

Figure 3.12 Reactions under each Web of the Good Beam; Flexural Test

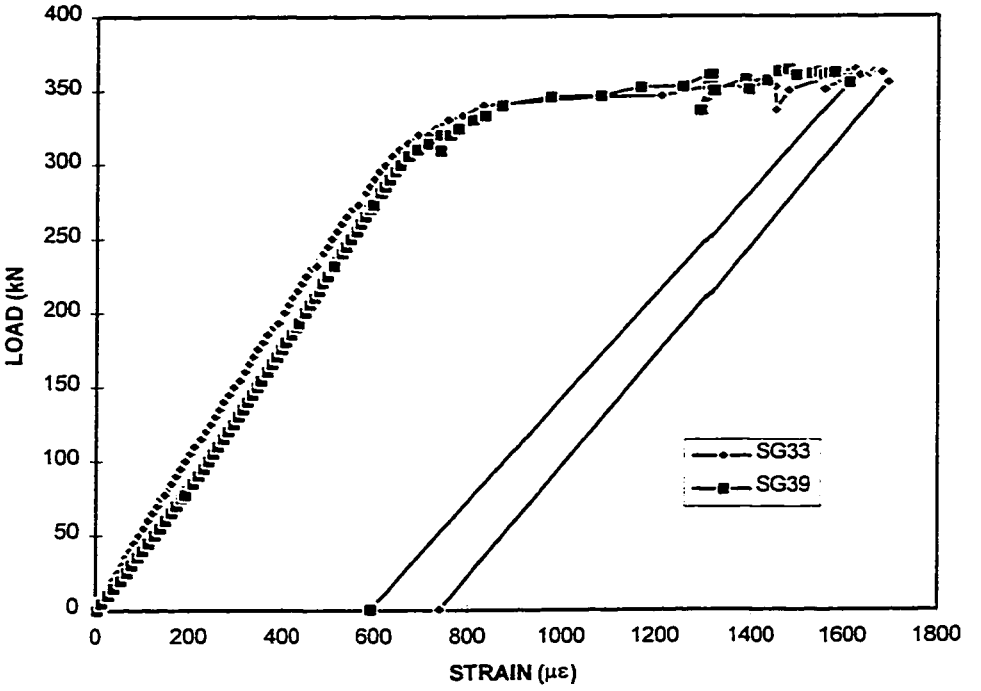

Figure 3.13 Strain measured in the Concrete on Top of the Good Beam; Flexural Test

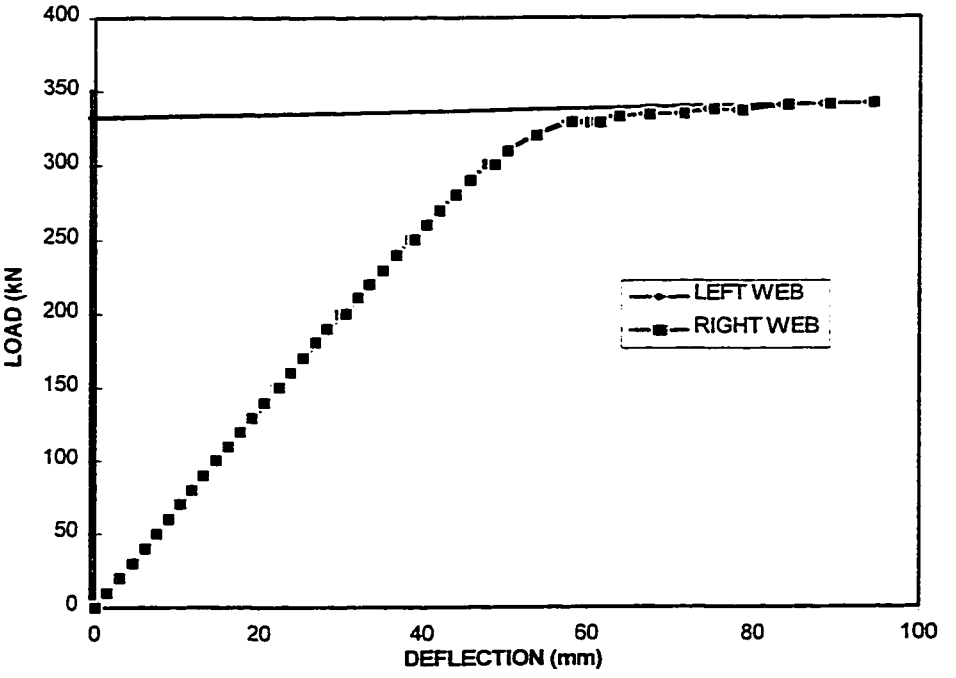

Figure 3.14 Deflection at Mid-span of Worst Beam; Flexural Test

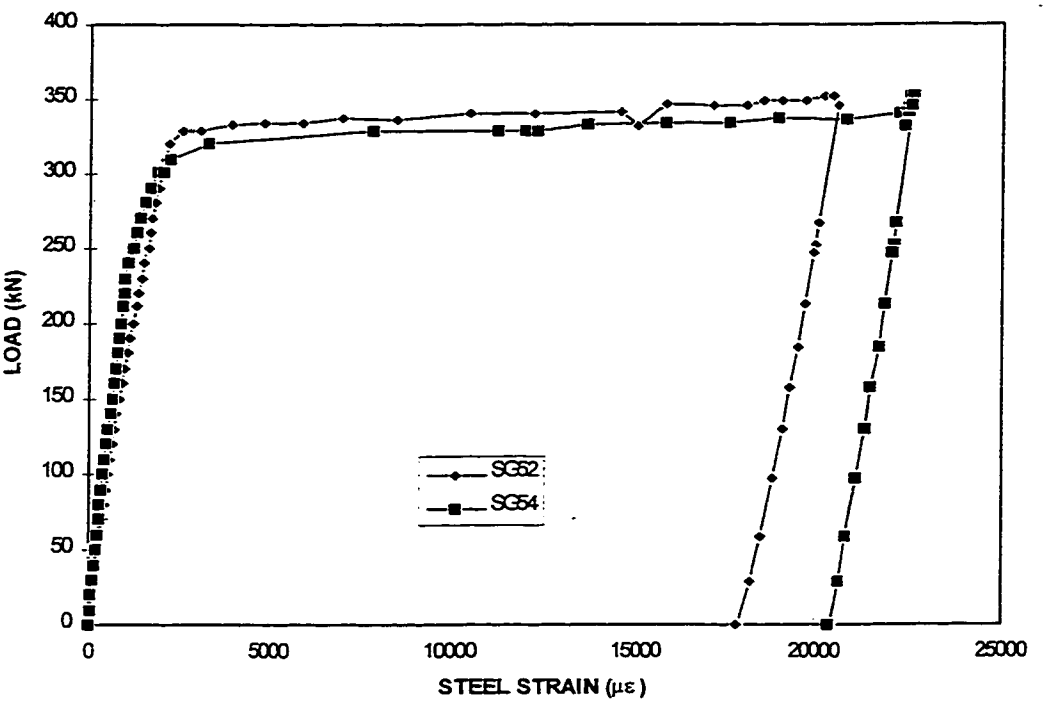

Figure 3.15 Strain Measured on the Bottom Steel of the Worst Beam; Flexural Test

CHAPTER 4

CFRP TESTING AND RESULTS

4. 1 Introduction

After the actual capacity of the beams had been verified, the need for rehabilitation and improved flexural capacity became evident. Four beams were therefore moved to an open yard to be patched with concrete mortar, and then brought back to the laboratory to be strengthened with CFRP-sheets/strips.

The testing programme for the rehabilitated beams, and an initial mathematical model to predict the beam's flexural capacity will be described. An important part of the programme was testing the beams under cyclic loading, as bridge beams are mainly subjected to moving loads. Two cyclic tests were performed on two beams in order to test the durability of different kinds of patching mortar, while the other two beams were subjected to a series of flexure and shear tests.

Analysis of a truss model provided an understanding of the mechanism of failure of the beams in flexure.

The need for some other tests to verify the truss model was obvious. Three other smaller beams with ateratCFRP-strips were therefore also tested. The results suggesteb a need for further research in this direction.

The results of all these tests indicated that for these beams, other means than CFRP would be required to provide the desired increase in strength.

4. 2 Bridge Girders under Static Loads

4.2. 1 Objective

The main goals of applying the CFRP-strips/sheets were to find an easy and economic way to enhance the strength of the beams in flexure. The use of the CFRP-strips seemed to be an easy to apply solution, which had the advantage of not being labour intensive. An additional benefit would be the ability to rehabilitate a bridge without interfering with the traffic on top of the bridges, which would avoid delays in work, and save money to the traffic department by not needing to provide detours. CFRP-strips applied to the soffits of the beams were intended to act as an external reinforcement to increase the capacity of the beams more than 24 %.

CFRP-sheets were wrapped at the ends of the webs on a 45° angle. The main goals of wrapping CFRP-sheets at the ends of the beams were to strengthen the girders in shear and give an appropriate anchor to the strips resisting flexure. The concept of applying sheets/strips is shown in Figure 4.1 and Figure 4.2. It was obvious from former work done on the strips that the two main problems needing consideration are the bond between the epoxy and the concrete and the anchorage at the end. The tensile strength of these strips is always high enough not to cause tensile failure in the strips.

4.2. 2 Properties of Materials Used in Rehabilitation

The materials used to enhance the capacity of the beams were "Sika Carbodur S1012" CFRP-strips and Mitsubishi CFRP-sheets. Each of these two different kinds of material has to be defined and its properties have to be known. The two materials were preliminarily used in the aerospace and automotive fields because of their high strength to weight ratio, durability and ability to form complex shapes. Carbon fibres have a very high elastic

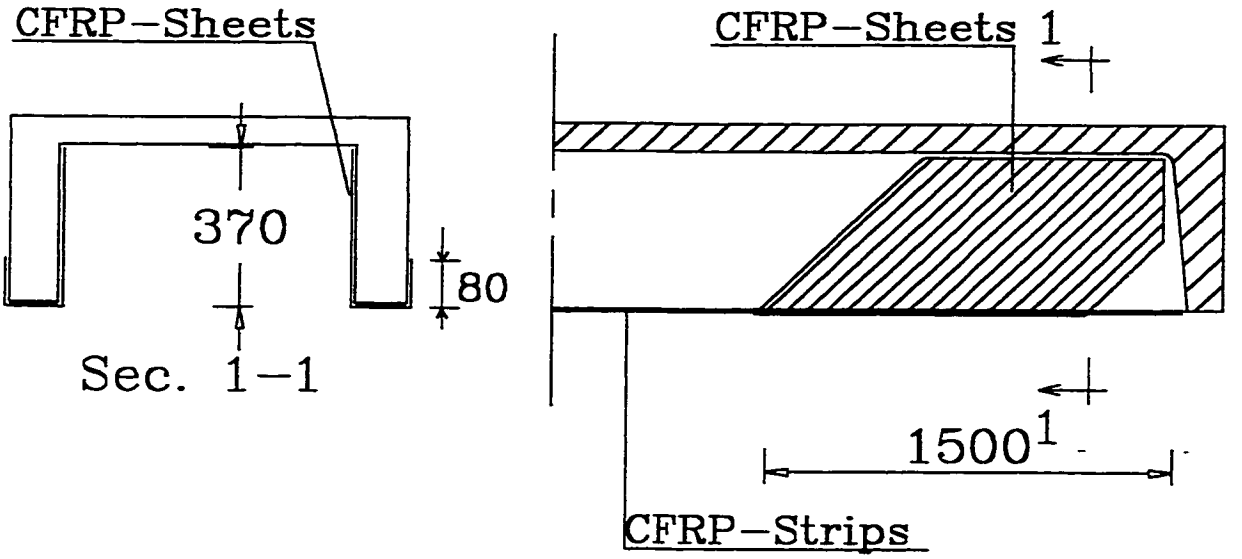

Figure 4. 1 Schematic Showing CFRP-Sheets/ Strips on the Beam (Dimensions in mm)

Figure 4. 2 Repaired Beam Ready for Testing

modulus and high strength in both tension and compression. The CFRP-strips consist of 60-70 % of unidirectional carbon fibers with an approximate diameter of 8 μm; these are embedded in an epoxy resin matrix. The Young's modulus of various carbon fibre types ranges from 240-900 GPa, and the tensile strength of the unidirectional carbon fibres is about 2000-7000 MPa. The CFRP-strips are over 1.2 mm in thickness, so they cannot be wrapped around the webs as easily as the 0.12 mm thick sheets. The main applications of the strips are in beams and slabs to enhance the flexural capacities of the structural members: and the Sika-strips are easy to apply in straight lengths. The sheets are more flexible, which is why the sheets can be used for wrapping columns for confinement or beams to enhance both shear and flexural capacities. Mechanical properties of the CFRP-strips/ sheets are given in Table 4.1, as provided by the manufacturers. These mechanical properties were not verified through experiment, since failure of the beams was not dependent on them. Tests for properties like bond strength and creep of the epoxy under shear need to be developed in the future, as such properties would be helpful for design.

	Sika Carbodur	Mitsubishi Replark
Modulus of Elasticity*	155 GPa	230 GPa
Tensile Strength*	2.4 GPa	3.4 GPa
Elongation at Break*	1.90%	
Thickness	1.2 mm	0.1 mm
Width	100 mm	250 mm
Length of Roll	250 m	25 m

* Mechanical value obtained from longitudinal direction of fibres

Table 4.1 Mechanical Properties of CFRP-Strips/Sheets

4.2. 3 Mathematical Model

4.2.3. 1 Utilizing CFRP-strips to Enhance Flexural Capacity

A mathematical model similar to the one introduced by Norris et al. (1997), based on strain compatibility between the steel, concrete and CFRP-strips is used to estimate the flexural capacity of the beams. The properties of the different materials used were based on the lab tests and the technical data provided by Sika construction about their product "Sika Carbodur S1012". Six steel reinforcement bars were taken from the beams tested in the first phase of the project. The reinforcement bars were taken mostly from areas where it could be safely assumed that the steel did not yield in the first tests. The six specimens were machined to reduce their diameter along the middle of their lengths. Each specimen was tested in tension; a curve was drawn until the specimen reached failure. According to these lab tests the yield stress of the reinforcing bars could be taken as 350 MPa. Four concrete cylinders were cored from the same tested beams and each specimen was compressed to failure. According to results of these tests, the average compressive strength of the concrete was 45 MPa. The ultimate strength of the strips was taken to be 2945 MPa. The factors used in the calculations of beam strength were α_1 and β_1 from the CSA A23.3. The predicted moment of resistance from the calculations was about 998 kN·m which meant an increase in the flexural capacity of the beam of about 24 %.

Input design data

$f'_c = 45\,\text{MPa}$ $\alpha_1 = 0.78$ $\beta_1 = 0.86$

$f_y = 350\,\text{MPa}$

$f_f = 2945\,\text{MPa}$

$$M_r = \phi_s T_s (d_s - \beta_1 c) + \phi_f T_f (d_f - \beta_1 c)$$

For initial calculation, assume Neutral Axis inside flange.

$c = 150\,\text{mm}$ for $\varepsilon_c = 0.0035$

$\varepsilon_s = 0.0072$ $\quad f_s = f_y = 350\,\text{MPa}$ $\quad A_s = 6550\,\text{mm}^2$

$\varepsilon_f = 0.0086$ $\quad f_f = 1338.0\,\text{MPa}$ $\quad A_f = 240\,\text{mm}^2$

$$C = \phi_c \alpha_1 f'_c b c$$
$$C = 0.65 \times 0.78 \times 45 \times 920 \times 150 \times 10^{-3} = 3149\,\text{kN}$$
$$T = T_s + T_f = \phi_s f_y A_s + \phi_f f_f A_f$$
$$T = 0.85 \times 350 \times 6550 + 0.9 \times 1338.2 \times 240 = 2238\,\text{kN} \neq C$$

Since $T \neq C$, there is a need to reduce c in order to reduce compression in flange.

Hence, assume:

$c = 75\,\text{mm}$ for $\varepsilon_c = 0.0035$

$\varepsilon_s = 0.0180$ $\quad f_s = f_y = 350\,\text{MPa}$ $\quad A_s = 4000\,\text{mm}^2$

$\varepsilon_f = 0.0207 > \varepsilon_{fult}$

$\varepsilon_{fult} = 0.019$

Now try to see if both concrete and CFRP-strips have the maximum strains:

at $\varepsilon_c = 0.0035$ and $\varepsilon_{fult} = 0.019$ $\quad f_{fult} = 2945\,\text{MPa}$

$c = 81\,\text{mm}$

$\varepsilon_s = 0.0164$ $\quad f_s = f_y = 350\,\text{MPa}$

$$C = 0.65 \times 0.78 \times 45 \times 920 \times 81 \times 10^{-3} = 1701\ \text{kN}$$
$$T = 0.85 \times 350 \times 6550 + 0.9 \times 240 \times 2945 = 2585\ \text{kN} \neq C$$

After several iterations of c, to equate the tension and the compression in the section the following is obtained:

$c = 113\,\text{mm} \qquad a = \beta_1 c = 97\,\text{mm}$

$\varepsilon_s = 0.007 \qquad f_s = f_y = 350\,\text{MPa}$

$\varepsilon_f = 0.013 \qquad f_f = 1954\,\text{MPa}$

$$C = 0.65 \times 0.78 \times 45 \times 920 \times 113 \times 10^{-3} = 2371\,\text{kN}$$

$$T = 0.85 \times 350 \times 6550 + 0.9 \times 240 \times 1954 = 2370\,\text{kN} \quad \text{OK.}$$

$$M_r = \phi_s \times T_s \times (d_s - \beta_1 c) + \phi_f \times T_f \times (d_f - \beta_1 c)$$

$$M_r = \left(0.85 \times 350 \times 6550 \times \left(460 - \frac{97}{2}\right) + 0.9 \times 240 \times 1954 \times \left(520 - \frac{97}{2}\right)\right) \times 10^{-6}$$

$$M_r = 998\,\text{kN} \cdot \text{m}$$

Knowing the nominal moment of resistance before and after attaching the strips, the mathematical model predicted an increase in the flexural capacity of 24 %, which now has to be proven experimentally.

4.2.3. 2 Introducing CFRP-sheets to Enhance Shear Capacity

The CFRP-sheets were mounted on the internal side of the webs of the beams on 45°for a length of 1.50 m to act like external shear reinforcement. The layout of the bridge is such that the beams are near each other without any space left between them. It is only possible to wrap the sheets from the inside, coming 80 mm from the outside of each web as shown in Figure 4.3. Based on the known properties of the CFRP-sheets (strength and cross-sectional area), the new shear capacity was calculated. The equations of the CSA-23 were used treating the CFRP-sheets as bent bars.

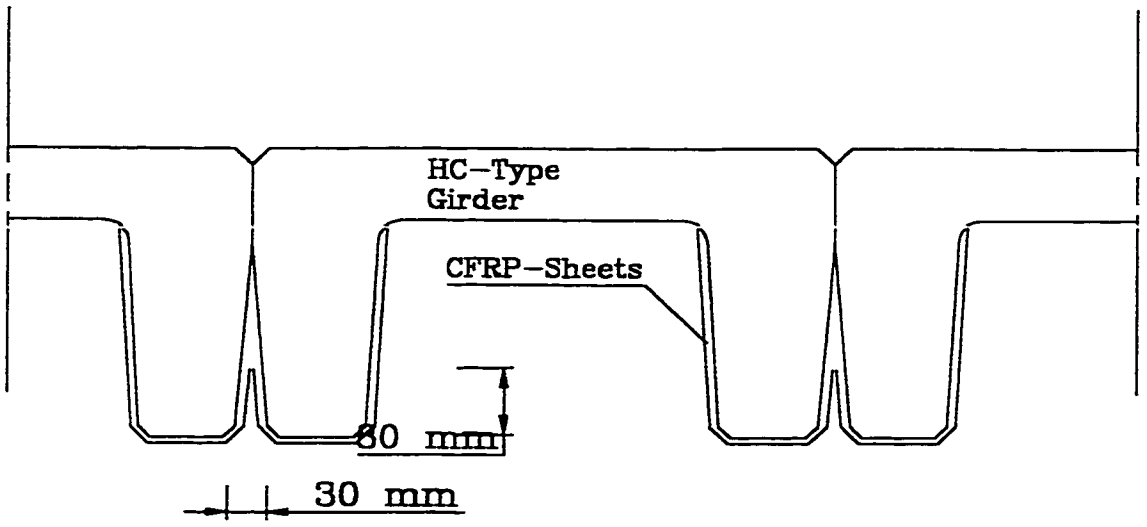

Figure 4. 3 The Webs of the Beams in The Bridge Layout

Calculation of area of sheets: $A_{fs} = 0.11 \times 10^{-1} \times 1000 = 11 \, mm^2/m$

Area for each sheet:

$A_{fs} / sheet = 1.1 \times 10^2 \times 0.25 = 27.5 \, mm^2/sheet$

For both webs:

$A_{fs} = 27.5 \times 2 = 55 \, mm^2/sheet$

Using the general method:

$f'_c = 45 \, MPa$

$d_v = 0.9 d = 0.9 \times 490 = 441 \, mm$

$b_w = 2 \times 150 = 300 \, mm$

$V_{rg} = V_{cg} + V_{sg} + V_{fg}$

$V_{cg} = 1.3 \lambda \beta b_w d_v \sqrt{f'_c}$

$V_{cg} = 1.3 \times 1 \times 300 \times 441 \times \sqrt{45} \times \beta$

$V_{cg} = 1153744 \beta$

$$V_{sg} = \frac{A_v f_y d_v \cot\theta}{s}$$

$\frac{A_v}{s} = \frac{4 \times 100}{180} = 2.22 \, mm^2/mm$ $\qquad f_y = 350 \, MPa$ $\qquad d_v = 441 \, mm$

$V_{sg} = 342657 \cot\theta$

$$V_{fg} = \frac{A_f f_{ult} d'_v (\cot\theta + \cot\alpha)}{s} \times \sin\alpha$$

For bent bars:

$\alpha = 45°$

$$V_{fg} = \frac{55 \times 3400 \times (520 - 150) \times (\cot\theta + 1)}{250} \times 0.707 = 197478(\cot\theta + 1)$$

We have to assume V_f and get the related value M_f, assume a value for θ and then get the related value β. Taking out numbers for V_{cg}, V_{sg} and V_{fg} a check is made if V_f is the same. This iteration process is followed until a solution as close as possible to the input value is obtained.

Assume:

$V_f = 750\,\text{kN}$ $\qquad$ $M_f = 1.15 \times 750 = 862\ \text{kN} \cdot \text{m}$

Assume:

$\theta = 38°$

$$\varepsilon_x = \frac{0.5 \times (N_f + V_f \cot\theta) + \frac{M_f}{d_v}}{E_s A_s}$$

$N_f = 0$

$E_s = 200 \times 10^3\ \text{MPa}$ $\qquad$ $A_s = 5600\,\text{mm}^2$

$\varepsilon_x = 2.17 \times 10^{-3} > 0.002$

Take $\varepsilon_x = 0.002$

$\frac{v_f}{\lambda f'_c} = 0.135$ $\qquad$ $\theta = 37°$ $\qquad$ $\beta = 0.11$

$V_{cg} = 127\,kN$

$V_{sg} = 455\,kN$

$V_{fg} = 459\,kN$

$V_f = V_{cg} + V_{sg} + V_{fg} = 1041\,kN \neq V_f$

Assume:

$V_f = 1000\,kN$ $\qquad M_f = 1.15 \times 1000 = 1150\,kN \cdot m$

$\theta = 37°$

$\varepsilon_x > 0.002,$ $\qquad$ take $\varepsilon_x = 0.002$

$\frac{v_f}{\lambda f_c'} = 0.167$ $\qquad \theta = 36°$ $\qquad \beta = 0.095$

$V_{cg} = 110\,kN$

$V_{sg} = 471\,kN$

$V_{fg} = 469\ kN$

$V_f = V_{cg} + V_{sg} + V_{fg} = 1050\,kN$ $\qquad$ close enough

$V_{rg} = V_f$

$V_f = 1.25\ V_{D.L.} + 1.5 V_{L.L.}$

$V_{D.L.} = 27\,kN$

$1025 = 1.25 \times 27 + 1.5 \times R_{expected}$

$R_{expected} = 650\,kN$

According to these calculations this final value (650 kN) will be the maximum expected reaction at the support. With the shear tests having the same geometry as the initial ones, the expected increase shear capacity would be about 18%.

4.2. 4 Process of Rehabilitation

The following procedures were interpreted to perform the rehabilitation process. The main idea was to patch the beams with different kinds of grout, to apply the strips, and then to wrap the sheets above them. Four beams were used in this phase. Two of them were repaired and had CFRP-strips and sheets bonded onto them, while the other two were used to test the efficiency of the grout repair under cyclic loading.

4.2.4. 1 Patching the Beams

The beams were transferred to an open yard for the patching work to be done. Sandblasting and the application of shotcrete were not possible in the laboratory.

1) Initial Sandblasting:

There were several areas with exposed corroded steel on the beams, and other areas where the cover had almost spalled off. This latter cover had to be broken off to provide access to as much of the corroded steel reinforcing bars as possible, and to get rid of the weak parts of the concrete. The exposed reinforcing bars were sandblasted to be rust free. The rust layer was found to be very shallow on the reinforcement bars so the process of sandblasting was not intensive.

2)Strain Gauges:

There was a good opportunity to measure the strain on the reinforcement bars, as the bars were now exposed. This chance did not exist in the initial tests as the bars were not exposed in most of the cases. So strain gauges were mounted on the exposed steel. Special precautions were taken to protect the gauges from being damaged during shotcreting in the yard. Two steel strain gauges were placed on reinforcement in each web where the steel was exposed in the mid-span. The strain gauges were placed in the constant moment zone

250 mm away from the centerline of the beam on each side. Three layers of protective material were used to cover each gauge to be sure the gauge was protected. Strain gauges on steel have the advantage of being more consistent than gauges on concrete, as the concrete is a non-homogeneous material. Adding strain gauges to the reinforcing bars was part of a plan to understand the changes in the strain profile through the beams while testing.

3)Shotcrete:

Two beams were repaired using the Sika 224 grout product. This material has a very high strength, very short hardening time and a low liquidity (Table 4.2). The material was mixed with water in the ratio of one bag (25 kg) to 2.75 L water in a mechanical mixer. The grout was applied manually to one beam. It took a long time to get the same shape of the beam's web as originally by applying this material by hand. In some areas where there has been extensive loss of concrete, it took up to five coats of material to achieve a profile similar to the original concrete. This was considered too time consuming and forms were erected to reconstitute the webs of the second beam. Pouring the material in the forms was much easier and took less time. The result with both methods was that the beams had a good straight shape after repair, which made the wrapping of the sheets easier. In all cases, special care was taken with the parts with the strain gauges, to ensure the strain gauges were not destroyed. The beams were wrapped with wet burlap to avoid shrinkage cracks and were soaked with water twice daily for a period of three days. The same procedure of forming was used when wet shotcrete was "shot" into the forms to reform the bottoms of the webs of the other two beams. These beams were also wrapped with wet

	Compressive Strength	Flexural Strength	Splitting Tensile Strength	Slant Shear
1 day	35 MPa	-	-	-
7 days	55 MPa	-	-	-
28 days	75 MPa	9.0 MPa	9.8 MPa	32 MPa

All properties are given at 23° C and 50 % R.H.

Table 4.2 Properties of the Sika224 Grout Used in the Tests

burlap to avoid shrinkage cracks and again the burlap was soaked with water twice daily for a period of three days.

4.2.4. 2 Application of the Strips

1) Sandblasting after Shotcrete:

One of the most important points required before the strips could be applied on the bottoms of the webs, was that the CFRP-strips have to be applied to a smooth surface, so that no obstructions appear to make the strips irregular. The shotcreted beams were not sufficiently smooth so the areas on which the strips were to be put were sandblasted again in order to obtain a fairly smooth surface.

2)Applying the strips:

The beams were moved back to the laboratory for the application of the strips and sheets. A length of 10.4 m of Sika-strips was applied to each web of two beams, recognizing that the bearing conditions in the field would prevent the contractor from using 600 mm from each end of the girder. One beam treated with Sika224 and one shotcreted beam were reinforced with the Sika-strips. Sikadur 30 epoxy is the manufacturers recommended product used to apply the Sika-strips to the concrete. An easy procedure was used to apply the strips. The beam's webs, as well as the strips, were cleaned using acetone to remove any sand or dirt on the two contact surfaces. Two strips of ordinary duct tape (20 mm wide) were stuck on the outer sides of the 150 mm wide bottom of the web to define accurately the path of the epoxy and the strip. The Sikadur 30 epoxy was mixed mechanically from its components A and B (the mixing ratio is 3:1 by weight). After mixing, a very thin layer (1 mm) of Sikadur 30 epoxy was gradually applied to the bottom of the web using a trowel. The strips were passed through an arched slot with a maximum

height of 3 mm to control the thickness of the epoxy applied to them as well (1.8 mm at the centre of the strip). The shape of the epoxy of the strip was like an arch. This made it easier to press the air bubbles from the centre to the outside of the strip easily, while applying the strip on the concrete as shown in Figure 4.4. Five people carried the strips, one in the middle, one on each end and one on each half of the strip. Five people were involved here not because of the weight of the strip (which is very light), but because of its length (10.4 m). The strip was then placed slowly on the bottom of the first web, first in the middle and moving to both outer ends at the same time. After that, uniform pressure was applied on the strip using a roller to be sure that all the unnecessary epoxy was squeezed out and only a thin layer of epoxy left between the beam and the strip. The duct-tape was then removed with any excess epoxy on it. The procedure was repeated on the other web and the beam was left for 24 hours to let the epoxy cure. The procedure of applying the strips can be shown in Figures 4.5 to 4.8.

3) Strain Gauging on the CFRP-Strips and the concrete:

Strain gauges were placed on the CFRP-strip at the same locations as the steel gauges (250 mm from each side of the centreline of the girder). The same type of gauges as used for steel reinforcing bars was used. Concrete gauges were mounted at the same distance from the centreline on the webs at the top fibre and 80 mm below the top fibre on each vertical line. A system of (LSCs) was put on the bottom fibre of the concrete to read the strain measurements between the steel and the CFRP-strips. The whole strain profile is shown in Figure 4.9. These readings were taken to provide an extra point on each strain profile. It was expected that some shear flow would occur between the concrete and the

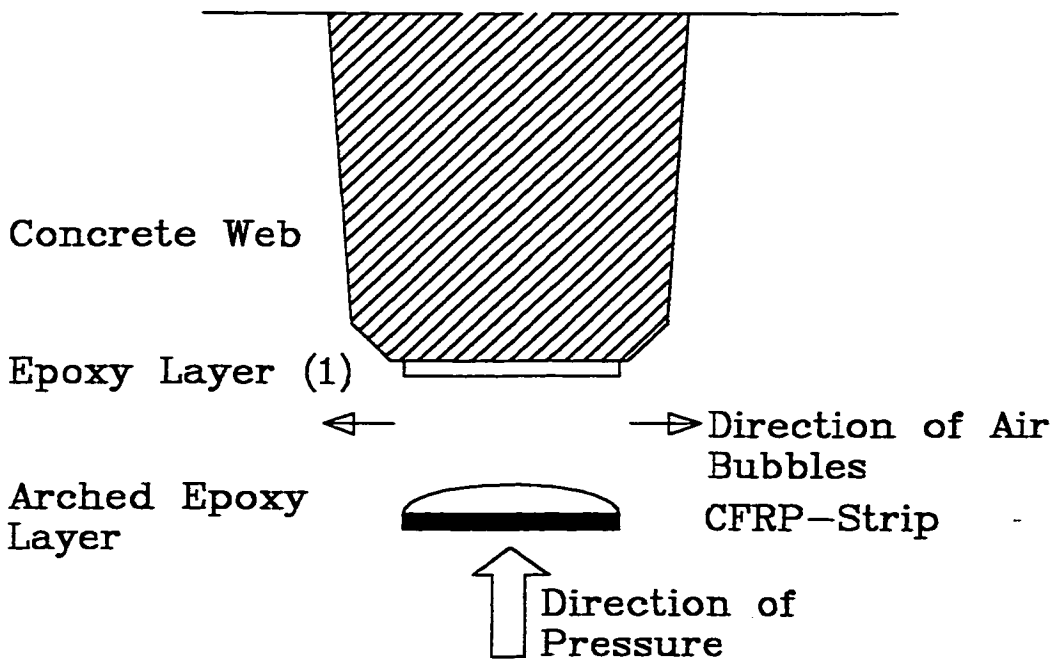

Figure 4. 4 Schematic Showing Arched Shape of Epoxy on CFRP-Strip

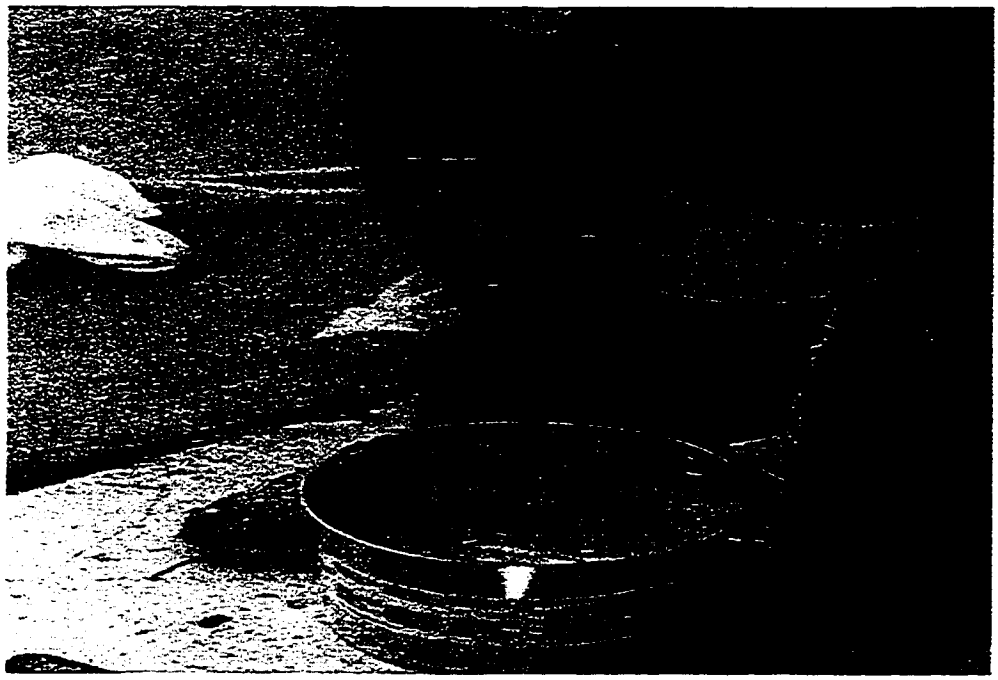

Figure 4.5 Mixing the Epoxy

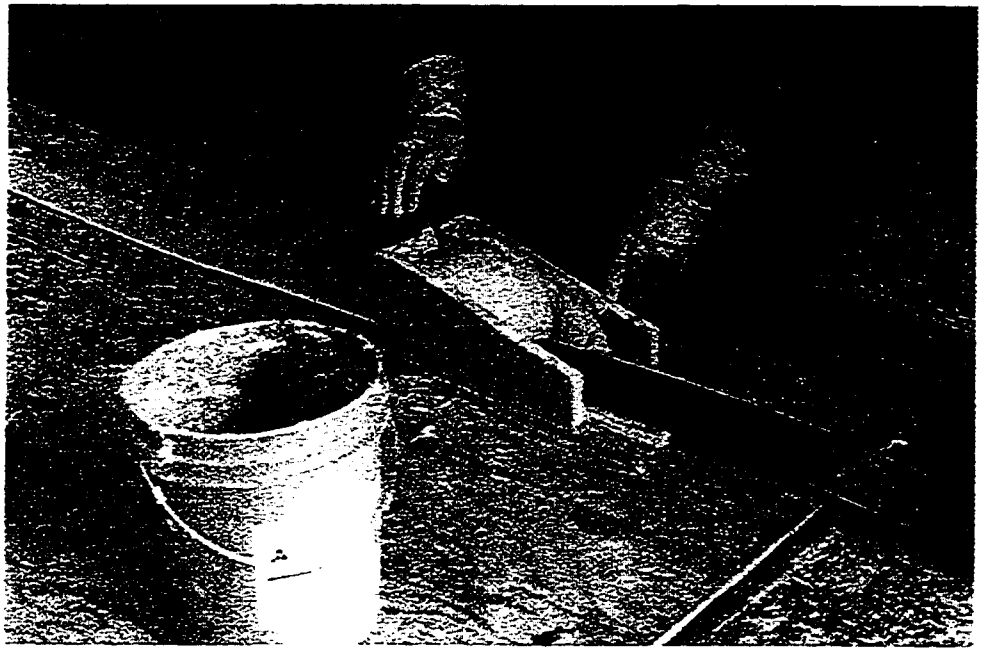

Figure 4.6 Applying the Epoxy on the Strips

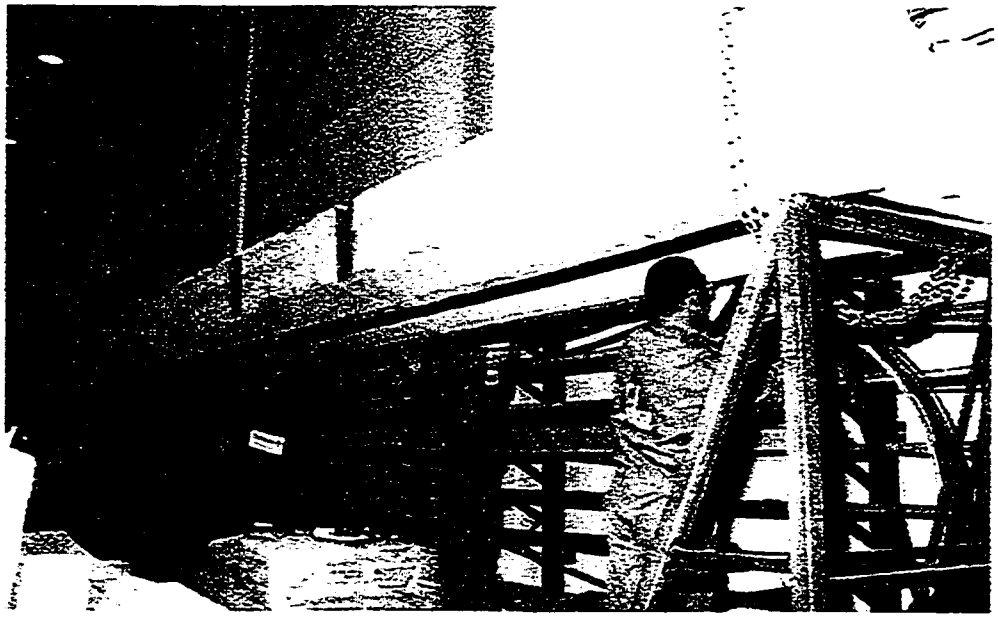

Figure 4.7 Applying the Strips on the Beam

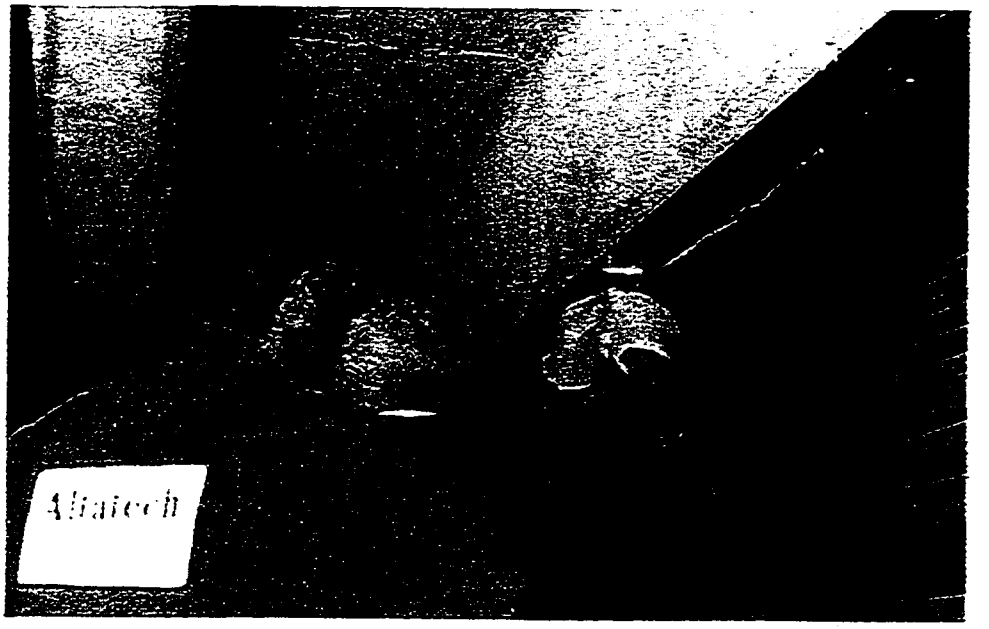

Figure 4.8 Uniform Pressure on the Strips

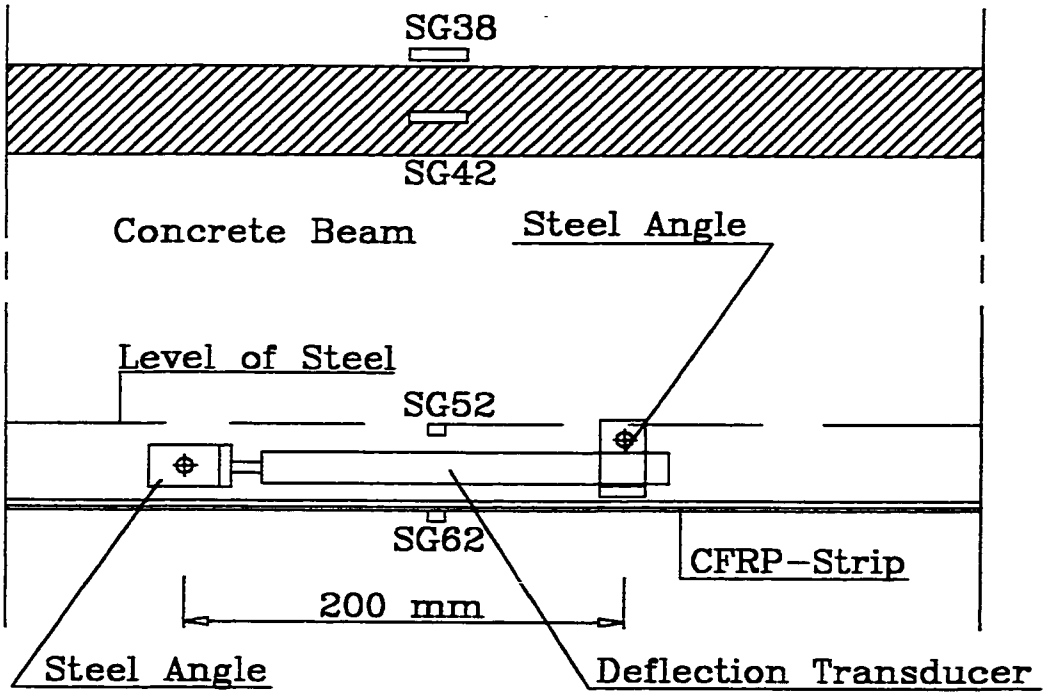

Figure 4. 9 Strain Profile in Beam under Test

epoxy and that the CFRP-strip would slip. A full strain profile could be drawn at each applied load level and compared with the mathematical model.

4.2.4. 3 Wrapping the CFRP-sheets for shear

Mitsubishi CFRP-sheets (Replark 20) were used for shear reinforcement and strip anchorage and needed to be wrapped around the webs of the beams. These sheets are about 10 times thinner than the Sika-strips. The small thickness gives the sheets the ability to be easily wrapped, as well as giving the sheets the flexibility to take any reasonable non-uniformity remaining in the concrete after the surface preparation. The modulus of elasticity of the sheets is higher than the Sika strips which gives a lower ultimate strain. The procedure for wrapping the CFRP-sheets was as follows:

1) Surface Preparation:

At a local level the surface for the CFRP-sheets has to be very smooth to avoid any areas of stress concentration. First the concrete was ground smooth to take the surface to a better shape. Sandblasting gave almost the same result but in a faster time. Subsequently the surface was cleaned with dry cloths to remove loose sand from the surface.

2) Applying of Primer:

The primer was mixed according to the manufacturer's instructions and then applied to the areas to be covered with the sheets. The primer was left to soak the concrete surface completely. The primer serves to prepare the surface of the concrete to accept the epoxy resin. The primer was left to cure for a few hours.

3) Applying of Putty

The putty is a kind of epoxy thicker than the resin and the primer. It was used to fill big holes still remaining in the concrete surface after grinding. The putty mix acts like

shotcrete for holes the size of a thumbnail. After the putty dries the surface of the concrete should be very smooth without any irregularities. The putty could be applied before or after the primer.

Application of Resin and Sheets:

After filling the remaining holes and letting the putty cure, the resin was applied as a final coat on which to stick the sheets. The sheets were applied directly onto the resin after the resin had been applied to the concrete. The sheets were applied over a length of 1.5 m at each end of the beam, on an angle of 45° on the inside of the beam. After crossing the Sika-strip, the sheets were taken only 80 mm up the other side of the web as shown previously in Figure 4.1. Figure 4.2 showed the whole beam after application of strips and sheets, ready for testing. The sheets took one week to cure before testing.

4.2. 5 Testing of Beams

The main focus in this series of tests was to provide information for recommendations concerning the design of beams strengthened by CFRP-strips.

Test 8:

The first flexural test was performed on the beam repaired with the Sika grout product "Sika 224", and reinforced with CFRP-sheets/ and strips. The same arrangement was used as the former tests. The vertical deflection was measured at the two webs in the constant moment zone closest to the mid-span using two deflection transducers (100 mm for each). At a certain point of the test (at a load of 260 kN) the vertical tension crack above of the reinforcing bars started to propagate at an angle of about 45° until it reached the level of the strips as shown in Figures 4.10, 4.11. This happened under the point of application of the concentrated load. The strips debonded from the bottom of the web. The

debonding began near the mid-span where the inclined crack reached the bottom of the beam. The debonding propagated to each end of the beam. The beam failed at a load of 401 kN, increasing the flexural capacity by only about 11 % of the original. The failure occurred when the sheets failed to hold the debonded strips at one end of the beam. Due to the high tensile force generated in the strips and the small transfer distance between the strips and the beam, the sheets failed to hold the strips any longer. This was an obvious example of arching action, where the tension developed in the tension-tie (the CFRP-strips in this case) was greater than the anchorage could hold. Simultaneous with the ripping of the anchor sheets compression failure of the concrete was beginning on the top of the beam.

Test 9:

After the flexural test, the same beam was tested for shear capacity at the end where the sheets did not fail. The shear span was chosen to be 2000 mm. Before the shear test, 7 strain gauges were put on the sheets of one web. One gauge was put on each of the four sheets 150 mm from the bottom of the web. The other three gauges were successively put on top of the sheet expected to strain the most (Figure 4.12). The gauges were spaced 50 mm apart beginning at the top of the beam. The beam carried a maximum load of 748 kN with a maximum reaction of 545 kN. The beam failed in flexure because the moment in the beam at this load was larger than the flexural capacity. The beam did not seem to be affected in terms of its shear capacity. There were a few minor diagonal cracks.

Test 10:

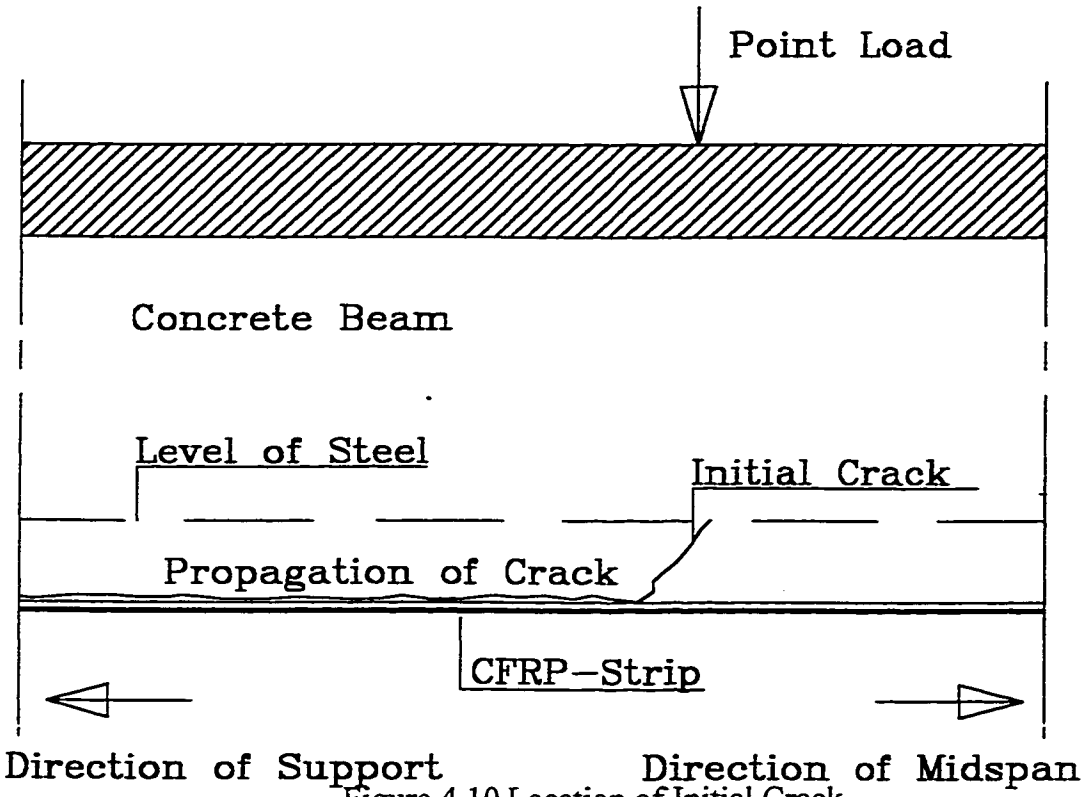

Figure 4.10 Location of Initial Crack

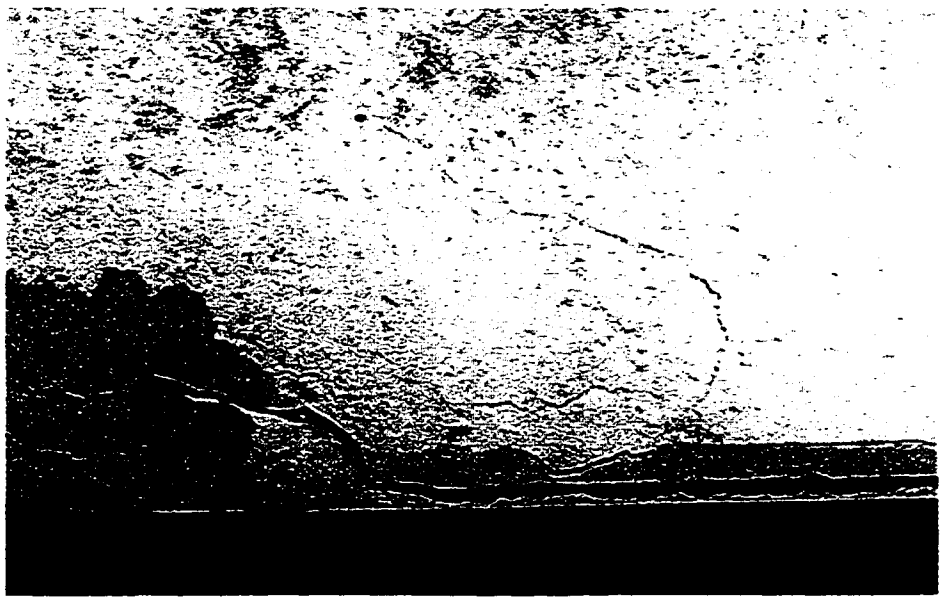

Figure 4.11 Critical Crack in Test

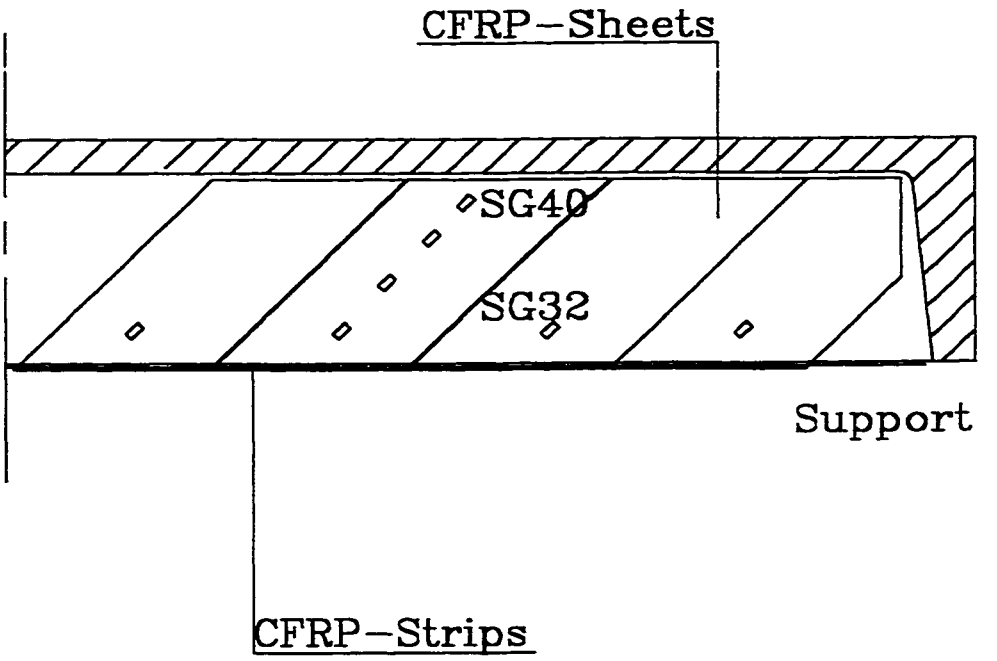

Figure 4.12 Orientation of Strain Gauges on the CFRP-sheets (Shear Test)

The second flexural test was performed on the beam with the same additional reinforcement as the previous beam but was repaired with ordinary shotcrete instead of the Sika 224 product. The same instrumentation was used. Four vertical strain profiles were assessed, as well as two vertical deflections. There seemed to be no difference, the strips being debonded from the concrete at almost the same load. The crack propagated from under the load points near mid-span to the support, but before the strips cut the sheets (as in test 8), compression failure occurred in the concrete. The load was 396 kN. This different ultimate failure affected neither the mode through which failure developed, which was similar in both beams (discussed later), nor the crack propagation noticed in both tests. The failure load was the same in both tests, which means that the gain in flexural capacity was the same in both experiments.

Test 11:

The shear test on the second beam was different to that on the first beam preventing flexural failure. The shear span was chosen to be 1115 mm. Shear cracks first appeared at a load of 400 kN but the load rose to 820 kN (with a maximum reaction of 630 kN) when the load dropped rapidly after two diagonal tension cracks opened, one on each web. Both cracks began under the concentrated load. The failure happened when the sheets started debonding from the concrete. It was noticed that the cracks were developing in the concrete almost in the same places as where the cracks developed when there were no sheets (see Chapter 3, initial capacity of the beams). The CFRP-sheets succeeded in delaying the failure by bridging the cracks until debonding began. Although there was no need for improvement in shear capacity, one layer of the sheets had improved the shear capacity by about 15%. With the results shown, this test result was not very far from the prediction of

the model introduced earlier. The test proved the sheets were an efficient method to strengthen the beams in shear.

4.2. 6 Failure Mechanism and Strain Compatibility

The interesting part of the failure was the crack propagating vertically (under the concentrated load) until the level of the reinforcing bar and then advancing at about 45° until it hits the strips (see Figure 4.11). Further propagation caused debonding of the strips from the concrete. The most suitable way to explain this propagation of the crack is to analyze the beam in a truss model (Figure 4.13). The vertical tension members are missing in the area between the steel and the CFRP-strips. The stirrups in the beam are stopped at the level of the steel and then plain concrete has to transfer the tension to the "lower tension chord" which is the CFRP-strips. The plain concrete fails to resist the combined stresses at the particular load and location where the crack begins. The crack propagates at an angle perpendicular to the maximum principle tension. The point of crack initiation is always the point where the maximum combined stresses occur. Checking several sections along the beam it will be noticed that the most critical section is the section under the concentrated load facing the outer sides of the beam. Here the combination of the highest bending moment and the highest shearing force occurs. Between the concentrated loads, the shear force would be zero (theoretically).

With the truss model, it can be shown that under the level of reinforcing bars the section becomes unsafe (plain concrete only) at a concentrated load of 290 kN. As was noticed in the tests the crack began to propagate at a load of 260 kN. Allowing for the approximations in the calculations, the theory therefore seems to give a reasonable explanation of the initiation of failure.

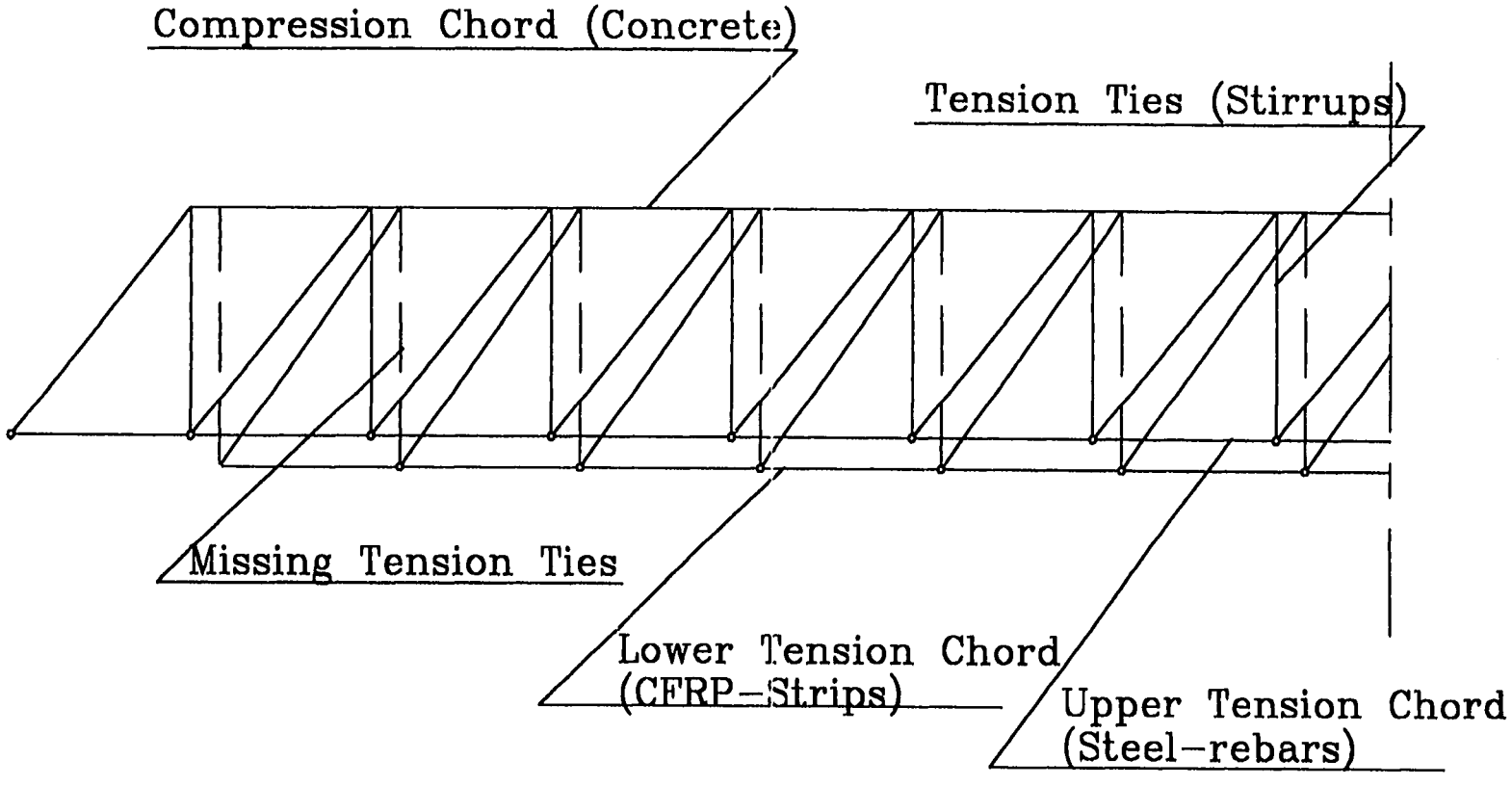

Figure 4.13 Truss Model for Beam

After that the crack propagates along the concrete, because the plain concrete is the weakest part in the structure. When the crack has propagated to the CFRP-sheets, the sheets stop further propagation, and thus the beam continues to carry load. When the tension in the strips is higher then the ability of the CFRP-sheets to resist, the sheets rip and the beam fails. The CFRP-strips had very little effect on the improvement of the capacity due to the lack of shear transmission: the CFRP-sheets prevented the beams from failing at an even lower load.

4.2. 7 Results of the Tests

4.2.7. 1 Results of Flexure Tests

The total results of the flexural tests are summarized in table 4.3. The flexural strength was improved by less than 12 %. Drawing curves expressing the real strains at the different stages of loading in the concrete, the steel and the CFRP-strips, it was found that compatibility of strain was lacking in the stages of loading after the critical crack appeared. It is obvious that the strain in the CFRP-strips increases at a faster rate than in the steel reinforcing bars until the steel begins to yield and the strips separate. This can be seen in Figures 4.14, 4.15 for the first beam, and Figures 4.16, 4.17 for the second beam. There is a clear trend for the results of the two beams. Four different stages can be defined to generalize the behaviour of these beams repaired with CFRP-strips.

Stage I: (Elastic loading: 0-90 kN)

In the early stages of loading, the strain in the CFRP-strips is higher than the strain in the steel reinforcing bars. The strains are roughly compatible.

Stage II: (To cracking of the concrete in tension: 90-250 kN)

In the later stages of the elastic zone the concrete cracks at the bottom fibre and begins to release some of its tension. The CFRP-strips take over much of the tension as they are glued to the bottom fibre. The strains in the strips increase suddenly and continue to increase at a faster rate than those in the steel.

Stage III: (To yielding of the steel: 250-320 kN)

In this stage, the concrete carries no tension. The concrete is cracked to the neutral axis, so that the tension above the steel is now carried by the reinforcing bar. The strain in the CFRP-strips remains high.

Stage IV: (Until the slippage of CFRP occurs: 320-Failure)

After the steel yields, it carries minimal additional force. Although the steel strain increases, the CFRP-strips have to carry any extra tension so the strain in the strips continues to increase. Due to the increasing forces in the strips, high shear flow occurs between the strips and the concrete. The concrete cracks due to shear flow and the strips debond from the beam. At debonding the strips release some of their force. The strain in the steel increases rapidly as the steel is the only material that can carry the tension released by the CFRP. At this stage the extra steel force must be occurring due to strain hardening. The CFRP-strips are now held by the CFRP-sheets only at the ends of the beam. All the force going to the strips is now transferred at that joint, which fails at about of 400 kN.

The maximum deflection was measured to be 180 mm (Figure 4.18).

4.2.7. 2 Results of Shear Tests

Only two shear tests were performed in this phase. One of them did not give a realistic indication about the shear capacity of the beam, due to an error in the mixing proportions in the putty. The other test showed that the CFRP-sheets could be used with

confidence in strengthening beams in shear. The test had no practical reason, as there was no need to increase the shear capacity. It was an opportunity, though, to examine the CFRP-sheets, if needed in the future. The results of the strain gauges put on the most critical sheet, show that the high strain starts at gauge number 40 for the beginning of the test. Gauge number 40 was positioned at the top of the web near the point loads. This was where the crack initiated. As the test progressed, strain gauge number 32 picked up the high strain. This gauge was positioned near the bottom of the web 500 mm apart from the point of the concentrated load. The previous statement means that the crack was moving similarly to an ordinary "shear" crack (see Chapter 3). The CFRP-sheets have managed to bridge the cracks and hence improve the shear capacity until the sheets debonded from the beam. The gauge readings are shown in Figure 4.19.

BEAM	B2	B5
Tested span in flexure	10500 mm	10500 mm
Maximum flexural load	401 kN	396 kN
Maximum nominal moment	932 kN·m	921kN·m
Expected nominal moment	991 kN·m	991 kN·m
Maximum vertical deflection	181 mm	185 mm
Maximum Shear Load	-	820 kN

Table 4.3 Summary of Results of Tests

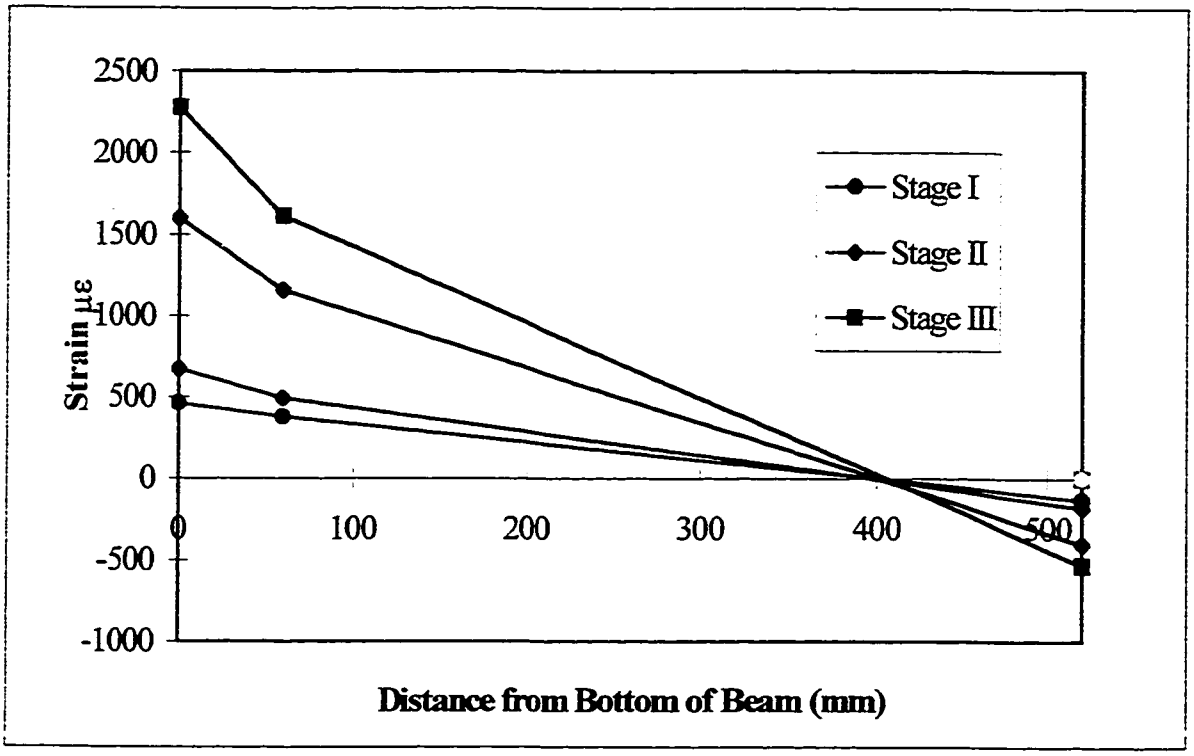

Figure 4.14 Strain Profile in Stages I, II and III for Beam 1

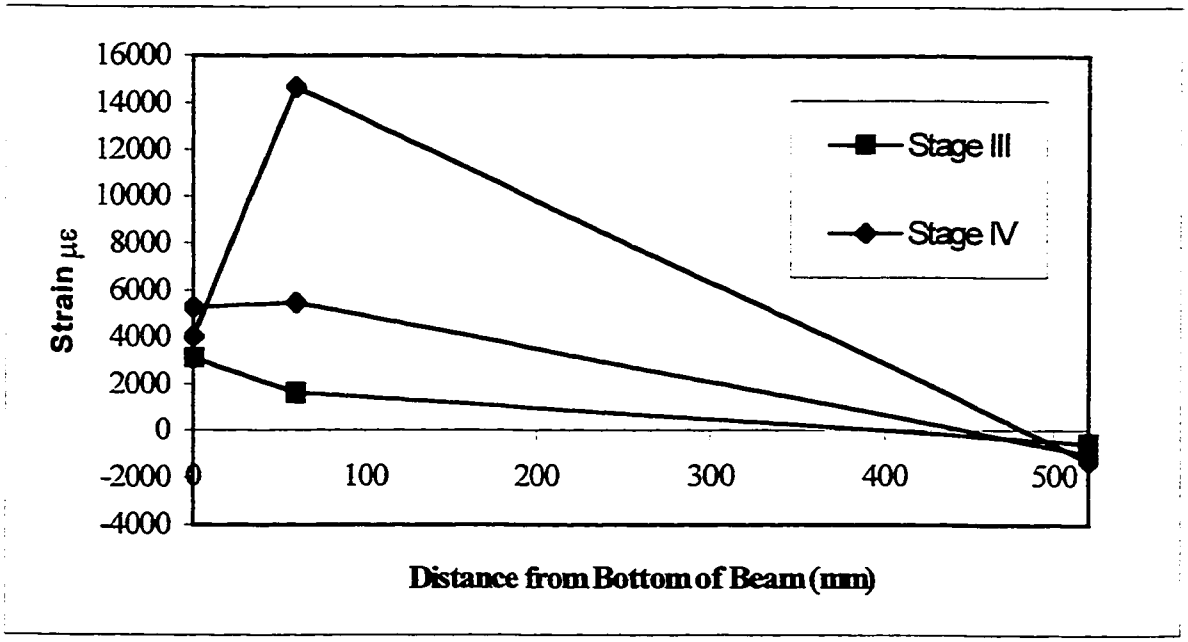

Figure 4.15 Strain Profile in Stages III, V for Beam 1

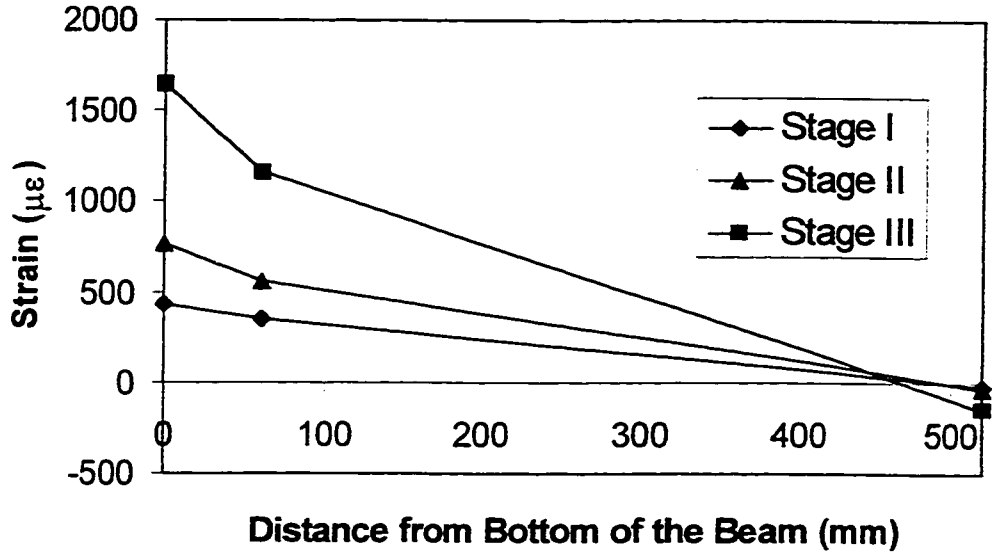

Figure 4.16 Strain Profile in Stages I, II and III for Beam 2

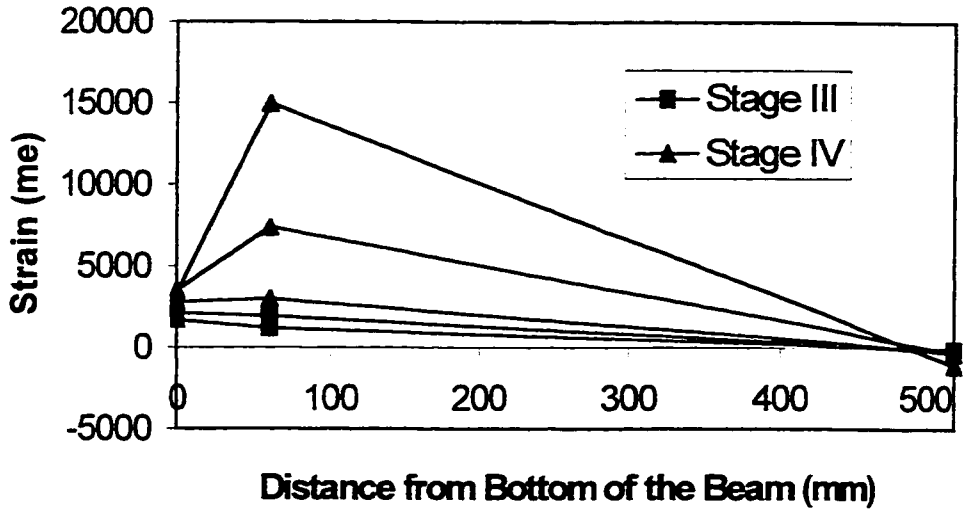

Figure 4.17 Strain Profile in Stages III, V for Beam 2

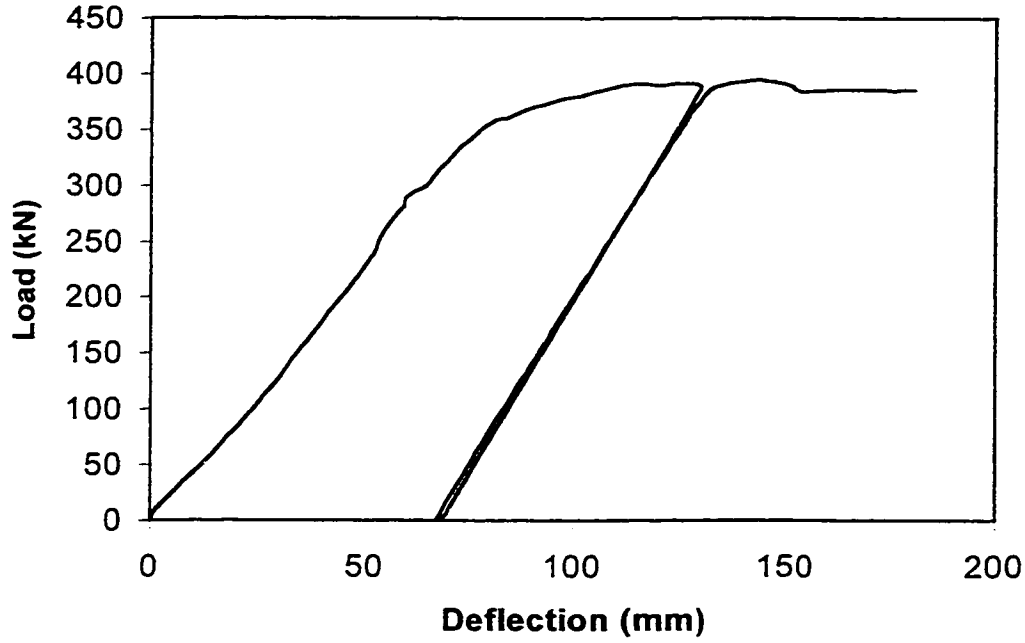

Figure 4.18 Vertical Deflection of Beam 1

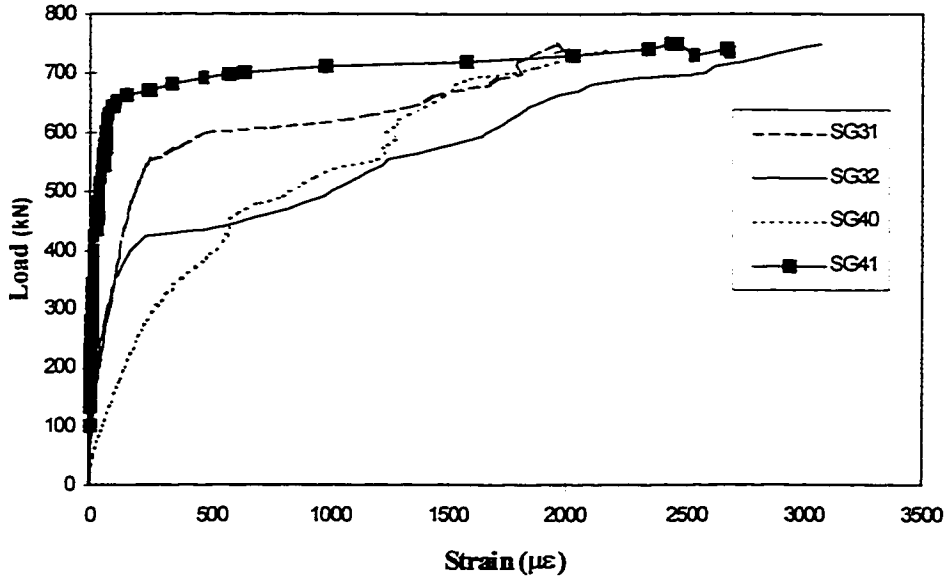

Figure 4.19 Strain in Shear Test

4. 3 Experimental Verification of Truss Model

4.3. 1 Introduction

It was obvious from the previous flexural tests and the analysis made after, that there are many factors affecting the performance of the CFRP-strips. The geometric shape of the beams (i.e. width and depth) is one dominant factor. The amount of reinforcement and the concrete strength are other factors, which could affect the performance of the strips. To verify the results of the tests a small parametric study was undertaken. The method was to fix certain parameters, that were expected to affect the results, in order to study other obvious parameters. Three beams were designed with three different geometric shapes, while the area of steel A_s and the concrete strength f_c' were fixed. There was a reference beam with the smallest width and depth, a beam with the same width but deeper and a third beam which had the same depth as the reference beam but was wider. The cross sections and the reinforcement are shown in Figure 4.20. Based on the common flexural equations the nominal moment was predicted for each beam with and without the CFRP-strips. The beams were over-designed in shear to prevent shear failure, as the beams have a relatively short span. It was expected that the geometric shape would affect the results of the tests significantly, i.e. the performance of the strips would be less than expected in the beams with narrower webs. The wide beam has a greater area between the steel and the CFRP-strips to transfer the shear.

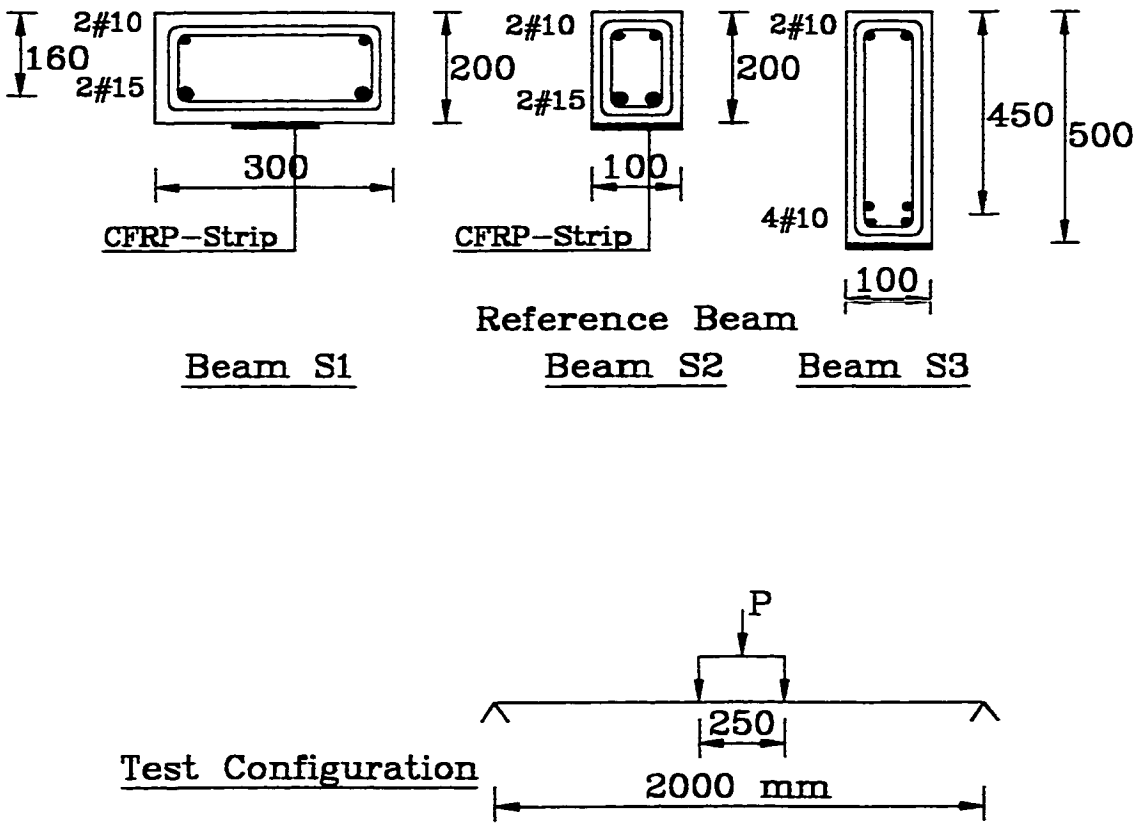

Figure 4.20 Cross-sections of Beams S1, S2 and S3 and Testing Configuration

Stirrups are #10@ 60 mm

4.3. 2 Test Setup

The test arrangement for these beams was previously discussed in Chapter 3.

4.3. 3 Preparation for the Tests

The beams were cast and cured for 28 days before application of the CFRP-strips. 6 cylinders were cast from the same batches of concrete, to be tested on the same day of the actual test. After 28 days the CFRP-strips were applied with the same procedure described in Chapter 4. The strips were left for more than one week for the epoxy to cure and then the beams and concrete cylinders were tested. The concrete had an average strength of 38 MPa. On the basis of knowing the actual concrete strength, the theoretical flexural capacities were calculated with and without the CFRP-strips. The results of the calculations and the tests are listed in Table 4.4. The goal of the tests was to determine whether there is a different rate of increase in the capacity, which cannot be predicted by the compatibility equations.

4.3. 4 Testing Beams S1, S2 and S3

Test 12:

The first test on this series was on the beam S1. Only the load and the vertical deflection were measured. At about 110 kN the beam started cracking at one of the supports, and the strips debonded at a maximum load of 130 kN, where it was expected to go to 140 kN. The inclined crack was not obvious as the beam had a high width, and debonding at the zones of stress concentrations caused the failure first. The deflection at the failure load was 17.5 mm (see Figure 4.21).

Test 13:

The second beam tested was the reference beam, S2. The same setup was used and again, only load and deflection were measured. The beam failed at an unexpectedly high load of 96 kN, whereas the maximum calculated capacity was about 78 kN. Although this number seems unreasonable, the mechanism of failure was obvious. The beam started cracking at about 45° almost under the concentrated load from the level of the reinforcing bar down to the level of the CFRP-strips. After that several cracks propagated at the same angle in the shear span (which was small). The total failure of the strips occurred suddenly at the end of the strips, with the same angle of crack. The deflection was expected: 17 mm at failure load (see Figure 4.22).

Test 14:

The third test in this series was performed on the beam S3. This beam had a narrow width and a relatively large depth. The beam simulates the case of the bridge beams tested before. The loading configuration was the same and vertical deflection was measured as well. The beam was more ductile than beams S1 and S2, and the beam started cracking in the same manner as beam S2. The beam failed at a load of 255 kN. This load means the beam only reached 45% of the expected capacity. This small improvement in the nominal capacity shows that the effect of the CFRP-strips on beams becomes less as the beam becomes narrower and deeper. Figures 4.23 to 4.26 show the setup of the tests and the different modes of failure for beams S1, S2 and S3.

4.3. 5Conclusions of Experimental Verification

This last series of experimental tests verified the concept, that the geometrical shape of the beam has an effect on the ability of the CFRP-strips to enhance strength. Results of

the tests are summarized in Table 4.4. The calculations of the flexural capacity based on strain compatibility may be reliable in the case of strengthening of slabs. However, one must be careful in the case of the beams. The test results from both series of tests show that conventional calculations can significantly overestimate the flexural capacity of the beams.

The shape of the deflection curve has become more ductile as the shape of the beam changed from deep and narrow to wide and shallow (like slabs). The calculations of the beam capacity verify this fact, as the calculations show that the reinforcing bars are subjected to a higher strain in the shallow beam. The effect of the geometric shape was very obvious in terms of the mode of failure. It became clear that the truss model explanation is the right one. The narrow web gives an obvious shear crack between the level of the reinforcement bars and the CFRP-strips, whereas in the wide webs the area of concrete is bigger and the failure load is closer to the expected one.

The anchorage of the strips at the end makes a difference in the capacity of the beam. If there was no anchorage (case of beams S1, S2 and S3) we find that although we get initially the same cracking mode, the beams fail near the supports where there is a high stress concentration due to shear transfer from the CFRP-strips to the beam again. In the first tests of the bridge beams the final failure was debonding from the middle until the anchorage was cut at the end.

The behaviour of the beams with the strips still needs more understanding. The several facts affecting the performance of CFRP-strips on the beams need further research and a general analysis to be able to come out with full design recommendations.

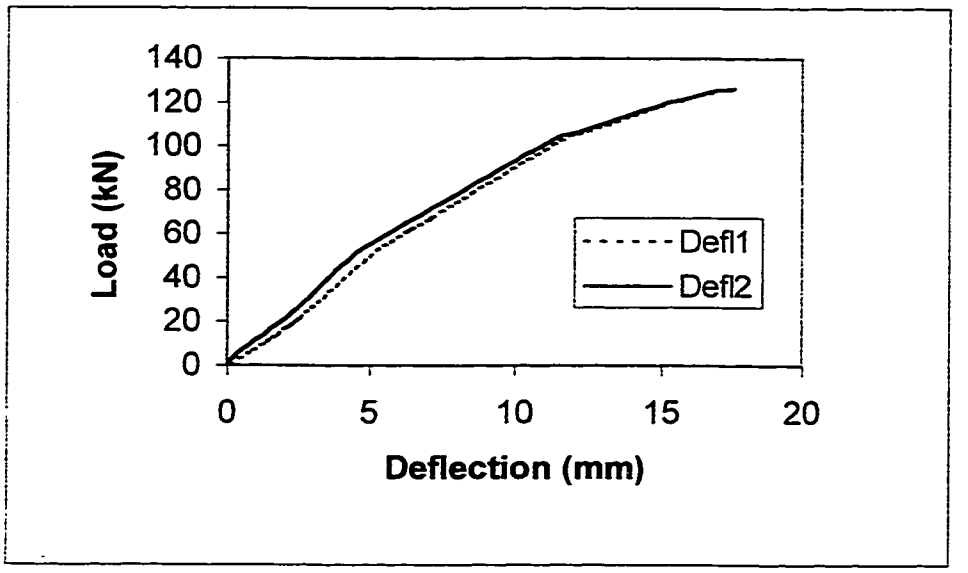

Figure 4.21 Load vs. Deflection for beam S1

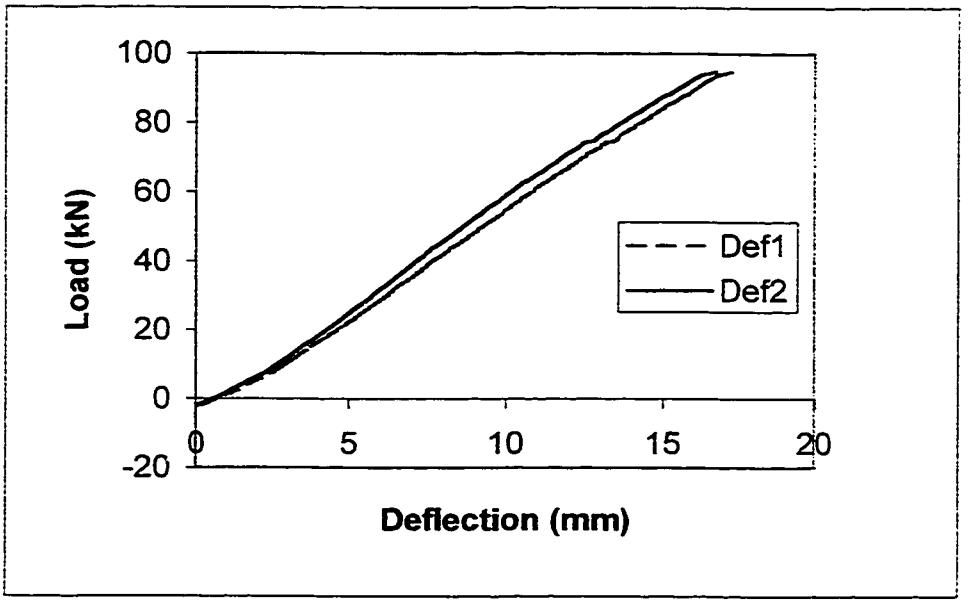

Figure 4.22 Load vs. Deflection for beam S2

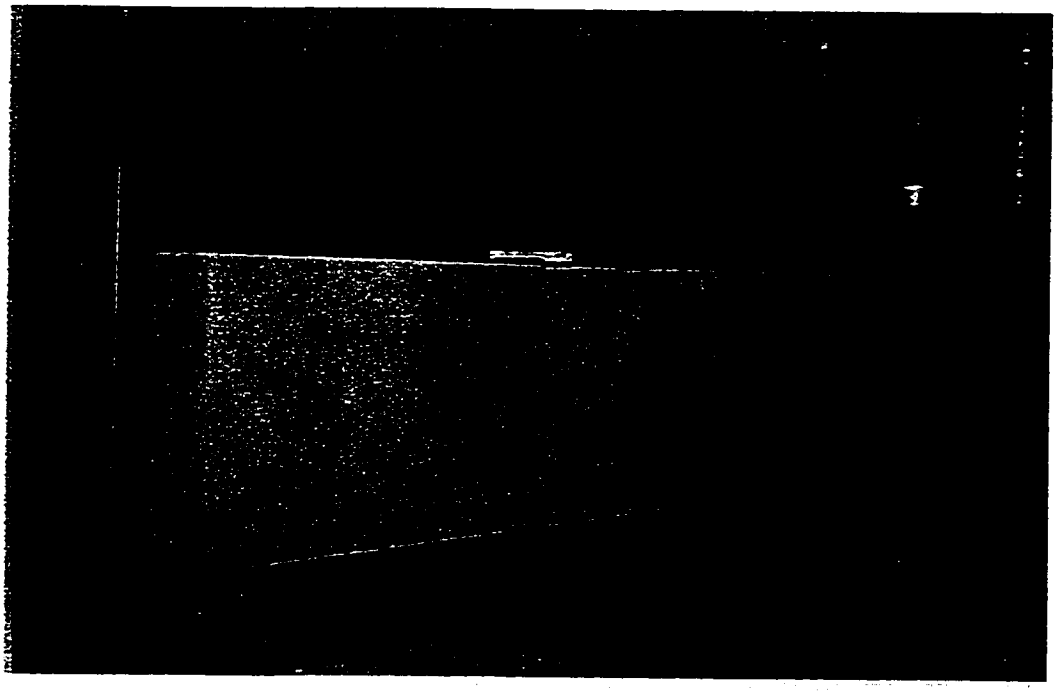

Figure 4.23 Beam S3 under Testing Frame

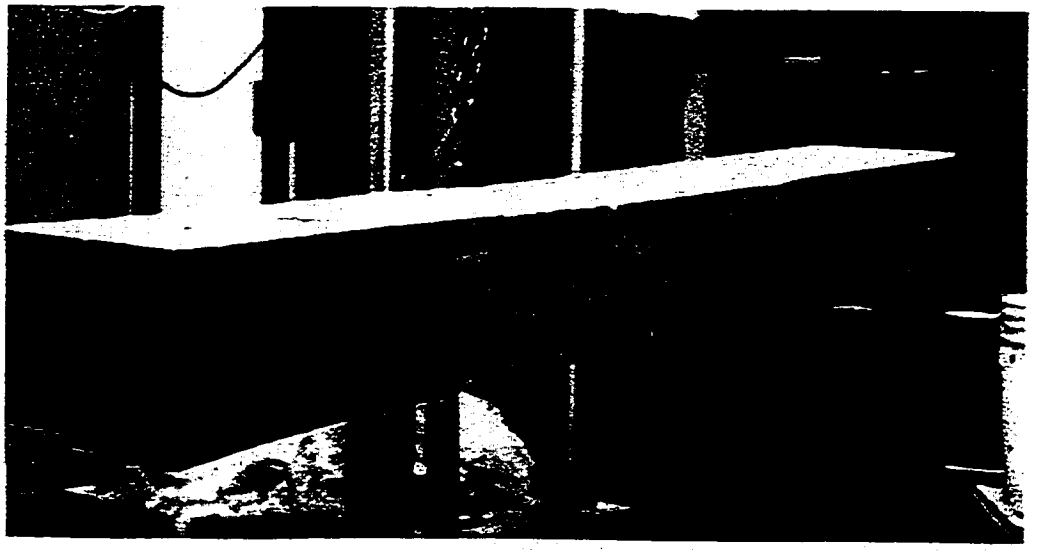

Figure 4.24 Failure of CFRP-strips in beam S1

Figure 4.25 Failure of CFRP-strips in beam S2

Figure 4.26 Failure of CFRP-strips in beam S3

	S1	S2	S3
Calculated Nominal Moment (kN·m)	25.7	22.9	69.2
Calculated Nominal Moment with CFRP(kN·m)	60	33	144
Expected Failure Load (kN)	141	78	339
Expected Increase in Capacity %	133	44	108
Actual Failure Load (kN)	130	96	255
Actual Nominal Moment (kN·m)	55.4	40.8	102
Actual Increase in Capacity %	116	78	45

Table 4.4 Summary of Results of Series S1, S2 and S3

4. 4 Cyclic Testing

4.4. 1 Objective

Patching the beam is necessary to be able to apply the strips to it. As mentioned before, some of the beams were poorly patched about 10 years ago. This patch has proven to be weak and badly bonded to the concrete. In most of the tests the mortar was the first to fall away when the beam was loaded. There was great concern that this would affect the whole process of rehabilitation, as it would be useless to apply strips and then have the cover fall with the strips. Two cyclic tests were performed on the two beams patched but not reinforced with CFRP-strips. The goal was to see how the mortar behaved under repeated loading that would represent a sufficient number of years in service. Such test would reveal if there was a significant difference between the Sika product Sika 224 (see Table 4.2), and normal cement patch subject to cyclic loading, as there was little or no difference in static loading. The patch in two webs was held in place by CFRP-sheets (Figure 4.27) to see if the CFRP-sheets would hold the mortar in place better. Hence, for each of the two beams, one web was covered with vertical sheets 100 mm long from the inside and 25 mm long from the outside, with a spacing of 50 mm between each two sheets. The other web was left as it was, only patched. To determine if the capacity of the beams was affected by the continuous cyclic loading, the beams were statically failed after the cyclic loading.

4.4. 2 Calculations

The range of the cyclic load has to be in the range of the maximum and the minimum expected service loads. The maximum expected service load is the dead load,

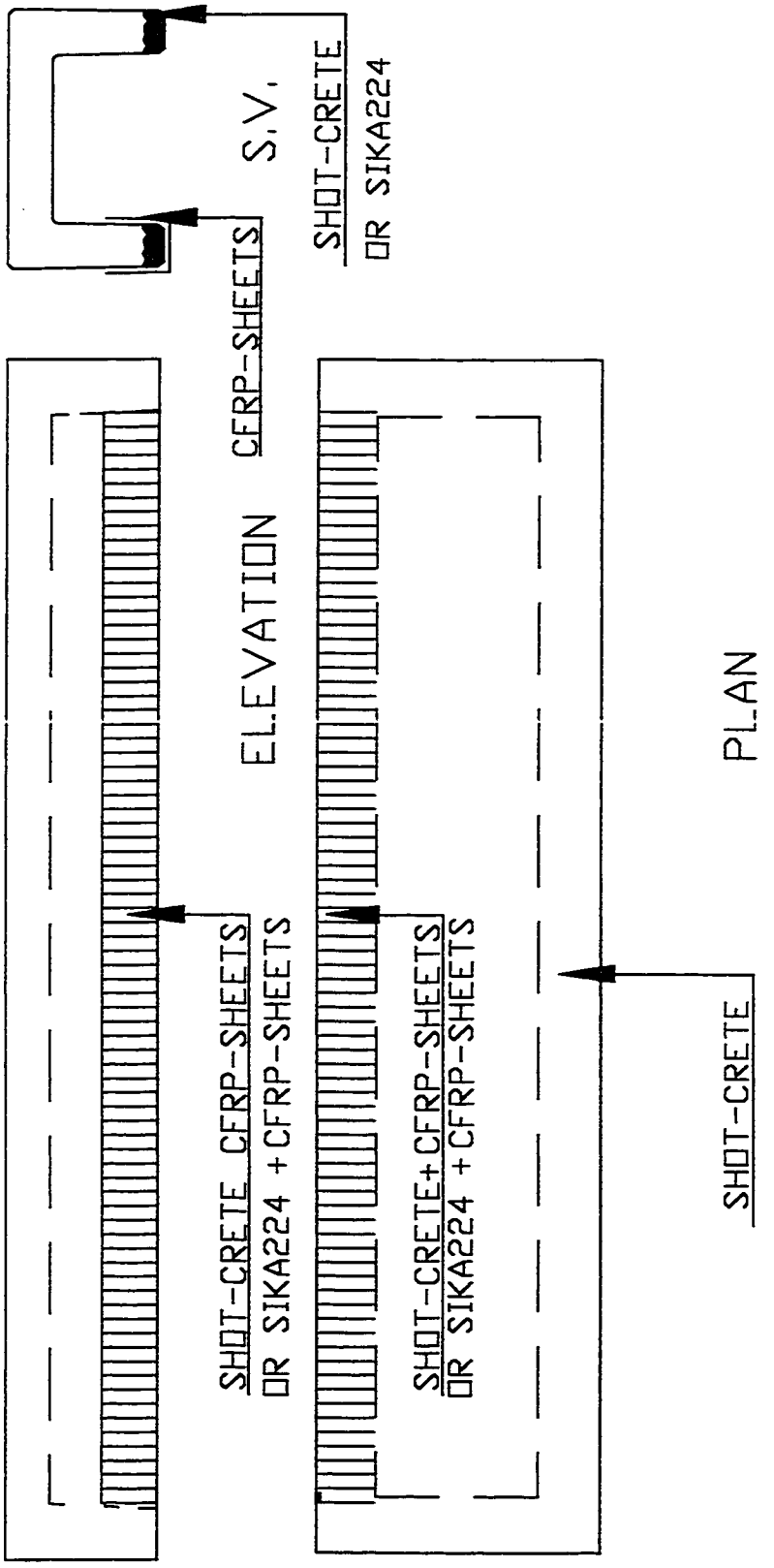

Figure 4.27 Layout of CFRP-sheets in Cyclic Testing

the assumed wearing surface and the 20 t truck as recommended by the Bridge Code, while the minimum load would be the floor cover and dead load only.

Full calculations of the maximum expected load and moment will follow. Present purposes:

$$M_{max} = M_{D.L.+F.C.+L.L.} = 14 + 86 + 360 = 470\,kN \cdot m$$
$$M_{min} = M_{sustained} = 86 + 14 = 100\,kN \cdot m$$

The ratio between M_{max}/M_n and the ratio between M_{min}/M_n represent the load ratios between maximum and minimum loads used in the tests and the nominal load.

$$\frac{M_{max}}{M_n} = \frac{470}{820} = 0.57$$

$$\frac{M_{min}}{M_n} = \frac{100}{820} = 0.12$$

Use:

$$P_{max} = 0.57\,P_n = 0.57 \times 353 \cong 200\,kN$$

$$P_{min} = 0.12\ P_n = 0.12 \times 353 \cong 40\,kN$$

For a more critical case use:

$$P_{min} = 10\,kN$$

4.4. 3 Tests

Test 15:

3500 cycles between 10 and 200 kN were applied at a frequency of 0.2 Hz. The maximum deflection of the beam remained at 37 mm from the beginning till the end of this stage of test. The amplitude of the load was increased to oscillate between 10 and 250 kN for another 3000 cycles at the same speed; it was noticed that the maximum deflection was also constant at 42 mm from the beginning till the end of the test. No cracks were observed, which indicated that the loading was within the elastic range and did not affect the strength

of the beam. After the cyclic loading the beam was unloaded and statically reloaded to failure. Failure was reached at a load of 368 kN, the same as in the flexural tests on the beams in their in-situ condition. The strains in the steel as well as the concrete, the reactions under each web and vertical deflection at midspan were measured. The strains in the steel and concrete were linear throughout the whole cyclic test sequence, which indicates that the cyclic loads did not affect the beam.

Test 16:

The second beam was subjected to the same loading regime: 3500 cycles between 10 and 200 kN at a rate of 0.2 Hz were applied. The maximum deflection of the beam remained at 41 mm from the beginning till the end of this stage. 41 mm is a larger deflection than occurred with the first beam but still in the elastic range. The amplitude of the load was raised again to be between 10 and 250 kN for another 3000 cycles at the same rate. This time the maximum deflection was constant at 44 mm from the beginning till the end of the test. After the cyclic loading the beam was unloaded and statically reloaded to failure. Failure was reached at a load of 370 kN, again slightly more but comparable to the ultimate loads of the beams tested originally. The strains in the steel as well as the concrete, the reactions under each web and vertical deflection at mid-span were measured.

4.4. 4 Results of Cyclic Tests

The strains in the steel and concrete, as well as the vertical deflection, were linear throughout the whole cyclic tests (Figures 4.28, 4.29 and 4.30), indicating only a minor effect of the cyclic loads on the beam. The results also indicated that the CFRP-sheets had only a minor effect, which makes use of them uneconomic for this application. There was no advantage in using the Sika224 product in these tests. This product may be useful in the

long run (requiring further research beyond the scope of this thesis). The beams should not be affected by cyclic truck-loads as shown in these tests.

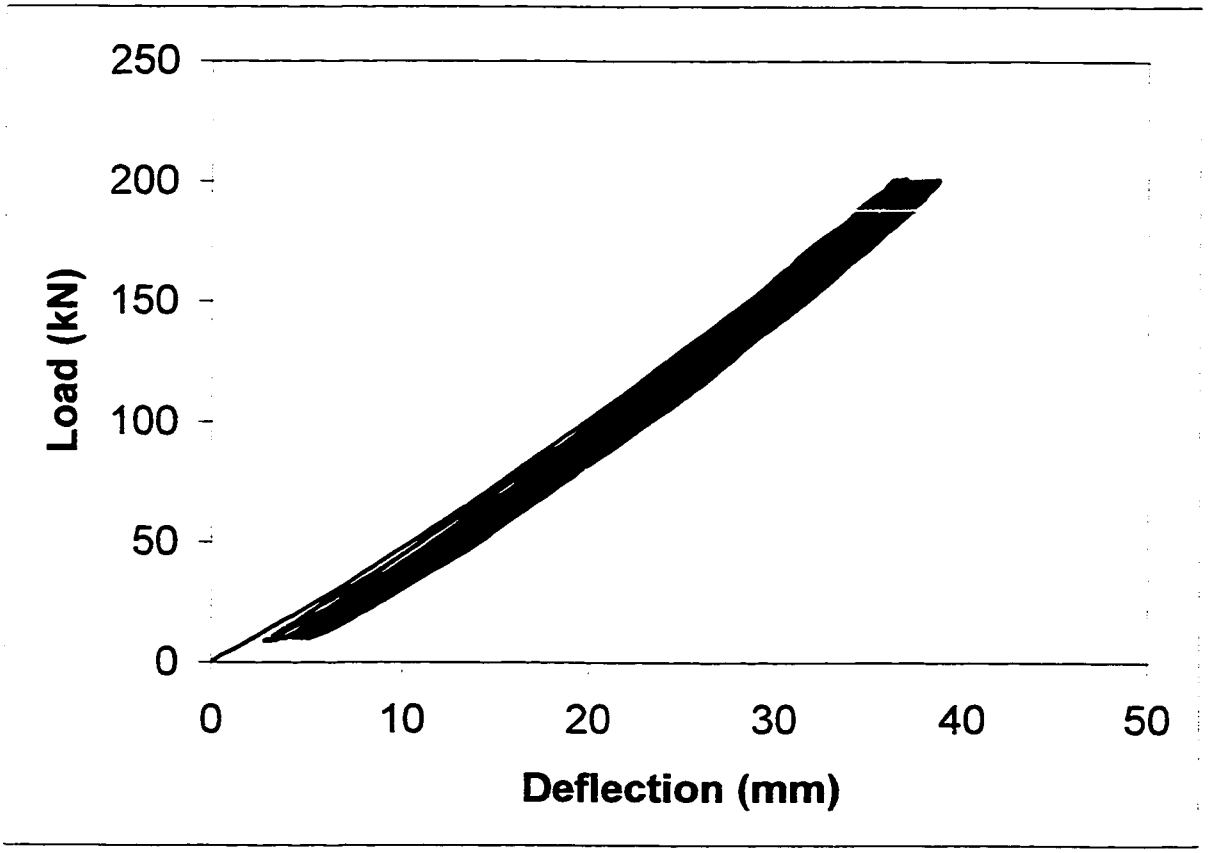

Figure 4.28 Vertical Deflection in Cyclic Test

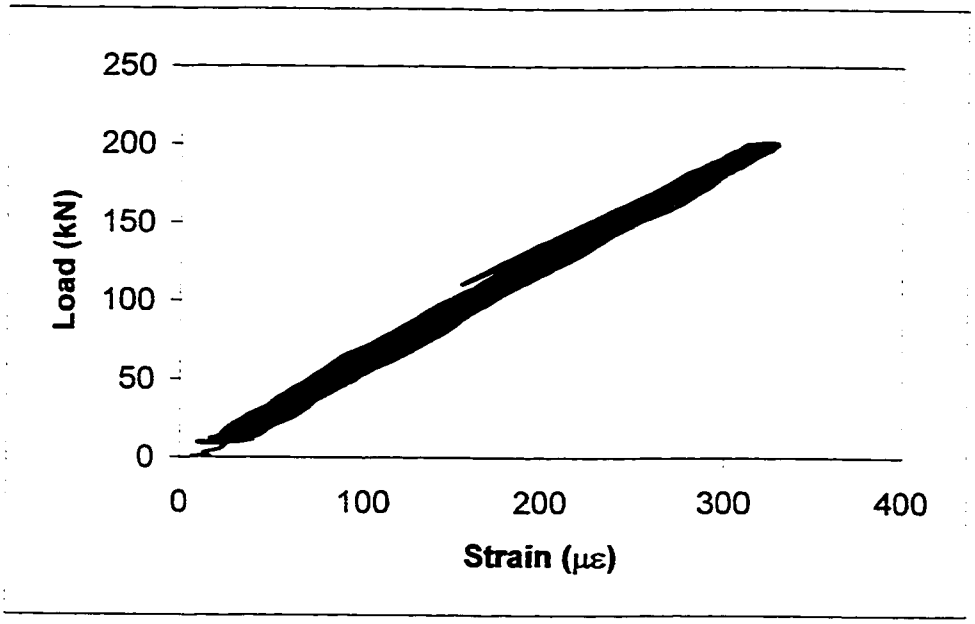

Figure 4.29 Concrete Strain in Cyclic Test

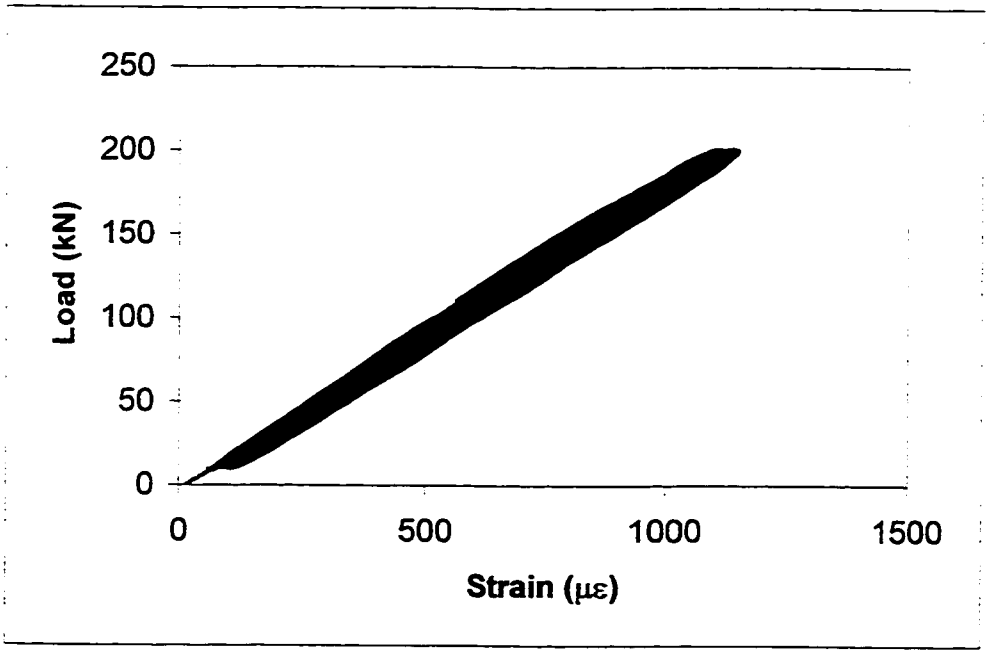

Figure 4.30 Steel Strain in Cyclic Test

CHAPTER 5

EXTERNAL POST-TENSIONING TO REHABILITATE THE BEAMS

5. 1 Introduction

The results of the tests using the CFRP-strips for rehabilitation of the bridge girders led to the conclusion that the method still needs more testing and research for this particular application. The need for a different method of rehabilitation was therefore essential. External post-tensioning was an attractive solution, which thus needed to be analyzed and tested to prove the efficiency of the method.

A detailed analysis of the bridge girder was made. The required capacity of the beams under the maximum specified truckloads was determined. This capacity was compared with the actual capacity of the beams to calculate the amount and location of post-tensioning needed. The bars were chosen from several commercial brands on the basis of the efficiency and true needs of the project.

The tendon layout was chosen to provide a number of effects, and with the method of post-tensioning, had to be practical for field installation. The anchorage of the bar to the beam was tested in part and then fully on two beams. The test results lead to a series of conclusions and recommendations.

5. 2 Analysis

5.2. 1 Objective

External post-tensioning is a reliable method to enhance the flexural capacity of concrete members. The main objective here was to enhance the flexural capacity of the members so that the beams could safely resist the truck loads in the CHBDC (Canadian Highway and Bridge Design Code). As Alberta Transportation requested, the traffic on top of the bridge must not be disturbed. The beams had to be post-tensioned by working from underneath the bridge only. This introduced the problem of anchoring the bars to the bridge beams. While increasing the shear capacity was not a specific objective, the shear capacity was increased as well because of the post-tensioning bars.

Two sets of calculations were performed: the actual capacity of the beams in their current condition and to increase the capacity of the beams to the required capacity using unbonded post-tensioning bars.

5.2. 2 The Capacity Including Post-Tensioning

The method used to calculate the flexural capacity of the girder with external post-tensioning was that specified in the CSA-A23.3-94. This method has proven to be efficient in the calculations of the moment of resistance of a beam externally prestressed (or post-tensioned), based on an approximate equation for calculating the stress in the bar. The cross-section of the beam was idealized as seen in Figure 5.1 to ease the calculations of the properties of the section.

The moment of the cross-section after external post-tensioning has to be bigger than the required factored moment calculated above. One 1-inch (25.4 mm) DYWIDAG bar was selected to produce the desired force needed for the section. The calculations were:

$$M_r = \phi_p f_{pr} A_p \left(d_p - \frac{a}{2} \right) + \phi_s A_s f_y \left(d_s - \frac{a}{2} \right)$$

$$f_{pr} = f_{pe} + \frac{8000}{l_e}(d_p - c_y)$$

These are the two main equations for the calculation of the moment of resistance.

The following are the constants in the equations:

$\phi_p = 0.9 \qquad \phi_s = 0.85 \qquad \phi_c = 0.65$

$A_s = 6550\,mm^2 \qquad f_y = 350\,MPa$

$d_p = 535\,mm \qquad d_s = 460\,mm$

$f_c' = 45\,MPa \qquad b = 920\,mm \qquad \alpha_1 = 0.72$

$l_e = 11000\,mm$

A prestressing DYWIDAG-bar of 1-inch diameter has the following properties:

$A_p = 548\,mm^2 \qquad f_{ult} = 1034\,MPa \qquad f_{py} = 827\,MPa$

$F_{ult} = A_p \times f_{ult} = 548 \times 1034 = 567000\,N$

$F_{max} = 0.7 \times F_{ult} = 0.7 \times 567 = 397\,kN$

As there is no need to deal with the maximum force of the bar, assume

$F_{max} = 320\,kN$

Assume 10 % losses;

$F_{max\,final} = 288\,kN$

$$f_{pe} = \frac{288 \times 10^3}{548} = 526\,MPa$$

$$c_y = \frac{\phi_p A_p f_{py} + \phi_s A_s f_y}{\alpha_1 f_c' b}$$

$$c_y = \frac{0.9 \times 548 \times 827 + 0.85 \times 6550 \times 350}{0.78 \times 0.65 \times 45 \times 920} = 110\,mm < 150\,mm \qquad \text{OK.}$$

$$f_{pr} = 526 + \frac{8000}{11000} \times (530 - 110) = 831\,MPa > 827\,MPa$$

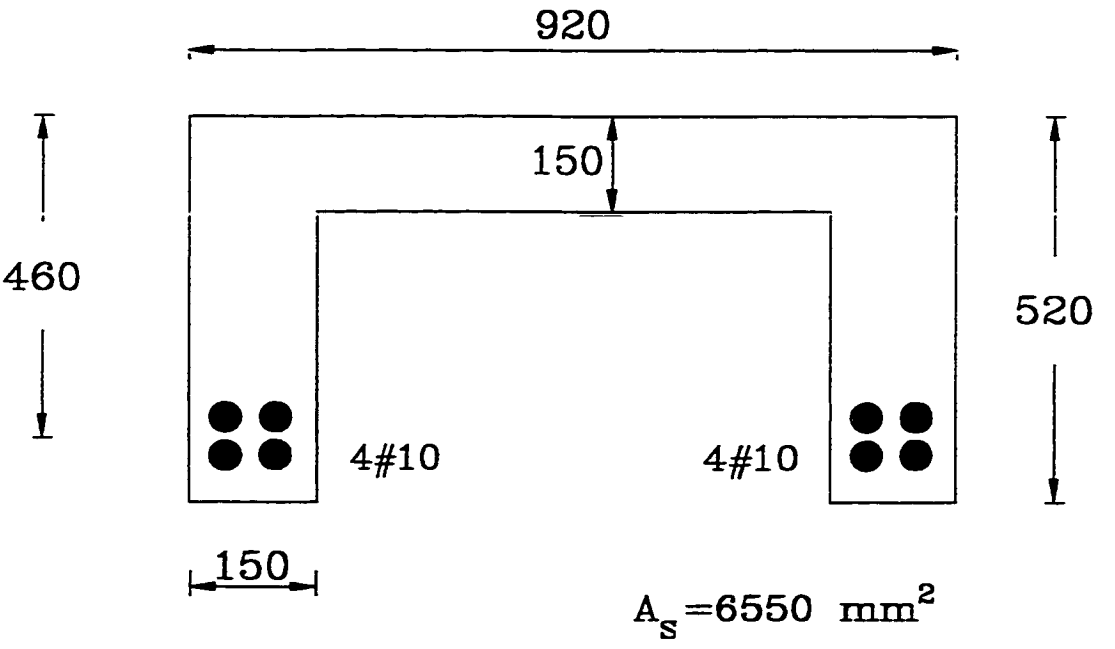

Figure 5.1 The Idealized Cross-section of the Beam

Use $f_{pr} = f_{py} = 827\,\text{MPa}$

$a \cong 0.9 \times c_y = 0.9 \times 110 = 99\,\text{mm}$

$$M_r = 0.9 \times 827 \times 548 \times \left(535 - \frac{99}{2}\right) + 0.85 \times 350 \times 6550 \times \left(460 - \frac{99}{2}\right)$$

$M_r = 987\ \text{kN} \cdot \text{m}$

This moment is larger than the required factored moment due to live loads, dead loads and impact. So the decision was to use one 1 inch prestressing bar with an initial post-tensioning force of 320 kN.

5. 3 Layout of the Bars

The layout of the bars can be seen in Figure 5.2. Several aspects were considered in the layout. Work had to be performed only from underneath the beams so that traffic would not be interrupted. The beams are in the field beside each other, so work cannot be done on the outside of the beams. The diaphragms of the beams in the laboratory were badly damaged. The low level of reinforcement indicates the diaphragms cannot be depended upon. The soffits of the beams are damaged mostly towards the ends of the beams, so it was better to use them as deflection points near the midspan.

The idea of the post-tensioning was to jack the whole system in one operation. This was done by connecting the four inclined bars with the straight bar by a steel hollow circular section. The circular shape was chosen to make it easier to drill holes at different angles. Teflon plates greased with vaseline were put between the circular sections and the soffits of the beams. As one end of the horizontal bar is stressed, the horizontal bar applies compression on the two circular pipes. The circular pipes move towards the centre of the beam and can slide along the soffits of the beam due to the existence of the teflon plates.

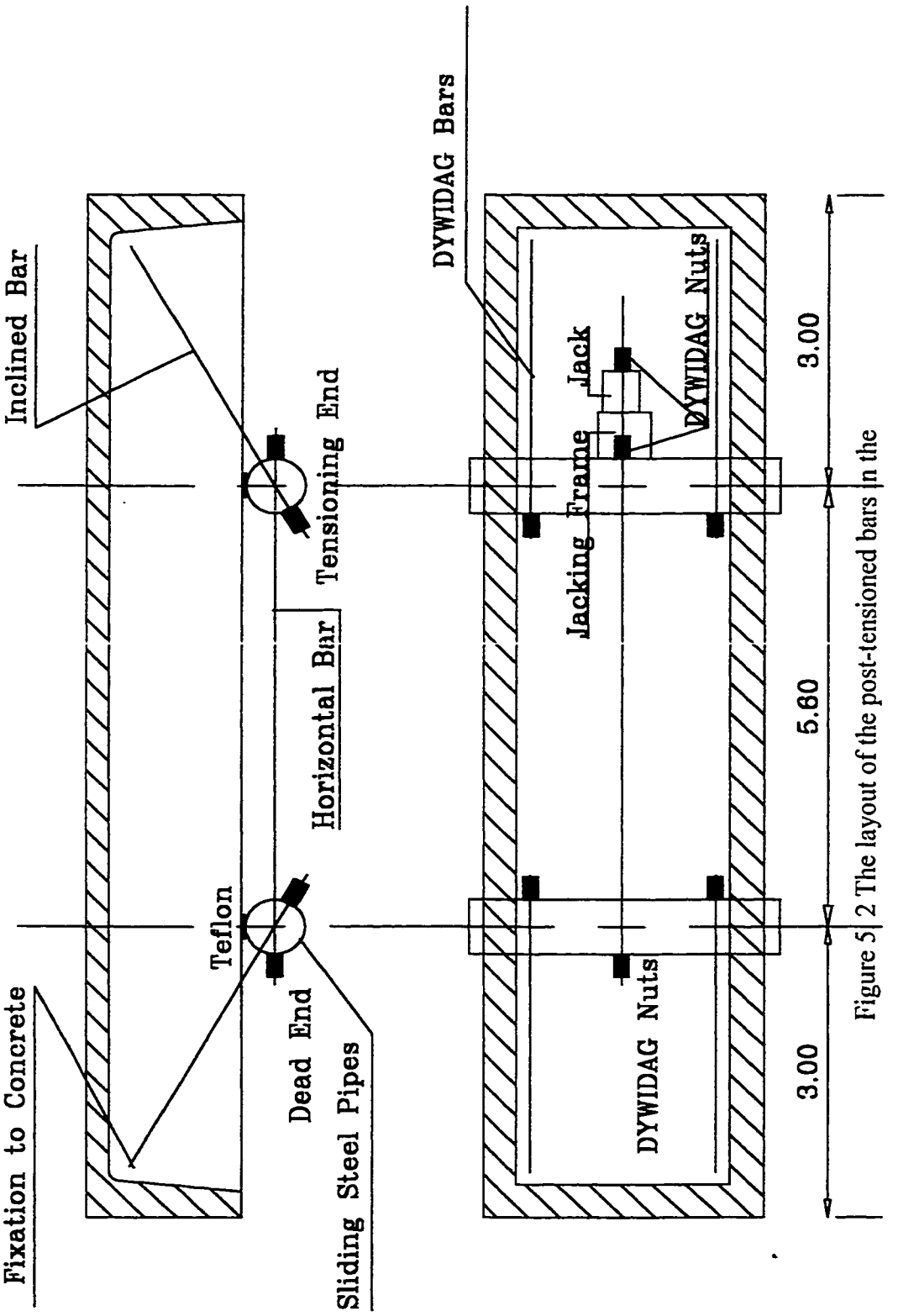

Figure 5| 2 The layout of the post-tensioned bars in the girders

This stretches the inclined bars at both ends of the beam, as they are fixed to the ends of the beam. The jacking details are shown in Figure 5.3. Another advantage of the stressing system devised is the production of a constant moment zone due to the post-tensioning around midspan. For aesthetic reasons one could hide half the circular section inside the girder to produce effective but better looking rehabilitation. Such a design detail would not affect the principle shown by the results of the tests.

5. 4 Connection to Fix the Bars (Design and Testing)

The idea of using a steel connection fixing the inclined bars to the concrete webs was raised after determining that it was not possible to fix the bars to the diaphragms of the beams directly and obtain sufficient resistance for the required post-tensioning force. The diaphragms were, as previously noted, damaged and weakly reinforced. The steel connection (Figure 5.4, and Figure 5.5) was designed to resist a force of 200 kN in service conditions. The connection is an eccentric connection, which resists direct shear, torsion and moment, as seen in the drawing. The places of the stirrups and the reinforcing bars, as well as the fillets on the inside of the beams were taken into consideration in the design (Figure 5.6). The connection was designed to be light weight with the least number of anchor bolts to be safe. The anchor bolts were high strength UCAN-fasteners with 12 mm diameter. The properties of the bolts are listed in Table 5.1.

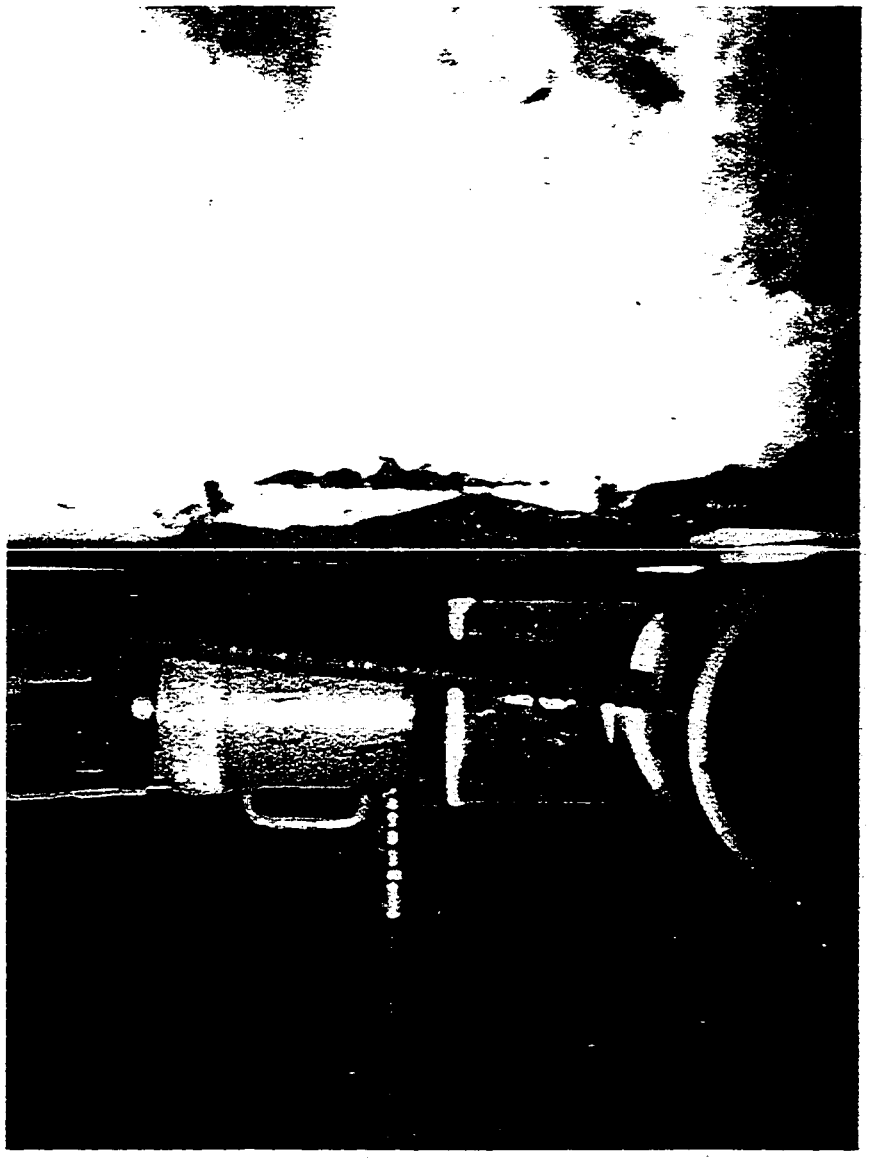

Figure 5. 3 The Jacking Detail

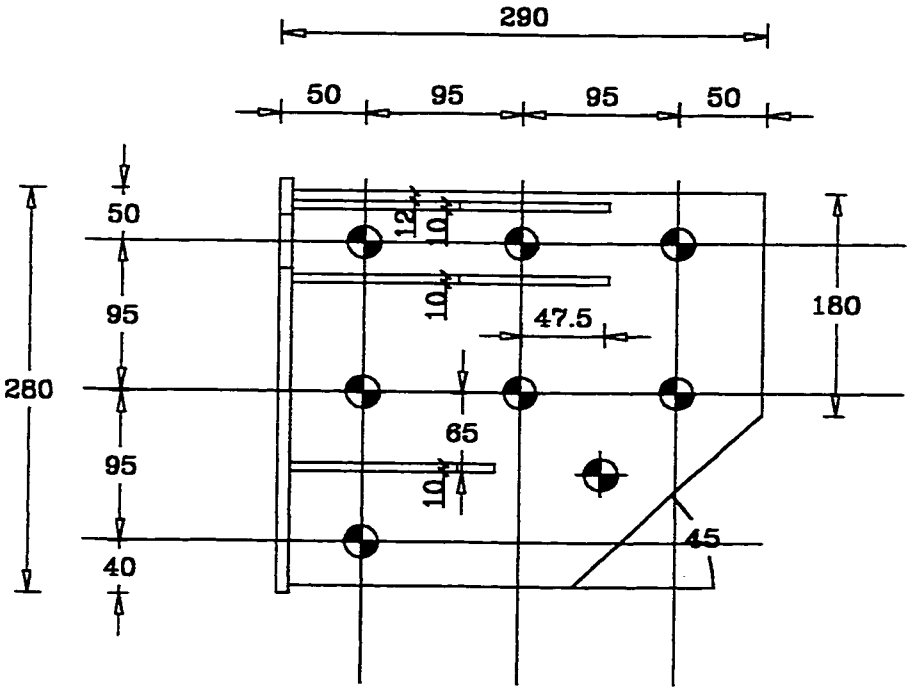

Figure 5. 4 The Dimensions of the Steel Connection

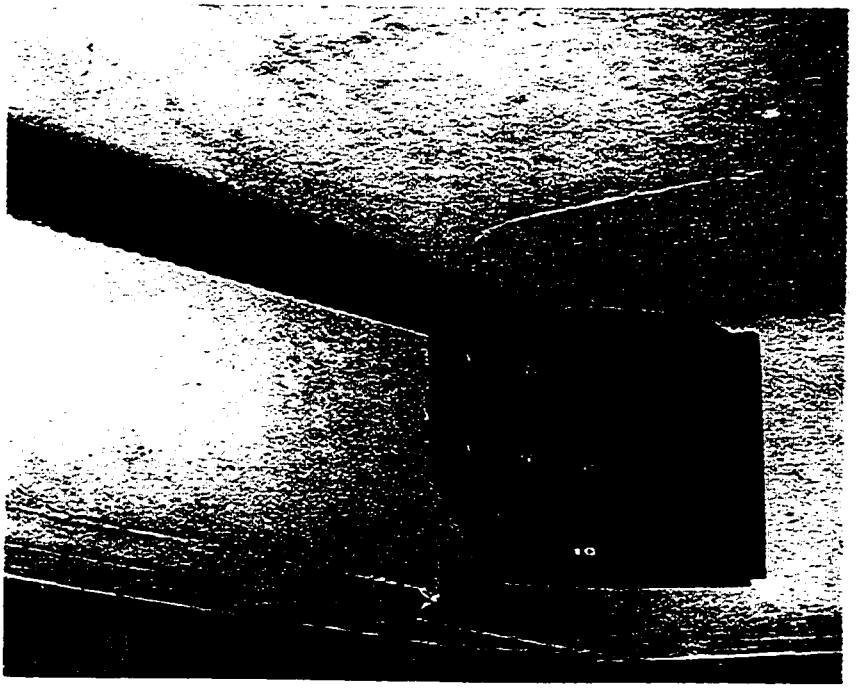

Figure 5. 5 The Used Steel Connection Mounted on the Web

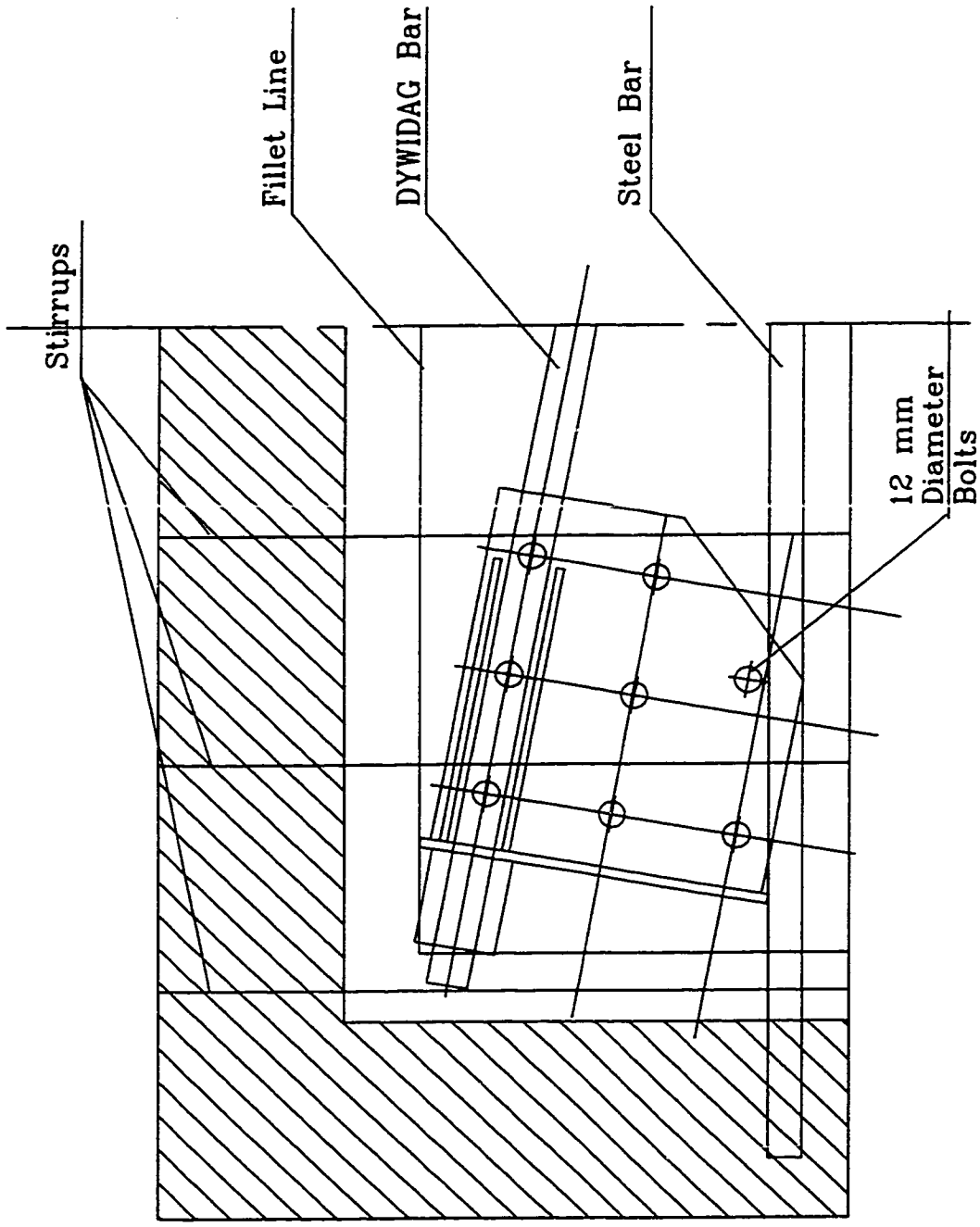

Figure 5.6 The location of the connection on the webs of the beams

Type of Load	Concrete Compressive Strength	Load Data	
		Tension	Shear
Average Ultimate Load	28 MPa	51 kN	85.9 kN
Average Working load	21 MPa	12.5 kN	23.3 kN
	28 MPa	14.6 kN	24.5 kN
	45 MPa	19.5 kN	27.4 kN

Table 5.1 Properties of Anchor Bolts used in Testing

The connection was designed for a maximum service load of 200 kN. This load results in a total shear force of 200 kN, a moment of 10 kN·m and a torsional moment of 20 kN·m between the connection and the beam. Summing up the total tension and shear on the most critical bolt and using the integration equation, it was found that these straining actions were safe with the number and configuration of the bolts shown in the figures.

To prove the safety of the design a pullout test was carried out. A trial connection was mounted on one part of a previously tested beam as shown in Figure 5.7. A DYWIDAG-bar was fixed to the connection and was jacked against a steel hollow section. The connection failed suddenly at an ultimate load of 335 kN. The failure was caused by direct shear on three of the bolts: two of them were in the row of bolts under the DYWIDAG-bar. The direct shear failure was not surprising, as shear is the dominant factor of the straining actions. The failure load was substantially higher than the maximum service load the connection will be exposed to, the factor of safety thus providing confidence in satisfactory performance.

5. 5 Preparation for the Tests

5.5. 1 Mounting of Connections and Bars

After proving the safety of the connection under high load, tests were performed on the beams. Two beams were randomly chosen to be tested. Eight connections were manufactured, four for each beam. A template was used while drilling the holes in the webs of the beams. The template assured the accuracy of the placement of the holes to ease the mounting of the connection. The place of the first bolt was determined, and then drilled. The place of the second hole was also determined and drilled. The template was then fixed to the web using the two bolts, and the other six bolts were drilled through the template.

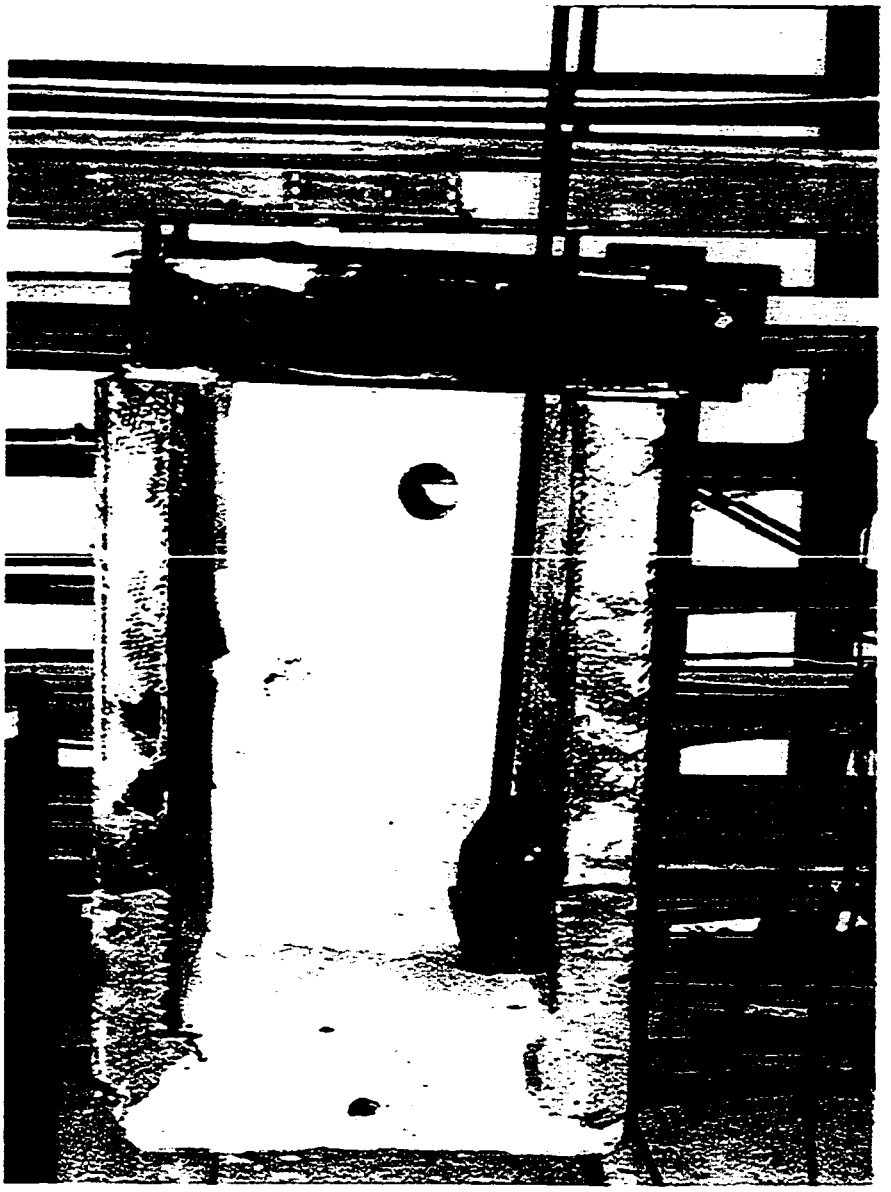

Figure 5. 7 The Pull-out Test on a Trial Connection

Due to the inaccuracy of the spacing of the stirrups, sometimes stirrups were hit and the connection had to be held by seven bolts only. The big factor of safety, though, permitted the use of seven bolts without concern for the safety of the connection. After the four connections had been mounted the inclined bars were bolted to the connection. The circular pipes, previously drilled at the angle and spacing needed, were put on the inclined bars and a nut and washer placed loosely behind the pipe on each bar. The central bar was inserted to connect the two circular pipes. To avoid local buckling of the circular pipe during tensioning, a stiffening plate was put between the end of the horizontal bar and the circular pipe. To hold the system in place, temporarily ropes were put around the bars.

5.5. 2 Strain-Gauging the Beam

A strain gauge was put on each DYWIDAG bar. The idea of the steel strain gauges was to monitor load during post-tensioning. The force is the central bar was measured, and the four inclined bars could be checked for almost equal forces. The strain gauges helped also to monitor losses in the bars after the post-tensioning procedure was complete to determine the final prestressing force in the bars during testing.

Four concrete gauges were planned to be mounted on the top of the beam after the post-tensioning procedure. The reason for waiting until after the post-tensioning was to avoid the damage of the gauges. The gauges on the top fibre of the beam could have been under tension and any crack in the concrete would have damaged the gauges.

The vertical deflection was also planned to be measured. After post-tensioning vertical deflection transducers were positioned to measure the deflection during flexural testing.

5.5. 3 The Post-Tensioning

Prior to post-tensioning the beam was moved under the flexural testing frame and placed for testing. To assure sliding of the pipes during post-tensioning two teflon plates separated by a thin stainless steel plate greased with vaseline were placed at the contact points between the circular pipes and the beam. Where the web was damaged, shims and neoprene pads were put on top of the Teflon plates to assure the distribution of the load on the soffit of the web. Figure 5.8 shows the sliding which happened between the Teflon plates due to post-tensioning.

The jacking frame was put on the pipe behind the nut, and then the loading ram, a thick plate (serving as a washer) and a second nut (Figure 5.9). The load was applied gradually to the bar with strain readings being taken every 50 kN to assess equal distribution of the strain as shown in Figures 5.10 and 5.11. When the load in the horizontal bar reached 320 kN the first nut was tightened against the pipe to hold the load and the loading ram was released. An expected loss of about 8 % happened in the bars after releasing the load to drop the load to about 295 kN. This was revealed by the strain readings taken after the release of the loading ram.

The day after post-tensioning, the concrete gauges and the deflection transducers were mounted as planned.

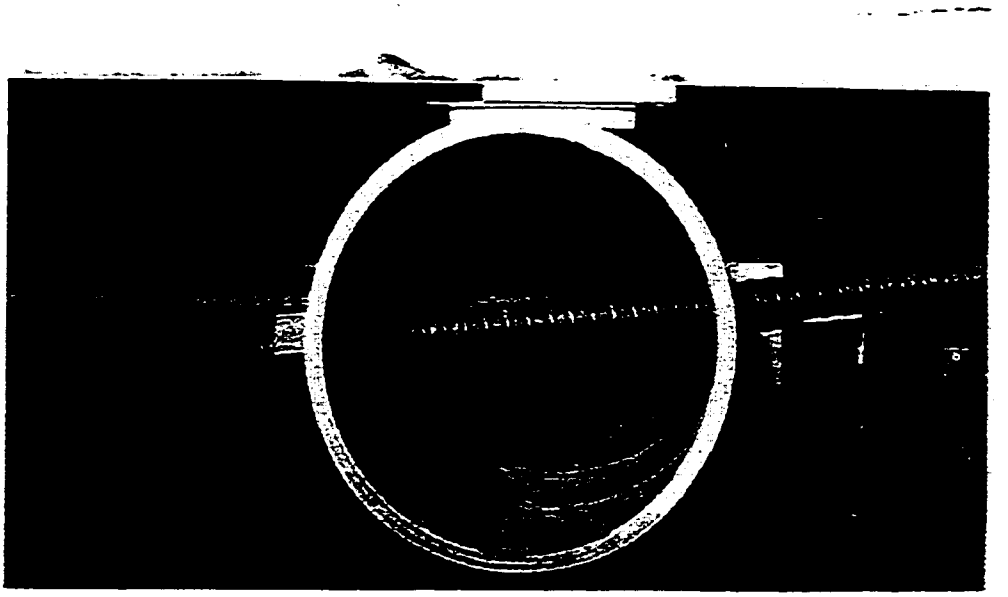

Figure 5. 8 The Sliding in the Teflon Plates due to the Axial Deformation of the Bar

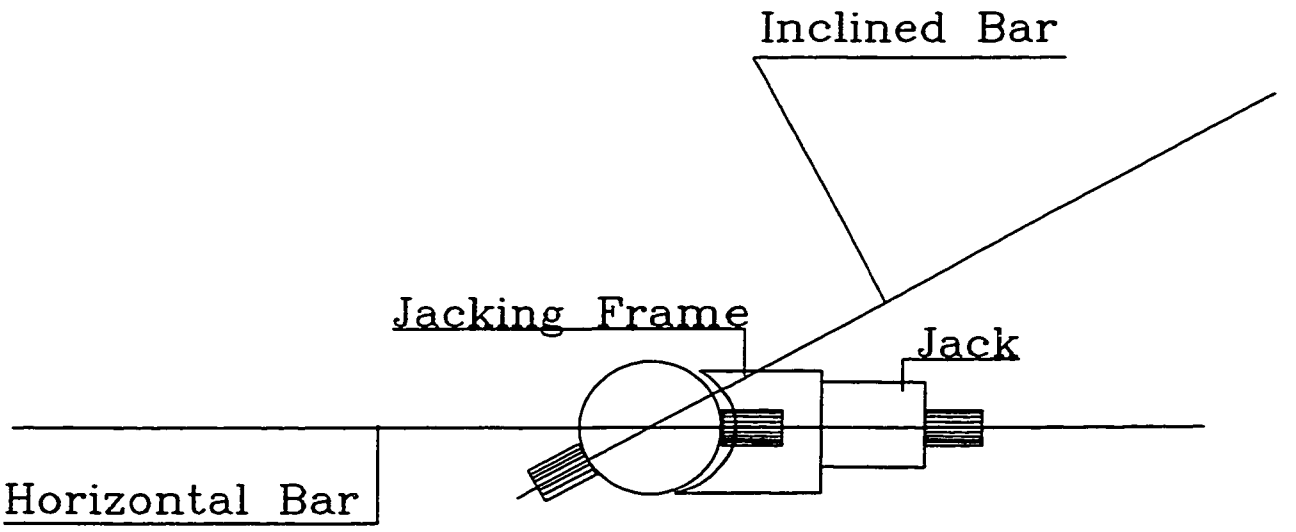

Figure 5. 9 The Jacking System Used in Post-Tensioning

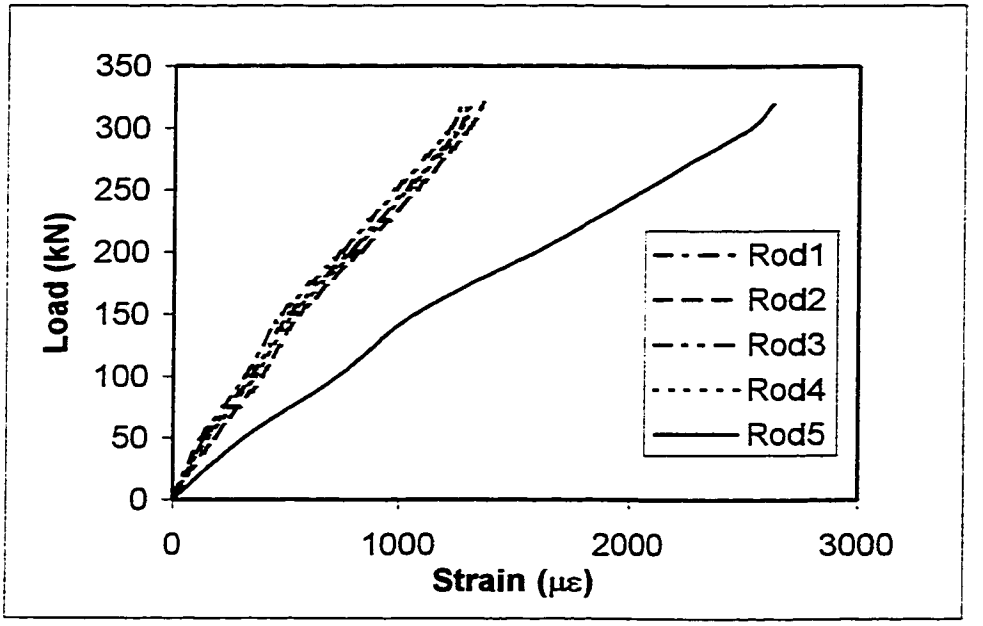

Figure 5. 10 The Strain in the Bars During Post-tensioning (First Beam)

Rods 1-4 inclined, 5 horizontal

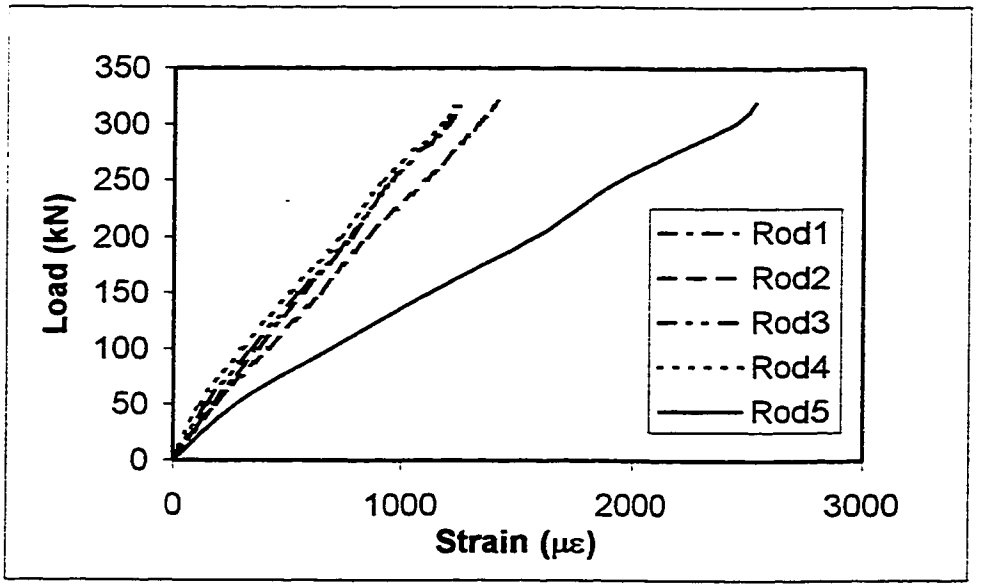

Figure 5. 11 The Strain in the Bars During Post-tensioning (Second Beam)

Rods 1-4 inclined. Rod 5 horizontal

5. 6 Testing

Test 17:

The beams were tested flexurally in four point loading, with two loading points on each web. The test span was 10.50 m (beam length 11.6 m). The same testing configuration as the previous flexural tests was used (Figure 5.12), to be able to compare the results between the different tests performed. The test was performed on the day after post-tensioning. Readings were taken every 5 seconds as the load (and stroke) could not be controlled. The strain in the DYWIDAG bars and the midspan deflection increased linearly during the test. The reinforcing steel inside the beam yielded at a load of 420 kN and the beam carried only a small amount of load beyond that. The test was stopped at 424 kN when traces of concrete crushing at the top fibre of the beam became apparent. During unloading, the beam almost returned to a state of zero deflection, which means that the DYWIDAG bars were still elastic, and able to release some tension at the bottom of the beam to return the beam almost to its original shape. The maximum deflection reached was 75 mm and the residual deflection of the beam was 15 mm.

Test 18:

This test was on the second post-tensioned beam. The same configuration and procedure as before was used. The objective was to verify the calculations done with more than one test to be sure that the results are consistent over all the beams. The reinforcing steel started yielding at about 430 kN and the test was stopped at a load of 437 kN. A margin of 3 % difference in failure load gives high confidence in the rehabilitation procedure. The maximum deflection was 76 mm returning to 16 mm after unloading the beam.

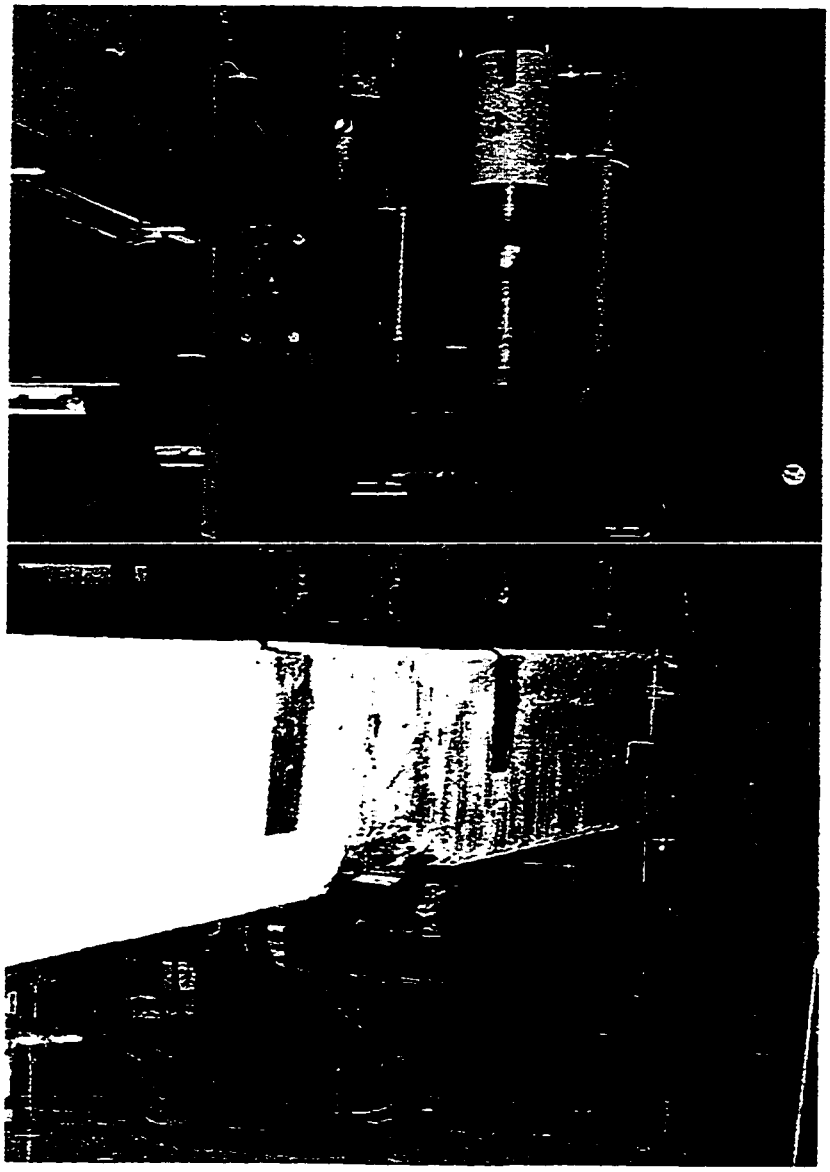

Figure 5. 12 Beam under Testing Frame

5. 7 Results and Conclusions

The major results of these two tests are shown in Table 5.2. The beams have achieved on average the capacity they were designed for. The results of the tests were consistent. Figure 5.13 shows the vertical deflection in both beams while Figure 5.14 shows the concrete strain in both beams. The sequence of the tests has shown the reliability of the calculations. Yield of the reinforcing steel was predicted to occur first followed by the crushing of concrete crushing of the concrete. The capacity of the beams was increased by 21% - 22% as aimed, giving the beams the strength needed with a reliable and predictable method. Smaller deflections compared to those in the tests on beams in their original state or the tests with the CFRP-strips was also expected, because the prestressing increases the stiffness of the beams. The strain in the DYWIDAG bars tends to increase less with increasing load as shown in Figures 5.15 and 5.16. This is understandable because there is no strain compatibility between the unbonded DYWIDAG bars and the concrete. As the concrete beam deflects with the load the DYWIDAG bars tend to be more straight than the beam.

One could conclude that the tests have proven the external post-tensioning used to be a reliable method to increase the flexural capacity of the beams. Unlike the CFRP-strips, the mode of failure was as predicted from the calculations and the loads and moments achieved were almost the same as expected.

BEAM	B7	B9
Tested span in flexure	10500 mm	10500 mm
Maximum flexural load	437 kN	424 kN
Maximum nominal moment	1016 kN·m	986 kN·m
Expected nominal moment	987 kN·m	987 kN·m
Maximum vertical deflection	76 mm	75 mm
Permanent Deflection	16 mm	15 mm

Table 5.2 Summary of Major Results

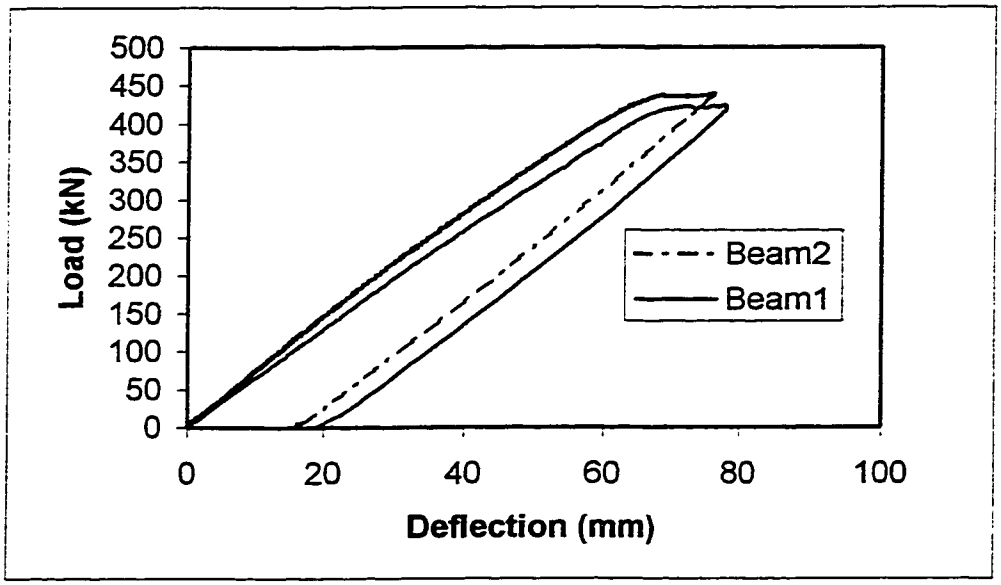

Figure 5. 13 The Vertical Deflection in Both Beams

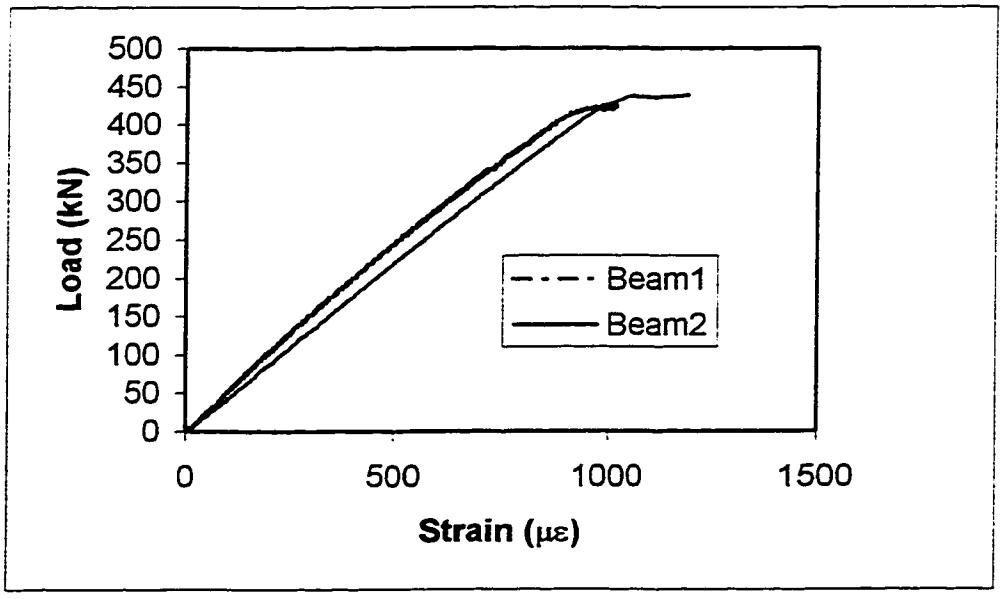

Figure 5. 14 The Concrete Strain in Both Beams

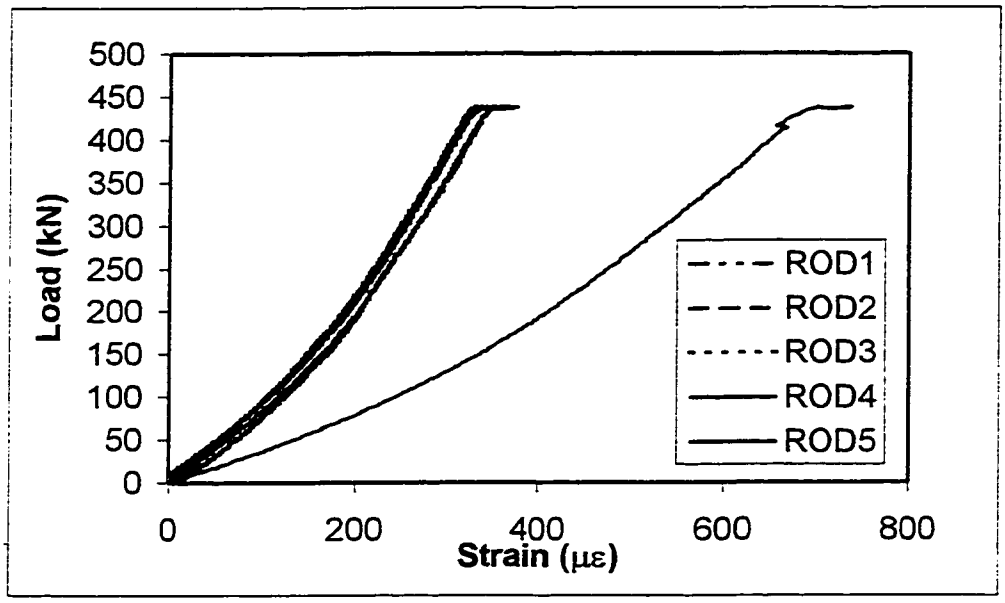

Figure 5. 15 The Strain in the Post-tensioned Steel During Testing of First Beam

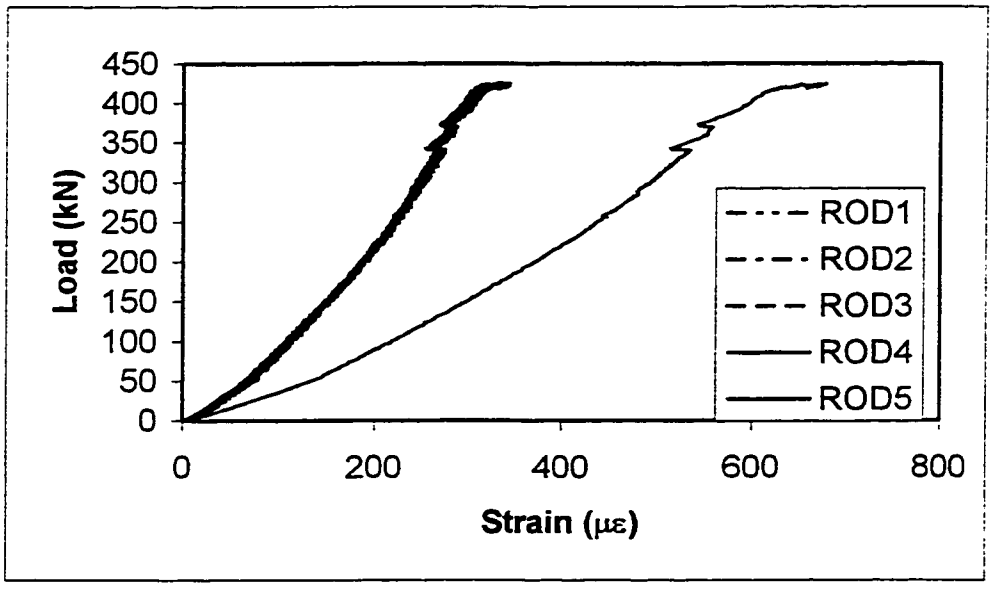

Figure 5. 16 The Strain in the Post-Tensioned Steel During Testing of Second Beam

CHAPTER 6

CONCLUSIONS AND RECOMMENDATIONS

6. 1 Introduction

The main objective of the project was to find a simple, economic and reliable method to increase the flexural capacity of the bridge beams. Several different tests were performed and the results were evaluated. The flexural capacity of the beams, rather than the shear capacity needed to be enhanced. Two methods of rehabilitation were examined. With the CFRP-strips there was less enhancement than expected: a truss model was used to explain this result. However sufficient strengthening was obtained with external post-tensioning, but some improvements with the technique are possible.

6. 2 Conclusions

6.2. 1 Current Condition of the Girders

It was proven that the flexural and shear capacities of the beams did not depend on their condition as extracted from the bridge. The beams have shown high resistance to flexure and shear loads, even if the reinforcing bars were corroded, the beams were cracked or the concrete cover had spalled. The need to enhance the capacity of the beams remained, though, because of the increase in permitted truck loads.

The tests showed that the shear capacity of the beams is higher than the flexural capacity. This is understandable, because a reinforced concrete beam should always be designed to have the ultimate flexural capacity less than the ultimate shear capacity. In this way, a ductile failure mode is always guaranteed.

6.2. 2 Strengthening Using CFRP-Strips/Sheets

6.2.2. 1 Flexural Strengthening Using CFRP-Strips

The results of the flexural tests performed on the bridge girders reinforced with CFRP indicated a sudden and unpredicted failure to the beams. These tests and the three tests performed on small beams showed that the geometric shape of a beam significantly affects the ability of CFRP-strips to strengthen that beam. For narrow webs there appears to be a lack of shear transfer to the level of the strips. This results in initial inclined cracks between the level of the steel reinforcement and the level of the CFRP-strips that start delamination of the strips. However with wider beams the area of plain concrete seemed to be wide enough to transfer the shear.

The truss model proposed, provides direction as to the mode of failure of the beams. The truss model is a good way of understanding how any reinforced concrete beam would behave if externally reinforced.

The strain profiles shown in Chapter 4 showed a clear trend in both tested beams that compatibility of strain was lacking in the stages of loading after the critical crack appeared. It is obvious that the strain in the CFRP-strips increases at a faster rate than in the steel reinforcing bars until the steel begins to yield and the strips separate. This latter statement raises doubt in the credibility of the compatibility method in the design of beams externally reinforced with CFRP.

6.2.2. 2 Shear Strengthening Using CFRP-Sheets

The CFRP-sheets were successful in resisting shear forces, and in anchoring the strips to let the beam carry a higher load. In shear, the inclined sheets served as external "bent bars" and helped the beam carry a shear load very close to that predicted. The sheets

did not prevent shear cracks from happening; the sheets just bridged the cracks to increase the load, and then the sheets failed through bond as expected, not by rupture.

In anchoring, the sheets held the strips at the ends of the beam. After the strips started debonding the beam worked as a tied arch, with the CFRP-sheets anchoring the "tie" of the beam. This let the beam carry more load than if the sheets had not been mounted.

6.2.2. 3 Cyclic Loading

The cyclic tests indicated no significant difference between the two grouts used to patch the beam. The failure loads in the two beams tested were the same. Furthermore, the static failure load remained the same as in the original tests after almost 7000 cycles to each beam. The beams behaved elastically until the end of the tests. Thus, the cyclic loading had no effect on the overall capacity of the beams, and had no effect on the grout up to the level tested.

6.2. 3 The External Post-Tensioning

The beams tested after being post-tensioned externally showed a significant increase in the flexural capacity. The maximum ultimate load was near the load predicted in the design. The external post-tensioning succeeded in increasing the flexural capacity of the beams by about 22 %, indicating that this is a suitable method to rehabilitate the bridge girders. The failure mode was ductile as the reinforcement bars started yielding inside the beam and the beam carried little or no more load. Small traces of compression failure could be seen in the top fibres of the beam towards the end of the test.

The shear capacity would be improved as well due to external post-tensioning, but no tests were performed to verify this statement.

6. 3 Recommendations for Further Research

6.3. 1 CFRP-Strips

More research is needed in the field of strengthening beams using externally bonded CFRP-strips. Three different directions of research are proposed:

1) As there was a lack of shear transfer in the beams, an experimental programme would be started to test beams with externally bonded stirrups. This would increase the flexural capacity of the beams as the initial inclined crack would be avoided. The external stirrups could to be CFRP-sheets or even GFRP-sheets as the latter are cheaper. Through a truss model the designated amount and bond length of these stirrups could be calculated and then tested.

2) Numerical modeling through a finite element analysis could be used to verify the experimental work done here. Finite element analysis would provide an opportunity to generalize the model and deduce design equations for the future design of externally reinforced beams.

3) An experimental and analytical parametric study is required to derive relations between the ability of the CFRP-strips to enhance flexural capacity and the geometric shape of the beams, the beams' reinforcement ratio, the yield strength of the steel and the concrete compressive strength.

6.3. 2 External Post-Tensioning

Research in the direction of external post-tensioning has indicated that the concept works. It is recommended that the method of post-tensioning presented be used to rehabilitate pre-cast bridges in Alberta. More refinements are needed, though, to improve

the method and make it applicable in the field. There are two types of refinement which can be introduced:

1) The steel connection fixing the DYWIDAG-bar to the web of the reinforced concrete beam could be redesigned in a more economical way. The steel connection is an eccentric one, so more work could be done to try to bring the force as close as possible to the centre of the bolt system. The steel connection could even be replaced by other safe means of connecting the DYWIDAG-bars to the beam.

2) The detail of the circular steel pipe can be refined. The clear height of roads underneath the bridges would be affected by the pipes, if employed as in the thesis. The pipes could either be half- or full imbedded inside the beam. (Figure 6.1, Figure 6.2). The latter two suggestions would produce a nicer aesthetic effect on the bridges. However such adjustment would affect the design of the DYWIDAG-bars. As the distance d_p would be less, a higher post-tensioning force would be required to get the same moment of resistance to the beams.

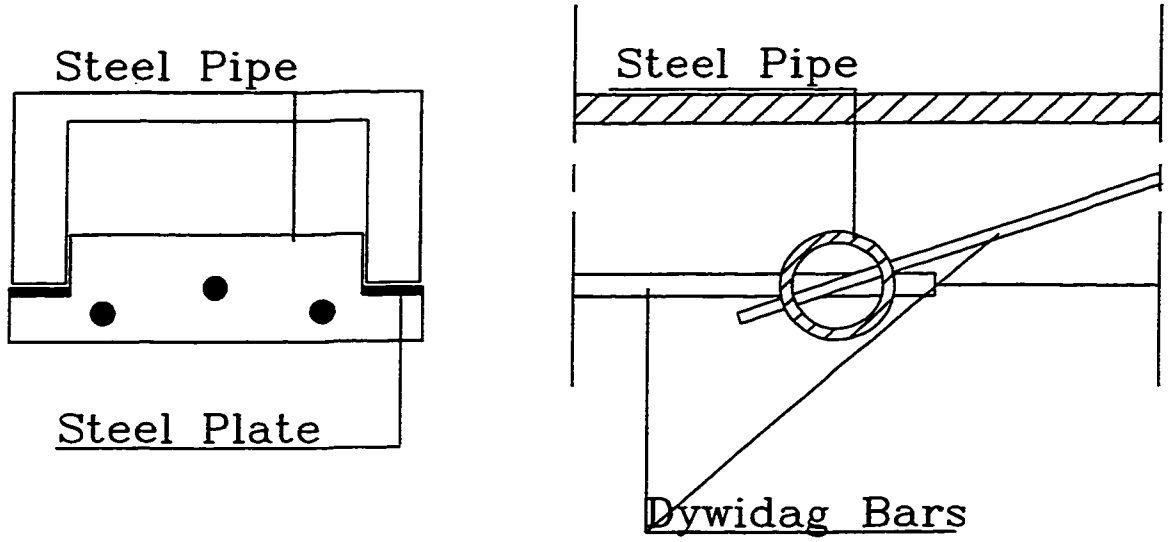

Figure 6. 1 Half- Imbeded Circular Pipe Supported by Flat Plate on Webs

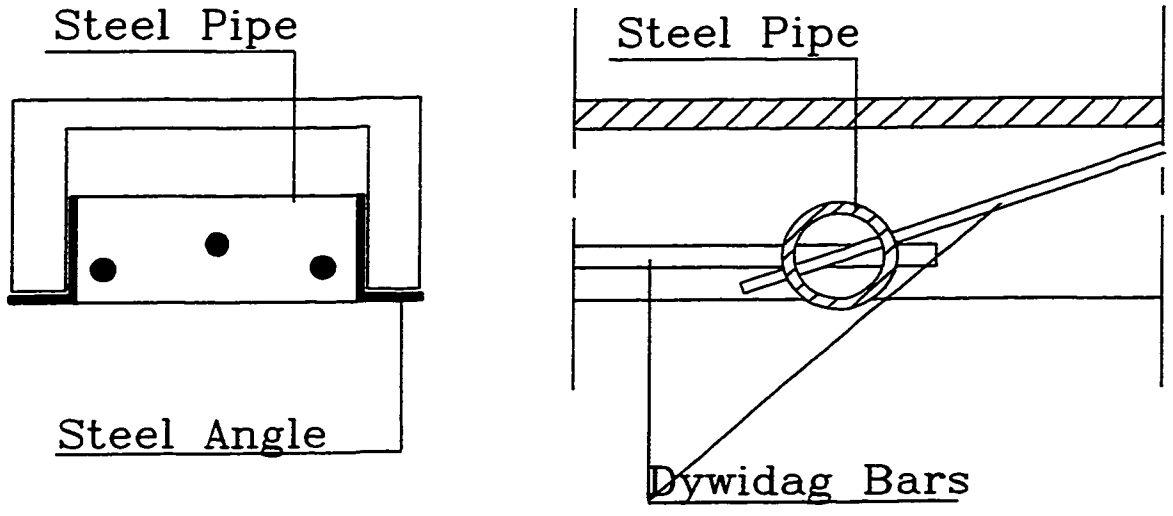

Figure 6. 2 Fully- Imbedded Circular Pipes Supported by Welded Steel Angle

LIST OF REFERENCES

Alexander, J. G. S., and Cheng, R., (1996), "Field Application and Studies of Using CFRP-Sheets to Strengthen Concrete Bridge Girders", *ACMBS-II Conference, Montreal,* August 1996.

Calder, A.J.J., (1982), "Exposure Tests on Externally Reinforced Concrete Beams- First Two Years," Transport and Road Research Laboratory, Crowthorne, England, Report SR529.

Chajes, M. J., Finch W. W. Jr., Januszka, T. F., and Thomson T. A. Jr., (1996), "Bond and Force Transfer of Composite Material Plates Bonded to Concrete", *American Concrete Institute Structural Journal, V.93, No. 2,* March-April 1996, pp208-217.

Cheng, R., Hutchinson, R., and Rizkalla, S., (1997), "Rehabilitation of Concrete Bridges for Shear Deficiency using CFRP-sheets", *42nd International SAMPE Symposium,* May 4th –May 8th 1997, pp. 325-335.

Crasto, A. S., Kim, R. Y., Mistretta J. P. and Dougherty, M., (1997), "Rehabilitation of Concrete Bridge Beams with Fiber-Reinforced Composites", *42nd International SAMPE Symposium,* May 4th –May 8th 1997, pp. 77-82.

CSA-A23.3-94, "Concrete Design Handbook", *Concrete Standards Association, Rexdale, Ontario.*

Dorton, R. A., (1994), "Development of Canadian Bridge Codes", *Proceedings of The Fourth International Conference on Short and Medium Span Bridges, Halifax,* August 8th-August 11th, 1994, pp. 1-12.

Drimoussis, E., and Cheng, R., (1994), "Shear Strengthening of Concrete Girders Using Carbon Fiber Reinforced Plastic Sheets", *Structural Engineering Report, University of Alberta, Department of Civil Engineering,* October 1994, 177p.

Garden H. N, Hollaway L. C., and Thorne A. M., (1997), "A Preliminary Evaluation of Carbon Fiber Reinforced Polymer Plates for Strengthening Reinforced Concrete Members", *Proceedings of the Institution of Civil Engineers, of Structures and Buildings,* May 1997, pp. 127-142.

Ghali, A., (1986), "Strength of Concrete Bridges Precast Stringers Type G", *Separate Report, Submitted to Bridge Engineering Branch, Alberta Transportation,* June 30th 1986.

Hisabe, N., Hiromichi, S., Ootaguro, H., Mitsui, Y., and Murakami, K., (1997), "Experimental Study on Carbon Fiber Sheet for Shear Strengthening", *International Conference on Engineering Materials, JSCE,* June 8th-June 11th, 1997.

Holzenkämpfer, P., (1994)," Ingenieurmodelle des Verbundens geklebter Bewehrung für Betonbauteile", Dissertation, Heft 108, August 1994, pp. 214.

Iványi, G., and Buschmeyer, W., (1996a), "Strengthening Bridge Superstructures due to External Prestressing: Experiences in Design and Construction", *FIP Symposium on Post-Tensioned Concrete Structures,* 1996, pp. 387-396.

Iványi, G., and Buschmeyer, W., (1996b), "Structural Evaluation of Prestressed Concrete Bridges", University of Dundee, International Congress "Concrete in the Service of the Mankind", Dundee, Scotland.

Jansze, W., (1997), "Strengthening of Reinforced Concrete Members in Bending by Externally Bonded Steel Plates", *Thesis, Technical University of Delft, Holland,* October 1997.

Japan Society of Civil Engineers (1986), "Standard Specification for Design and Construction of Concrete Structures", *Part 1*, (Design).

Karbhari, V. M., (1995), "Characteristics of Adhesion Between Composites and Concrete as Related to Infrastructure Rehabilitation", *27th International SAMPE Technical Conference,* October 9th –October 12th 1995, pp. 1083-1094.

Karbhari, V. M., (1997), "On the Use of Composites for Bridge Renewal: Materials, Manufacturing and Durability", *42nd International SAMPE Symposium,* May 4th –May 8th 1997, pp. 915-926.

Karbhari, V. M., and Seible, F., (1996), "On the Use of Fiber Reinforced Composites for Infrastructure Renewal – A Systems Approach", *Proceedings of The Materials Engineering Conference: Materials For The New Millennium,* 1996, V. 2, pp. 1091-1100.

Karbhari, V. M., Engineer, M., (1996a), "Effect of Environmental Exposure on the External Strengthening of Concrete with Composites – Short Term Bond Durability", *Journal of Reinforced Plastics and Composites*, December 1996, V. 15, pp. 1194-1216.

Karbhari, V. M., Engineer, M., (1996b), "Investigation of Bond between Concrete and Composites: Use of a Peel Test", *Journal of Reinforced Plastics and Composites*, February 1996, V. 15, pp. 208-227.

Karbhari, V. M., Engineer, M., and Eckel II, D. A., (1997), "On the Durability of Composite Rehabilitation Schemes for Concrete: Use of a Peel Test", *Journal of Materials Science,* V. 32, pp. 147-156.

Klaiber, F., Dunker, K., Wipf, T., and Sanders, W., (1987), "Methods of Strengthening Existing Highway Bridges", *Transportation Research Board, Crowthorne, England, NCHRP Research Report No. 293*, September 1987.

Lloyd, G.O., and Calder, A.J.J., (1982), "The Microstructure of Epoxy Bonded Steel-to-Concrete Plates," Transport and Road Research Laboratory, Crowthorne, England, Report SR705.

Loov, R. E.,(1997), "The Direct Computation of Stirrup Spacing Based on Shear Friction", *Proceedings Symposium on Advanced Design of Concrete Structures, Chalmers University of Technology, Goteberg*, June 12th-June 14th, 1997.

Mao, S., Alexander, S. D. B., and Rogowsky, D. M., (1997), " Tests of Alberta HC-Type Stringers", *Report for Bridge Engineering Branch, Alberta Transportation and Utilities.*

Mattock, A. H., Yamazaki, J., and Kattula B. T., (1971), "Comparative Study of Prestressed Concrete Beams with and without Bond", *American Concrete Institute Journal,* V. 68, pp. 116-125.

McKenna, J. K., and Erki, M. A., (1994), "Strengthening of Reinforced Flexural Members Using externally Applied Steel Plates and Fiber Composite Sheets- A Survey" *Canadian Journal for Civil Engineers, V. 21,* 1994, pp. 16-24.

Meier, U., (1992), "Carbon Fibre Reinforced Polymers: Modern Materials in Bridge Engineering" *Structural Engineering International*, V.2, pp. 7-12.

Muller, J., Gauthier, Y., (1990), "Ultimate Behaviour of Precast Segmental Box Girders with External Tendons", *American Concrete Institute, Detroit, Michigan, Special Publication SP120-17*, pp. 355-354.

Munley, E., (1994), "Federal Highway Administration Research Program: Fiber Reinforced Polymer Composite Materials", *10th ASM/ESD Advanced Composites Conference, Dearborn, MI*, November 8th , 1994.

Naaman, A. E., and Alkhairi, F. M., (1991), "Stress at Ultimate in Unbonded Post-Tensioning Tendons. Part 1: Evaluation of the State-of-the-Art", *American Concrete Institute Journal,* V. 88, pp. 641-651.

Naaman, A. E., and Alkhairi, F. M., (1991), "Stress at Ultimate in Unbonded Post-Tensioning Tendons. Part 2: Proposed Methodology", *American Concrete Institute Journal,* V. 88, pp. 683-692.

Neale, K. W. (1997), "Advanced Composites and Integrated Sensing for Rehabilitation", *ISIS Canada annual report* p. 6.

Neale, K. W., and Labossière, P., (1991), "Advanced Composite Materials with Applications to Bridges", *State of the Art report, Canadian Society for Civil Engineering,* Montreal, Que., pp. 21-69.

Neubauer, U., and Rostásy, F. S., (1996), "Design Aspects of Concrete Structures Strengthened with Externally Bonded CFRP-Plates", (*Personal Communication*).

Norris, T., Sadaatmanesh, H., and Ehsani, M. R., (1997),"Shear and Flexural Strengthening of R/C Beams With Carbon Fiber Sheets", *American Society for Civil Engineers, Journal of Structural Engineering*, July 1997, V. 123, No. 7., pp. 903-911.
Okada, K., Kobayashi, K., and Miyagawa, T., (1988), "Influence of Longitudinal Cracking to Reinforcement Corrosion on Characteristics of Reinforced Concrete Members", *American Concrete Institute Structural Journal,* March-April 1988, pp134-140.

Pichler, D., (1993), "Die Wirkung von anpressdrücken auf die Verankerung von Klebelamellen", Dissertation, Technical University of Innsbrück, Innsbrück.

Pisani, M. A., (1996), "A Numerical Model for Externally Prestressed Beams", *Journal of Structural Engineering and Mechanics*, V. 4, No. 2, pp. 177-190.

Pisani, M. A., and Nicoli, E., (1996), "Beams Prestressed with Unbonded Tendons at Ultimate", *Canadian Journal of Civil Engineering*, V. 23, 1996, pp. 1220-1230.

Raoof, M., and Lin, Z., (1997), "Structural Characteristics of R/C Beams with Exposed Main Steel", *Proceedings of the Institution of Civil Engineers, of Structures and Buildings*, February 1997, pp. 35-51.

Robson, A., and Craig, J. M., (1996), "The Design of the Strengthening of the A3/A31 Flyover – Guildford", *FIP Symposium on Post-Tensioned Concrete Structures,* 1996, pp. 406-415.

Rozvany, G. I. N., and Woods, J. F., (1969), "Sudden Collapse of Unbonded Underprestressed Structures", *American Concrete Institute Journal*, V. 66, pp. 129-135.

Saeki, N., Shimura, K., Izumo, K., and Horiguchi, T., (1997), "Rehabilitation of Reinforced Concrete Beams using Prestressed Fiber Sheets", *International Conference on Engineering Materials, JSCE,* June 8th-June 11th, 1997.

Shawwaf, K., (1996), "Rehabilitation and Strengthening of Concrete Structures by Post-Tensioning Methods", *FIP Symposium on Post-Tensioned Concrete Structures,* 1996, pp. 416-423.

Walser, R., and Steiner, W., (1997), "Strengthening a Bridge with Advanced Materials", *Part of Technical Report: "Structural Strengthening with Carbon Fiber Plastic Laminates-The Sika® CarboDur System or Steel Plates.* February 1997.

Walter, R., and Miehlbradt, M., (1990), "Dimensionnement des Structrures en Béton. Bases et Technologie", *Presses Polytechniques et Universitaires Romandes, Lausanne, Switzerland.*